

การศึกษาสมบัติเชิงโครงสร้างและเชิงพลวัตของโปแตสเซียมไอโอไดด์ในแอมโมเนียเหลว  
โดยโมเลกุลาร์ไดนามิกส์เชิงโมเลกุล

นาย อนันต์ ทองระอา



วิทยานิพนธ์นี้เป็นส่วนหนึ่งของการศึกษาตามหลักสูตรปริญญาวิทยาศาสตรมหาบัณฑิต

ภาควิชาเคมี

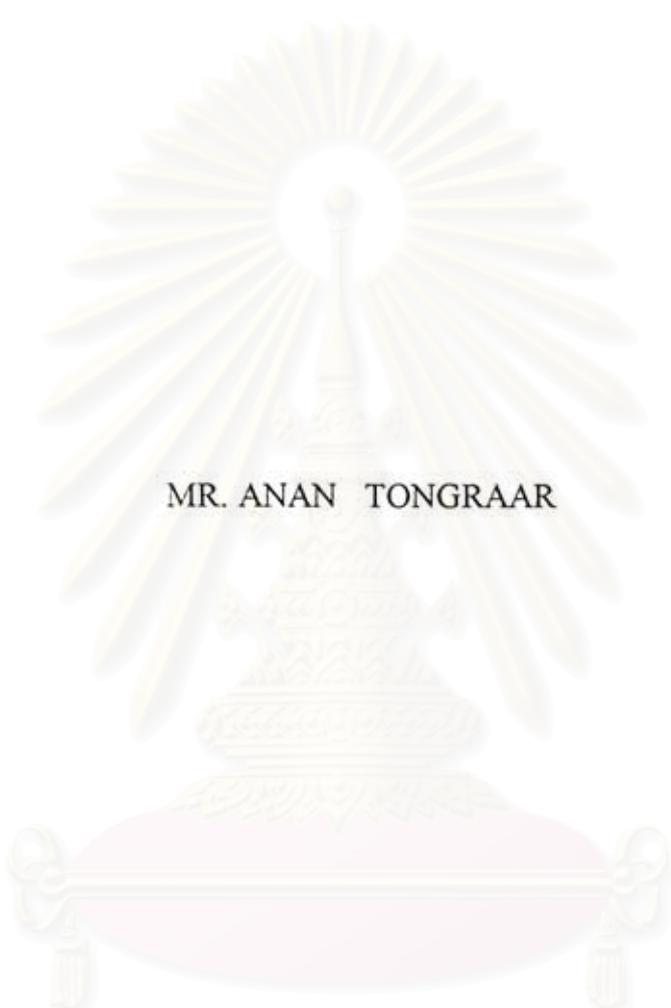
บัณฑิตวิทยาลัย จุฬาลงกรณ์มหาวิทยาลัย

พ.ศ. 2538

ISBN 974-631-452-1

ลิขสิทธิ์ของบัณฑิตวิทยาลัย จุฬาลงกรณ์มหาวิทยาลัย

STUDY OF STRUCTURAL AND DYNAMICAL PROPERTIES OF  
POTASSIUM IODIDE IN LIQUID AMMONIA BY MOLECULAR  
DYNAMICS SIMULATION



MR. ANAN TONGRAAR

สถาบันวิทยบริการ

A Thesis Submitted in Partial Fulfillment of the Requirement

จุฬาลงกรณ์มหาวิทยาลัย

for the Degree of Master of Science

Department of Chemistry

Graduate School

Chulalongkorn University

1995

ISBN 974-631-452-1

**Thesis Title** Study of Structural and Dynamical Properties of Potassium Iodide in Liquid Ammonia by Molecular Dynamics Simulation  
**By** Mr. Anan Tongraar  
**Department** Chemistry  
**Thesis Advisor** Associate Professor Supot Hannongbua, Ph.D.  
**Co-advisor** Professor Bernd Michael Rode, Ph.D.



Accepted by the Graduate School, Chulalongkorn University in Partial Fulfillment of the Requirement for the Master's Degree.

*Santi Thoongsuwan*

..... Dean of Graduate School  
(Associate Professor Santi Thoongsuwan, Ph.D.)

**Thesis Committee**

*Siri Varothai*

..... Chairman  
(Associate Professor Siri Varothai, Ph.D.)

*S. Hannongbua*

..... Thesis Advisor  
(Associate Professor Supot Hannongbua, Ph.D.)

*B. M. Rode*

..... Co-advisor  
(Professor Bernd Michael Rode, Ph.D.)

*Sirirat Kokpol*

..... Member  
(Associate Professor Sirirat Kokpol, Ph.D.)

*K. Sagarik*

..... Member  
(Associate Professor Kritsana Sagarik, Ph.D.)

พิมพ์ต้นฉบับบทคัดย่อวิทยานิพนธ์ภายในกรอบสี่เหลี่ยมนี้เพียงแผ่นเดียว

อนันต์ ทองระอา : การศึกษาสมบัติเชิงโครงสร้างและเชิงพลวัตของโปแตสเซียมไอโอไดด์ในแอมโมเนียเหลวโดยโมเลคิวลาร์ไดนามิกส์ซิมูเลชัน (STUDY OF STRUCTURAL AND DYNAMICAL PROPERTIES OF POTASSIUM IODIDE IN LIQUID AMMONIA BY MOLECULAR DYNAMICS SIMULATION) อาจารย์ที่ปรึกษา : รศ.ดร.สุพจน์ หารหนองบัว, ศ.ดร.เมธรัตน์ ไมเคิล โรด, 98 หน้า. ISBN 974-631-452-1

ได้ทำการศึกษาสารละลายที่ประกอบด้วยโปแตสเซียม 1 ไอออน ในแอมโมเนีย 215 โมเลกุล สารละลายที่ประกอบด้วยไอโอไดด์ 1 ไอออน ในแอมโมเนีย 215 โมเลกุล และสารละลายที่ประกอบด้วยทั้งโปแตสเซียมและไอโอไดด์อย่างละ 1 ไอออน ในแอมโมเนีย 214 โมเลกุล โดยโมเลคิวลาร์ไดนามิกส์ซิมูเลชันที่อุณหภูมิเฉลี่ย 240 เคลวิน โดยใช้แบบจำลองฮาร์ดคอร์สำหรับโมเลกุลแอมโมเนีย ส่วนศักย์คู่ระหว่างไอออนโปแตสเซียม-แอมโมเนีย ไอออนไอโอไดด์-แอมโมเนีย และ ไอออนโปแตสเซียม-ไอออนไอโอไดด์นั้น ได้พัฒนาขึ้นใหม่จากการคำนวณ แอบ อินิซิโอ ซึ่งมีการแก้ไขความผิดพลาดของเบซิส เซต จูเปอร์โพสิชัน เอียร์เรอร์สมบัติเชิงโครงสร้างของสารละลาย ได้อธิบายในรูปของฟังก์ชันการกระจายเชิงรัศมีและเลขอินทิเกรชัน ผลการศึกษาพบว่าเลขโคออร์ดิเนชันของไอออนโปแตสเซียมมีค่า 8.7 และ 8.9 สำหรับระบบไอออนโปแตสเซียม-แอมโมเนีย และระบบไอออนโปแตสเซียม-ไอออนไอโอไดด์-แอมโมเนีย ตามลำดับ ค่าเดียวกันนี้ของไอออนไอโอไดด์มีค่า 15.9 และ 15.1 สำหรับระบบไอออนไอโอไดด์-แอมโมเนีย และระบบไอออนโปแตสเซียม-ไอออนไอโอไดด์-แอมโมเนีย การมีอยู่ของเคาน์เตอร์ไอออนในสารละลาย ส่งผลให้รัศมีโซลเวชันของไอออนโปแตสเซียมสั้นลง 0.2 อองสตรอม ก่อให้เกิดการหันเหของโมเลกุลที่อยู่ในเชลแรกของไอออนโปแตสเซียม ทำให้เกิดการแยกของพีกที่สองของกราฟการกระจายในเชิงรัศมีของไอออนโปแตสเซียม-อะตอมไนโตรเจน และทำให้เกิดการหายไปของพีกที่สองของการกระจายในเชิงรัศมีของอะตอมไนโตรเจน-อะตอมไนโตรเจน เป็นต้น สมบัติเชิงพลวัตของสารละลายซึ่งได้ศึกษาในรูปของฟังก์ชันออรัคคอรี่เลชันและฟูเรียร์ทรานสฟอร์ม มีความสอดคล้องกับผลที่ได้จากการศึกษาทั้งทางด้านทฤษฎีและทางด้านการทดลอง



ภาควิชา .....  
สาขาวิชา .....  
ปีการศึกษา .....

ลายมือชื่อนิสิต .....  
ลายมือชื่ออาจารย์ที่ปรึกษา .....  
ลายมือชื่ออาจารย์ที่ปรึกษาร่วม .....

## C625038 : MAJOR PHYSICAL CHEMISTRY

KEY WORD: MOLECULAR DYNAMICS SIMULATION/ METAL-AMMONIA SOLUTION

ANAN TONGRAAR : STUDY OF STRUCTURAL AND DYNAMICAL PROPERTIES OF POTASSIUM IODIDE IN LIQUID AMMONIA BY MOLECULAR DYNAMICS SIMULATION. THESIS ADVISER : ASSOC. PROF. SUPOT HANNONGBUA, Ph.D. AND PROF. BERND MICHAEL RODE, Ph.D. 98 pp. ISBN 974-631-452-1

The solution of one  $K^+$  in 215 ammonia, one  $I^-$  in 215 ammonia and one KI in 214 ammonia have been investigated by Molecular Dynamics simulation at an average temperature of 240 K, using flexible ammonia model. The  $K^+$ -ammonia,  $I^-$ -ammonia and  $K^+ - I^-$  pair potentials were newly developed, based on *ab initio* calculations, in which the basis set superposition error (BSSE) was corrected. The structural properties of the solution are described in terms of radial distribution functions (RDFs) and running integration numbers. The coordination numbers of  $K^+$  of 8.7 and 8.9 were found for the  $K^+$ -ammonia and the  $K^+ - I^-$ -ammonia systems, respectively. The corresponding values of  $I^-$  are 15.9 and 15.1 for the  $I^-$ -ammonia and the  $K^+ - I^-$ -ammonia systems. The presence of the counter ion causes the shift of the solvation radius of the  $K^+$  of 0.2 Å to the shorter distance, the reorientation of its first shell molecules, the split of the second peak of the  $K^+ - N$  RDF and so on. The dynamical properties of the solution, which are investigated in terms of autocorrelation functions and their Fourier transforms are in good agreement with those reported by both theoretical and experimental investigation.

สถาบันวิทยบริการ  
จุฬาลงกรณ์มหาวิทยาลัย

ภาควิชา.....

สาขาวิชา.....

ปีการศึกษา.....

ลายมือชื่อนิสิต.....

ลายมือชื่ออาจารย์ที่ปรึกษา.....

ลายมือชื่ออาจารย์ที่ปรึกษาร่วม.....

## ACKNOWLEDGMENTS

This thesis was made completely and fast with full speed ahead helping of my kindful advisor, Associate Professor Supot Hannongbua. I would like to express my deep gratitude to him for his guiding, advising, understanding and encouraging. I owe a great dept of gratitude to my co-advisor, Professor Bernd Michael Rode who was taken me through a lot of problems and supported me a scholarship for the period of my M.Sc. studies. I am very obliged to Associate Professor Sirirat Kokpol and Associate Professor Kritsana Sagarik for their valuable suggestions as thesis examiners.

In addition, I am grateful to Austrian-Thai Center for Computer Assisted Chemical Education and Research for computer resource supplements. Financial supports by Austrian Ministry of Foreign Affairs and Graduate School are also gratefully acknowledged.

Finally, I would like to give my gratitude to my parents for their understanding and encouragement and gave me a continuous supports during the whole studying.



สถาบันวิทยบริการ  
จุฬาลงกรณ์มหาวิทยาลัย

# CONTENTS



pages

ABSTRACT IN THAI .....	iv
ABSTRACT IN ENGLISH .....	v
ACKNOWLEDGEMENT .....	vi
LIST OF FIGURES .....	x
LIST OF TABLES .....	xiv
CHAPTER 1 INTRODUCTION .....	1
Motivation and applications of computer simulations .....	1
A non-aqueous solvent system .....	2
CHAPTER 2 QUANTUM THEORY .....	4
2.1 Quantum mechanics methods .....	5
2.2 The Schrödinger's equation .....	6
2.3 Separation of nuclear motion : Born-Oppenheimer approximation .....	7
2.4 Molecular orbital theory and linear combination of atomic orbital (LCAO) approximation .....	8
2.5 Basis functions .....	9
2.6 Hartree-Fock theory and Hartree-Fock self-consistent-field methods .....	10
2.7 Basis set superposition error (BSSE) .....	12
2.8 Interaction potential in the statistical simulation .....	13
2.9 Specification of the systems for this study .....	15
2.9.1 Intermolecular potential energy functions .....	16
2.9.2 Construction of the intermolecular pair potential functions .....	16
2.9.3 Investigation of non-additivity of pair potentials .....	19

	pages
CHAPTER 3 MOLECULAR DYNAMICS METHOD .....	22
3.1 Molecular Dynamics procedure .....	24
3.2 The predictor-corrector algorithm .....	26
3.3 Periodic boundary conditions .....	28
3.4 Cut-off limit .....	29
3.5 Long-range interaction .....	31
3.5.1 The Ewald sum .....	31
3.5.2 The reaction field method .....	32
3.6 Shift and shift-force potentials .....	32
3.7 Neighbouring algorithm .....	33
3.8 Calculation of macroscopic properties .....	34
3.8.1 Structural properties .....	34
3.8.2 Dynamical properties .....	34
CHAPTER 4 RESULTS .....	37
Part A : Intermolecular potentials .....	37
4.1 Suitable basis sets for the atoms of the systems .....	37
4.2 Intermolecular pair potentials .....	39
4.2.1 $K^+$ -ammonia pair potential .....	39
4.2.2 $I^-$ -ammonia pair potential .....	41
4.2.3 $K^+ - I^-$ pair potential .....	43
4.3 SCF calculation on the non-additivity .....	45
Part B : Molecular Dynamics simulation .....	46
4.4 Structural properties .....	46
4.4.1 $K^+$ -ammonia system .....	46
4.4.2 $I^-$ -ammonia system .....	49
4.4.3 $K^+ - I^-$ -ammonia system .....	52

	pages
4.5 Dynamical properties .....	56
4.5.1 $K^+$ -ammonia system .....	56
4.5.2 $I^-$ -ammonia system .....	61
4.5.3 $K^+I^-$ -ammonia system .....	66
CHAPTER 5 DISCUSSION .....	72
Part A : Intermolecular potentials .....	72
5.1 Suitable basis sets for the atoms of the systems .....	72
5.2 Intermolecular pair potential .....	73
5.3 SCF calculations on the non-additivity .....	73
Part B : Molecular Dynamics simulation .....	75
5.4 Structural properties .....	75
5.5 Dynamical properties .....	80
REFERENCES .....	85
APPENDIXES .....	90
Appendix 1 Exponents and coefficients for 4 basis sets .....	90
Appendix 2 Gaussian 92 input file .....	95
CURRICULUM VITAE .....	98

สถาบันวิทยบริการ  
จุฬาลงกรณ์มหาวิทยาลัย

## LIST OF FIGURES

pages

2.1 a) The hard-sphere potential ; b) The square-well potential ; c) The soft-sphere potential .....	15
2.2 Definition of geometric variables for the configurations of ion-ammonia system .....	18
2.3 Geometries of their $K^+-(NH_3)_n$ complexes .....	20
3.1 The steps in Molecular Dynamics simulation .....	25
3.2 The periodic boundary condition .....	29
3.3 The minimum image convention in a two-dimensional system .....	30
4.1 Comparison of the stabilization energies obtained from the SCF calculation with BSSE, $\Delta E_{BSSE}$ and from the potential function, $\Delta E_{FIT}$ using the final values of the fitting parameters as given in Table 4.1 .....	40
4.2 Comparison of the $\Delta E_{BSSE}$ and $\Delta E_{FIT}$ .....	40
4.3 Comparison of the stabilization energies obtained from the SCF calculation with BSSE, $\Delta E_{BSSE}$ and from the potential function, $\Delta E_{FIT}$ using the final values of the fitting parameters as given in Table 4.2 .....	42
4.4 Comparison of $\Delta E_{BSSE}$ and $\Delta E_{FIT}$ .....	42
4.5 Comparison of the stabilization energies obtained from the SCF calculation with BSSE, $\Delta E_{BSSE}$ and from the potential function, $\Delta E_{FIT}$ using the final values of the fitting parameters as given in Table 4.3 .....	44
4.6 Comparison of the $\Delta E_{BSSE}$ and $\Delta E_{FIT}$ .....	44
4.7 Atom-atom radial distribution functions and running integration numbers from the Molecular Dynamics simulation of one $K^+$ in liquid ammonia at 240 K. (a) $K^+-N$ ; (b) $K^+-H$ .....	47

4.8 Atom-atom radial distribution functions and running integration numbers from the Molecular Dynamics simulation of one $K^+$ in liquid ammonia at 240 K. (a) N-N ; (b) N-H ; (c) H-H .....	48
4.9 Atom-atom radial distribution functions and running integration numbers from the Molecular Dynamics simulation of one $I^-$ in liquid ammonia at 240 K. (a) $I^-$ -N ; (b) $I^-$ -H .....	50
4.10 Atom-atom radial distribution functions and running integration numbers from the Molecular Dynamics simulation of one $I^-$ in liquid ammonia at 240 K. (a) N-N ; (b) N-H ; (c) H-H .....	51
4.11 Atom-atom radial distribution functions and running integration numbers from the Molecular Dynamics simulation of one $K^+$ and one $I^-$ in liquid ammonia at 240 K. (a) $K^+$ -N ; (b) $K^+$ -H .....	53
4.12 Atom-atom radial distribution functions and running integration numbers from the Molecular Dynamics simulation of one $K^+$ and one $I^-$ in liquid ammonia at 240 K. (a) $I^-$ -N ; (b) $I^-$ -H .....	54
4.13 Atom-atom radial distribution functions and running integration numbers from the Molecular Dynamics simulation of one $K^+$ and one $I^-$ in liquid ammonia at 240 K. (a) N-N ; (b) N-H ; (c) H-H .....	55
4.14 Normalized velocity autocorrelation function functions of (a) $K^+$ ; (b) N atom and (c) H atom, obtained from the Molecular Dynamics simulation of one $K^+$ in liquid ammonia at 240 K .....	57
4.15 (a) Normalized velocity autocorrelation functions of ammonia molecules about the x and z axis ; (b) their Fourier transforms, calculated from the Molecular Dynamics simulation of one $K^+$ in liquid ammonia at 240 K .....	58
4.16 (a) Normalized center-of-mass velocity autocorrelation functions of ammonia molecules ; (b) their Fourier transforms, calculated from the Molecular Dynamics simulation of one $K^+$ in liquid ammonia at 240 K .....	59

pages

4.17 Fourier transforms of the hydrogen velocity autocorrelation functions for bulk ammonia and ammonia in the solvation shell of $K^+$ , calculated from the Molecular Dynamics simulation of one $K^+$ in liquid ammonia at 240 K .....	60
4.18 Temperature changes of the Molecular Dynamics simulation of one $K^+$ in liquid ammonia .....	60
4.19 Normalized velocity autocorrelation function functions of (a) $I^-$ ; (b) N atom and (c) H atom, obtained from the Molecular Dynamics simulation of one $I^-$ in liquid ammonia at 240 K .....	62
4.20 (a) Normalized velocity autocorrelation functions of ammonia molecules about the x and z axis; (b) their Fourier transforms, calculated from the Molecular Dynamics simulation of one $I^-$ in liquid ammonia at 240 K .....	63
4.21 (a) Normalized center-of-mass velocity autocorrelation functions of ammonia molecules; (b) their Fourier transforms, calculated from the Molecular Dynamics simulation of one $I^-$ in liquid ammonia at 240 K .....	64
4.22 Fourier transforms of the hydrogen velocity autocorrelation functions for bulk ammonia and ammonia in the solvation shell of $I^-$ , calculated from the Molecular Dynamics simulation of one $I^-$ in liquid ammonia at 240 K .....	65
4.23 Temperature changes of the Molecular Dynamics simulation of one $I^-$ in liquid ammonia .....	65
4.24 Normalized velocity autocorrelation function functions of (a) $K^+$ ; (b) $I^-$ ; (c) N atom and (d) H atom, obtained from the Molecular Dynamics simulation of one $K^+$ and one $I^-$ in liquid ammonia at 240 K .....	67

4.25 (a) Normalized velocity autocorrelation functions of ammonia molecules about the x and z axis ; (b) their Fourier transforms about the x axis ; (c) their Fourier transforms about the z axis, calculated from the Molecular Dynamics simulation of one $K^+$ and one $I^-$ in liquid ammonia at 240 K .....	69
4.26 (a) Normalized center-of-mass velocity autocorrelation functions of ammonia molecules ; (b) their Fourier transforms, calculated from the Molecular Dynamics simulation of one $K^+$ and one $I^-$ in liquid ammonia at 240 K .....	70
4.27 Fourier transforms of the hydrogen velocity autocorrelation functions for bulk ammonia and ammonia in the solvation shell of $K^+$ and $I^-$ , calculated from the Molecular Dynamics simulation of one $K^+$ and one $I^-$ in liquid ammonia at 240 K .....	71
4.28 Temperature changes of the Molecular Dynamics simulation of one $K^+$ and one $I^-$ in liquid ammonia .....	71
5.1 Two-dimensional dipole orientation of ammonia molecules ; (a) The ammonia molecule in the first solvation shell of $K^+$ in the system consisting of one $K^+$ in ammonia ; (b) The dipole orientation of ammonia molecules in the system consisting of one $K^+$ and one $I^-$ in ammonia ; (c) The orientation changed of ammonia molecules in the solvation shell of $K^+$ in the $K^+$ - $I^-$ -ammonia system .....	76

## LIST OF TABLES

pages

2.1 Ammonia-ammonia intermolecular potential, energies are given in units of kcal/mol and distance in Å .....	16
4.1 Testing of basis sets for the $K^+$ -ammonia. (interaction energies and $r$ in kcal/mol and Å, respectively) .....	38
4.2 Testing of basis sets for the $I^-$ -ammonia. (interaction energies and $r$ in kcal/mol and Å, respectively) .....	38
4.3 Testing of basis sets for the $K^+ - I^-$ -ammonia system. (interaction energies and $r$ in kcal/mol and Å, respectively) .....	38
4.4 Final optimized parameters for the interaction of N and H atoms of ammonia with $K^+$ . (interaction energies and $r$ in kcal/mol and Å, respectively) .....	39
4.5 Final optimized parameters for the interaction of N and H atoms of ammonia with $I^-$ . (interaction energies and $r$ in kcal/mol and Å, respectively) .....	41
4.6 Final optimized parameters for the interaction of $I^-$ with $K^+$ . (interaction energies and $r$ in kcal/mol and Å, respectively) .....	43
4.7 The $K^+$ -ammonia interactions complexes, as defined in equation (2.33) - (2.37), and optimized nitrogen distances ( $r_{M-N}$ ) for the different $K^+-(NH_3)_n$ (interaction energies and $r$ in kcal/mol and Å, respectively) .....	45
4.8 Characteristic values of the radial distribution functions, $g_{\alpha\beta}(r)$ for the $K^+$ -ammonia solution ; $r_{M1}$ , $r_{M2}$ and $r_{m1}$ are the distance in Å, where $g_{\alpha\beta}(r)$ has first and second maximum and first minimum, respectively. $n_{\alpha\beta}(r_{m1})$ is running integration numbers, integrated up to $r_{m1}$ .....	46
4.9 Characteristic values of the radial distribution functions, $g_{\alpha\beta}(r)$ for the $I^-$ -ammonia solution ; $r_{M1}$ , $r_{M2}$ and $r_{m1}$ are the distance in Å, where $g_{\alpha\beta}(r)$ has first and second maximum and first minimum, respectively. $n_{\alpha\beta}(r_{m1})$ is running integration numbers, integrated up to $r_{m1}$ .....	49

4.10 Characteristic values of the radial distribution functions, $g_{\alpha\beta}(r)$ for the $K^+ - I^-$ -ammonia solution. $r_{M1}$ , $r_{M2}$ and $r_{m1}$ are the distance in Å, where $g_{\alpha\beta}(r)$ has first and second maximum and first minimum, respectively. $n_{\alpha\beta}(r_{m1})$ is running integration numbers, integrated up to $r_{m1}$ .....	52
5.1 Comparison of non-additivity effect for some complexes with respect to $n=6$ , energies and $r_{\text{shift}}$ from $n=1$ to 6 in kcal/mol and Å, respectively .....	74
5.2 Comparison of the characteristic values of the first solvation shell for some dilute ion-water solutions and ion-ammonia solutions. $\alpha\beta$ , $r_{M1}$ and $n_{\alpha\beta}$ are pair of species, the first maximum distance in Å and coordination numbers, respectively .....	79
5.3 Comparison of the self-diffusion coefficient from simulations, calculated separately for bulk ammonia and ammonia in the solvation shell of ions, and from experimental result .....	81
5.4 Comparison of various vibrational frequencies taken from the simulations, calculated separately for bulk ammonia and ammonia in the solvation shell of ions, and from the experimental results .....	84

# CHAPTER 1

## INTRODUCTION

### Motivation and applications of computer simulations

In the past few years, computer technology has rapidly developed. Computers play a significant role in many fields, including studies and research. Especially *Computational Science* makes use of computer simulations instead of experiments for evaluating interesting informations of systems, particularly, of those systems for which experiments cannot be easily performed. Computer simulations have been enlarged and merged into a new field of stochastic simulations and extended to cover quantum mechanical as well as classical systems.

The problems in statistical mechanics are exactly soluble. By this, a complete specification of the microscopic properties of a system (such as a Hamiltonian of an idealized model like the perfect gas or the Einstein crystal) leads directly, and perhaps easily to a set of interesting results or macroscopic properties. When not being exactly soluble, the problem succumb readily to analysis based on a straightforward approximation scheme. Computers may have an incidental and calculational part to play in such work. Computer simulations have a valuable role to play in providing essentially exact results for problems in statistical mechanics which would otherwise only be soluble by approximate methods, or might be quite intractable. In this sense, computer simulation is a test of theories and, historically, simulations have indeed discriminated between well-founded approaches (such as integral equation theories) [1] and idea that are plausible but, in the event, less successful (such as the old cell theories of liquid) [2-3]. The results of computer simulations may also be compared with those of real experiments

Computer simulations can fill the gap between theory and experiment. As mentioned above, some quantities or behaviour may be impossible or difficult to measure in an experiment. With computer simulations such quantities can be

computed. Computer simulations provided a direct route from the microscopic details of a system to macroscopic properties of experimental interest.

Computer simulation methods, such as Monte Carlo (MC) practically introduced by Metropolis [4], and Molecular Dynamics (MD), introduced by Alder [5], are important tools for studying statistical and dynamical properties of liquids and solutions. The results from Monte Carlo and Molecular Dynamics methods have been published [for example, 6-26], displayed the structural properties, for example, molecular distribution, molecular orientation, coordination number and energy distribution. Molecular Dynamics methods show not only the structural properties but also the dynamical properties, for example, in terms of velocity autocorrelation function, self diffusion coefficient, intramolecular geometry and molecular motion.

### A non-aqueous solvent system

Studies of the structure of aqueous solutions, particularly of salts in water, have been possible for long time already, both by experimental and theoretical approaches. Therefore, the solvation structure and related properties of numerous systems are already known.

A non-aqueous solvent of widespread interest is ammonia. Several differences between water and ammonia are compared. Water has the higher low-frequency relative permittivity (80 versus 22 at 0° C) and the lower polarizability (1.45 Å<sup>3</sup> versus 2.26 Å<sup>3</sup>). Hydrogen bonding is more important in solvent-solvent interactions in water than ammonia. In addition, the ammonia molecule is more stable against dissociation in the liquid than the water. The equilibrium concentrations of H<sup>+</sup> and OH<sup>-</sup> in water are near 0.1 p.p.m. as compared to H<sup>+</sup> and NH<sup>-</sup> concentrations of 10 p.p.m. in ammonia. On the other hand, the water molecule is more stable in the vapour phase.

Most studies of ammonia solution systems, have focussed on its solution of alkali or alkali earth metals because of their remarkable properties such as high electrical conductivity [27-29]. Alkali or alkali earth metals can be dissolved to large amounts in liquid ammonia, showing the characteristics of liquid metals. When the solution has the concentration range of metal between 1-3 mole percent metal, the solution show the characteristics of solvated electron. Metal is dissolved to metal ions and electrons that would be solvated by ammonia molecules. If the

concentration of the metal has the range between 3-8 mole percent metal, the properties of the solution are typically of a transition state that cannot indicate the exact characteristic. The metal-ammonia solutions containing more than 8 mole percent metal may be described as a binary mixture of solvated metal ions and solvent molecules, permeated by the free electron. These systems have been studied and compared by means of both experimental and theoretical methods. However, the study of most other metals in liquid ammonia is difficult or impossible by contemporary experimental apparatus, which is not capable of supplying results for very dilute solution. Therefore, considering solutions containing little metal is more satisfactorily treated by theoretical than experimental approaches. The dilute solution containing one cation or/and one anion in a solvent is a good model and a useful tool for understanding the effect of salt to the solvent species surrounding it.



สถาบันวิทยบริการ  
จุฬาลงกรณ์มหาวิทยาลัย

## CHAPTER 2

### QUANTUM THEORY

A theoretical model has the concept of an approximate solution of the Schrödinger's equation. It should possess a number of important characteristics. First, it should be both unique and well defined. The procedure for obtaining an energy and a wavefunction should be completely specified in terms of nuclear positions, numbers and spins of the electrons in the molecule. The second desirable feature is continuity, all potential surfaces should be continuous with respect to nuclear displacements. Special procedures must not be used for symmetrical molecules which might lead to results which are discontinuous with those for structures in which the nuclei are slightly displaced to nonsymmetrical positions. A theoretical model should also be unbiased. No appeal to "chemical intuition" should be made in setting up the details of the calculation. For example, while calculations in which electrons are assigned to certain "bond orbitals" might be satisfactory for many molecules, there are not suitable for those nuclear configurations where the locations of "bonds" are apt to be ambiguous. A theory can only be used for the analysis of such concepts as bonding if presuppositions have not been built into its formulation.

Another important requirement for a satisfactory theoretical model is size-consistency, relative errors involved in a calculation should increase more or less in proportion to the size of the molecule. This is particularly important if the model is to be used in a comparative manner, relating properties of molecules of different sizes. While it is generally not possible to satisfy this condition fully, it is often possible to construct models that are size-consistent for infinitely separated systems. This means that application of the model to a system of several molecules at infinite separation will yield properties that equal the sum of the same properties for the individual molecules.

## 2.1 Quantum Mechanics Methods

Quantum mechanics methods are based on the following principles ;

- Nuclei and electrons are distinguished from each other.
- Electron-electron (usually averaged) and electron-nuclear interactions are explicit.
- Interaction are governed by nuclear and electron charges (i.e. potential energy) and electron motions.
- Interaction determine the spatial distribution of nuclei and electrons and their energies.

The search for accurate electronic wavefunctions is usually based on molecular orbital (MO) theory. Molecular quantum mechanical methods are classified as either *ab initio* or semiempirical. Semiempirical methods use a simpler Hamiltonian than the correct molecular Hamiltonian and use parameters that compensate for neglecting some of the time consuming mathematical terms in Schrödinger's equation. The parameters used by semiempirical methods can be derived from experimental measurements or by performing *ab initio* calculations on model systems. In contrast, an *ab initio* calculation uses the full Hamiltonian and does not use experimental data other than the values of the fundamental physical constants. The differences between these methods are described and list, for example,

- ***Ab initio***

- Limited to about fifty atoms and best performed using a high performance computer.
- Can be applied to all kind of molecule, and molecular fragments (e.g. catalytic components of an enzyme).
- Vacuum or implicit solvent environment.
- Can be used to study ground, transition, and excited states.

- *Semiempirical*

- Limited to some hundred atoms.
- Can be applied to mostly only to organic molecules, including small oligomers (peptide, nucleotide, saccharide).
- Can be used to study ground, transition, and excited states (certain methods).

## 2.2 The Schrödinger's equation

Schrödinger's equation addresses the following questions ;

- Where are the electrons and nuclei of a molecule in space?  
==> configuration, conformation, size, shape, etc.
- Under a given set of conditions, what are their energies?  
==> heat of formation, conformational stability, chemical reactivity, spectral properties, etc.

According to quantum mechanics [30], the energy and many properties of a stationary state of a molecule can be obtained by solution of the Schrödinger partial differential equation,

$$H\psi = E\psi \quad \dots\dots\dots(2.1),$$

where  $\psi$  is the normalized total wavefunction of the system and  $H$  is the Hamiltonian, a differential operator representing the total energy.  $E$  is the numerical value of the energy of the state that relative to a state in which the constituent particles (nuclei and electrons) at infinitely separated and at rest.  $\psi$  is the wavefunction. The square of the wavefunction, (or  $|\psi|^2$  if  $\psi$  is complex) is interpreted as a measure of the probability distribution of the particles within the molecule. The total energy is thus obtained, as expectative value of  $H$ ,

$$E = \langle \psi | H | \psi \rangle \quad \dots\dots\dots(2.2).$$

The Hamiltonian  $H$ , like the energy in classical mechanics, is the sum of kinetic and potential parts,

$$\begin{aligned}
 H &= T + V \\
 &= -\frac{1}{2} \sum_A M_A \nabla_A^2 - \frac{1}{2} \sum_i \nabla_i^2 - \sum_A \sum_i \frac{Z_A}{r_{iA}} + \sum_{i < j} \frac{1}{r_{ij}} + \sum_{A < B} \sum \frac{Z_A Z_B}{r_{AB}} \\
 &\dots\dots\dots(2.3).
 \end{aligned}$$

The kinetic energy operator  $T$  is the sum of differential operators and the potential energy operator,  $V$  is the coulomb interaction.

$$T = -\frac{1}{2} \sum_A M_A \nabla_A^2 - \frac{1}{2} \sum_i \nabla_i^2 \dots\dots\dots(2.4),$$

$$V = -\sum_A \sum_i \frac{Z_A}{r_{iA}} + \sum_{i < j} \frac{1}{r_{ij}} + \sum_{A < B} \sum \frac{Z_A Z_B}{r_{AB}} \dots\dots\dots(2.5),$$

where  $\nabla^2 = \frac{\partial^2}{\partial x^2} + \frac{\partial^2}{\partial y^2} + \frac{\partial^2}{\partial z^2}$ ,  $r$ ,  $M$ ,  $Z$ , and  $m$  are distance, mass of nuclei, charge of nuclei, and mass of electrons, respectively.  $A$  and  $B$  are nuclei, and  $i, j$  represent electrons.

### 2.3 Separation of nuclear motion : Born-Oppenheimer approximation

The first approximation of Schrödinger's equation is a non-relativistic model of electrons in the system. The primary major step in simplifying the general molecular problem in quantum mechanics is the separation of the nuclear and electronic motions. Because the nuclear masses are much greater than those of electrons, therefore, nuclei move much more slowly. As a consequence, the electrons in a molecule adjust their distribution to changing nuclear position rapidly. This make it a reasonable approximation to suppose that the electron distribution depends only on the instantaneous position of the nuclei and not on their velocities. This separation is frequently called the adiabatic or Born-Oppenheimer approximation [31], therefore, the kinetic energy of the nuclei can be neglected. The repulsion between the nuclei, thus becomes constant and can be

separately calculated. Consequently, the electronic Hamiltonian, corresponds to motion of electrons only in the field of fix nuclei,

$$H^{elec} = T^{elec} + V \quad \dots\dots\dots(2.6),$$

where  $T^{elec}$  is the electronic kinetic-energy operator,

$$T^{elec} = -\frac{1}{2} \sum_i \nabla_i^2 \quad \dots\dots\dots(2.7).$$

#### 2.4 Molecular orbital theory and linear combination of atomic orbital (LCAO) approximation

Molecular orbital theory is an approach to molecular quantum mechanics which use one-electron functions or orbitals to approximate the full wavefunction. This approximate treatment of electron distribution and motion assigns individual electrons to one-electron function termed spin orbitals. These comprise a product of spatial functions, termed molecular orbital, and a spin function, ( $\alpha$  or  $\beta$ ).

For a wavefunction, this approximation is equivalent to setting up the n-electron probability function as a product of n one-electron functions, i.e.,

$$\psi^{n\text{-elec}} = \chi_1(1)\chi_2(2)\chi_3(3)\dots\dots\dots\chi_n(n) \quad \dots\dots\dots(2.8),$$

or as the product of spatial wavefunctions and spin wavefunctions of the form,

$$\psi^{n\text{-elec}} = \phi_1(1)\alpha(1)\phi_1(2)\beta(2)\dots\dots\phi_{n/2}(n-1)\alpha(n-1)\phi_{n/2}(n)\beta(n) \quad \dots\dots\dots(2.9),$$

This is so called the Hartree product. However, such a wavefunction is not acceptable, as it does not have the property of antisymmetry that correctly follows the Pauli antisymmetry principle. To ensure antisymmetry, the spin orbitals may be arranged in a determinantal wavefunction, which is widely known as Slater determinants,

$$\psi^{\text{n-elec}} = \frac{1}{\sqrt{n!}} \begin{vmatrix} \varphi_1(1)\alpha(1) & \varphi_1(1)\beta(1) & \dots & \varphi_{n/2}(1)\beta(1) \\ \varphi_1(2)\alpha(2) & \varphi_1(2)\beta(2) & \dots & \varphi_{n/2}(2)\beta(2) \\ \dots & \dots & \dots & \dots \\ \varphi_1(n)\alpha(n) & \varphi_1(n)\beta(n) & \dots & \varphi_{n/2}(n)\beta(n) \end{vmatrix} \dots\dots\dots(2.10).$$

The one-electron spin-orbitals are still fairly complicated functions. In practical application of the theory, a further restriction is imposed, requiring that the individual molecular orbitals be expressed as linear combinations of a finite set of  $N$  prescribed one-electron functions known as basis functions ( $\phi$ ). These functions are often called atomic orbitals. A molecular orbital ( $\varphi_i$ ) is then obtained by a linear combination of atomic orbitals (LCAO method),

$$\varphi_i = \sum_{\mu=1}^N c_{\mu i} \phi_{\mu} \dots\dots\dots(2.11),$$

where  $c_{\mu i}$  are the molecular orbital expansion coefficients.

## 2.5 Basis functions

The quality of the molecular orbitals is related to the quality of the basis functions used. Two types of atomic basis functions have received widespread use, Slater-type atomic orbital (STOs) [32] and the Gaussian-type atomic functions (GTOs). The STOs are labelled like hydrogen atomic orbitals and are mostly used for the calculations of small molecules. The type form of STOs is denoted by the expression,

$$\phi^{\text{STO}} = N r^{(n-1)} \exp(-\beta r) Y_{l,m}(\theta, \phi) \dots\dots\dots(2.12),$$

where  $\beta$ ,  $n$ ,  $Y_{l,m}$  are the exponent coefficient, principle quantum number and the angular part of the wavefunction, respectively.

The GTOs are expressed as,

$$\phi^{\text{GTO}} = N r^{(n-1)} \exp(-\beta_1 r^2) Y_{l,m}(\theta, \phi) \dots\dots\dots(2.13).$$

Gaussian-type functions were introduced into molecular orbital computations by Boy [33]. They are less satisfactory than STOs as representations of atomic orbitals, particularly, because they do not have a cusp at the origin. Nevertheless, they have the important advantage that all integrals in the computations can be evaluated explicitly without recourse to numerical integration.

## 2.6 Hartree-Fock theory and Hartree-Fock self-consistent-field methods

Since we have described how a determinantal wavefunction may be constructed from molecular orbitals, and in turn, how the orbitals may be expanded in terms of a set of basis functions. It remains to specify a method for fixing the expansion coefficients. This is the realm of Hartree-Fock theory.

Hartree-Fock theory is based on the variational method in quantum mechanics [34]. This method may be applied to determine optimum orbitals in single-determinant wavefunctions. We select a basis set for orbital expansion, and the coefficients  $c_{\mu i}$  may then be adjusted to minimize the expectation value of the energy  $E$ ,

$$\frac{\partial E}{\partial c_{\mu i}} = 0 \quad (\text{all } \mu, i) \quad \dots\dots\dots(2.14).$$

The resulting value of  $E$  will then be as close to the exact energy as is possible within the limitations imposed by the single-determinant wavefunction and the particular basis set employed. We first deal with these equation for close-shell systems. The variational condition leads to a set of algebraic equation for  $c_{\mu i}$  were derived independently for the close-shell wavefunction (obtained from Slater determinant) by Roothaan [35] and by Hall [36]. The Roothaan-Hall equation are in form,

$$\sum_{\nu=1}^N (F_{\mu\nu} - \epsilon_i S_{\mu\nu}) c_{\nu i} = 0 \quad \mu = 1, 2, 3, \dots, N \quad \dots\dots\dots(2.15),$$

$$\sum_{\mu=1}^N \sum_{\nu=1}^N c_{\mu i}^* S_{\mu\nu} c_{\nu i} = 1 \quad \text{.....(2.16).}$$

where,  $\epsilon_i$  is the one-electron energy of molecular orbital  $\phi_i$ ,  $S_{\mu\nu}$  are the elements of  $N \times N$  matrix, termed the overlap matrix,

$$S_{\mu\nu} = \int \phi_{\mu}^*(1) \phi_{\nu}(1) dx_1 dy_1 dz_1 \quad \text{.....(2.17),}$$

and  $F_{\mu\nu}$  are the elements of another  $N \times N$  matrix, termed the Fock-matrix,

$$F_{\mu\nu} = H_{\mu\nu}^{\text{core}} + \sum_{\lambda=1}^N \sum_{\sigma=1}^N P_{\lambda\sigma} [(\mu\nu|\lambda\sigma) - \frac{1}{2}(\mu\lambda|\nu\sigma)] \quad \text{.....(2.18).}$$

Here,  $H_{\mu\nu}^{\text{core}}$  is a matrix representing the energy of a single electron in a field of "bare" nuclei. Its elements are,

$$H_{\mu\nu}^{\text{core}} = \int \phi_{\mu}^*(1) \hat{H}^{\text{core}}(1) \phi_{\nu}(1) dx_1 dy_1 dz_1 \quad \text{.....(2.19),}$$

$$\hat{H}^{\text{core}}(1) = -\frac{1}{2} \nabla_1^2 - \sum_{i=1}^n \sum_{A=1}^M \frac{Z_A}{r_{iA}} \quad \text{.....(2.20).}$$

Here,  $Z_A$  is the atomic number of atom A and summation is carried out over all atoms. The quantities  $(\mu\nu|\lambda\sigma)$  are two electron repulsion integrals,

$$(\mu\nu|\lambda\sigma) = \iint \phi_{\mu}^*(1) \phi_{\nu}(1) \left( \frac{1}{r_{12}} \right) \phi_{\lambda}^*(2) \phi_{\sigma}(2) dx_1 dy_1 dz_1 dx_2 dy_2 dz_2 \quad \text{.....(2.21).}$$

The elements of the one-electron density matrix,  $P_{\lambda\sigma}$ , have the form

$$P_{\lambda\sigma} = 2 \sum_{i=1}^{\text{occ}} c_{\lambda i}^* c_{\sigma i} \quad \text{.....(2.22).}$$

The Roothaan-Hall equation can be written more compactly as the single matrix equation,

$$\mathbf{FC} = \mathbf{SC}\epsilon \quad \dots\dots\dots(2.23),$$

where  $\mathbf{F}$  is the Fock operator matrix,  $\mathbf{C}$  is the matrix of the linear combination coefficients  $c_{\mu i}$ ,  $\mathbf{S}$  is the overlap matrix and  $\epsilon$  is the diagonal matrix of the one-electron-energy eigenvalues.

A guess is made for the set of molecular orbital expansion coefficients to construct a trial molecular orbitals. The first matrix of the Fock-operator is constructed using the first guess of  $c_{\mu i}$ . From the first approximation of the Fock-matrix, the new matrix of  $\mathbf{C}$  can be obtained by solving the Roothaan-Hall equations. The process is repeated until the linear combination coefficients  $\mathbf{C}$  approach constant values, normally  $10^{-5}$  Hartree, yielded the total electronic energy. This technique is frequently called self-consistent-field (SCF) procedure.

### 2.7 Basis set superposition error (BSSE)

Performing of SCF procedure, the interaction energy,  $\Delta E$  between species A and species B are defined by the formula,

$$\Delta E = E_{AB}(r) - (E_A + E_B) \quad \dots\dots\dots(2.24),$$

where  $E_A$  and  $E_B$  are the total energies of the isolated species A and B, respectively.  $E_{AB}(r)$  is the total energy when the species A and B are brought to the internuclear at distance  $r$ . If finite basis sets are used to calculate molecular and atomic energies, an erroneous result for  $\Delta E$  would be obtained when the above formula is used.

The erroneous result is called the basis set superposition error [37]. The reason is from the fact that at the finite separation of two species sites A and B, the basis set located on B improves the incomplete basis set on A, consequently, lowers the essentially energy of species A, and vice versa. To estimate this effect, one will calculate the energy of species A by keeping all basis sets on the site

species A and B but remove the species B by representing of the ghost orbital on species B at the distance  $r$ . This quantities are denoted as  $E_{A(B)}$  and  $E_{B(A)}$ . Therefore, the corrected interaction energies formula,  $\Delta E_C$  would be

$$\Delta E_C = E_{AB}(r) - [E_{A(B)} + E_{B(A)}] \quad \dots\dots\dots(2.25).$$

## 2.8 Interaction potential in the statistical simulation

Quality of the results obtained from a computer simulation of Monte Carlo or Molecular Dynamics is depends mainly on the quality of the potential functions used. In general, the potential energy of the system containing  $N$  atoms may be derived into terms depending on the coordinates of individual atoms, pair, triplet, etc.,

$$\Delta E = \sum_i E_1(r_i) + \sum_i \sum_{i < j} E_2(r_i, r_j) + \sum_i \sum_{i < j} \sum_{i < j < k} E_3(r_i, r_j, r_k) + \dots \quad \dots\dots\dots(2.26).$$

The first term,  $E_1(r_i)$ , represents the effect of an external field (for example, the container wall). The second term,  $E_2(r_i, r_j)$ , represents the pair potential, is the most important term depends only on the magnitude of the pair separation  $r_{ij} = |r_i - r_j|$ , known as the pairwise additive approximation. The remaining term are three-body term,  $E_3$ , four-body term,  $E_4$ , etc., often meant to as non-additive corrections. In case of condensed systems, three-body term may be become very significant. However, involving the time consuming on a computer, this term was not included. Four-body term or higher are expected to be small in comparison to  $E_2$ ,  $E_3$ .

Fortunately, the pairwise approximation gives a remarkably good description of liquid properties because the average three-body effects can be partially include by defining an "effective" pair potential. By this, the potential energy can be written in the form,

$$\Delta E = \sum_i E_1(r_i) + \sum_i \sum_{i < j} E_2^{\text{eff}}(r_{ij}) \quad \dots\dots\dots(2.27).$$

One of the commonly function used is a simple Lennard-Jone 12-6 potential,

$$V^{LJ}(r) = 4\varepsilon[(\sigma/r)^{12} - (\sigma/r)^6] \quad \dots\dots\dots(2.28),$$

where  $\varepsilon$  and  $\sigma$  are the appropriate parameters. This provides a reasonable description of attractive tail of the form  $1/r^6$ , and repulsive interaction of the form  $1/r^{12}$ .

There are some proposes of investigating general properties of liquids, and for comparison with theory. Three forms, which although unrealistic and very simple and convenient to use in computer simulation, are

a) *The hard-sphere potential*

$$V^{HS}(r) = \begin{cases} \infty & (r < \sigma) \\ 0 & (\sigma \leq r) \end{cases} \quad \dots\dots\dots(2.29),$$

b) *The square-well potential*

$$V^{SW}(r) = \begin{cases} \infty & (r < \sigma_1) \\ -\varepsilon & (\sigma_1 \leq r < \sigma_2) \\ 0 & (\sigma_2 \leq r) \end{cases} \quad \dots\dots\dots(2.30),$$

c) *The soft-sphere potential*

$$V^{SS}(r) = \varepsilon(\sigma/r)^m \quad \dots\dots\dots(2.31).$$

where  $m$  is a parameter, often chosen to be an integer. The soft-sphere potentials contain no attractive part. The differences of these three potentials are shown in Fig. 2.1.

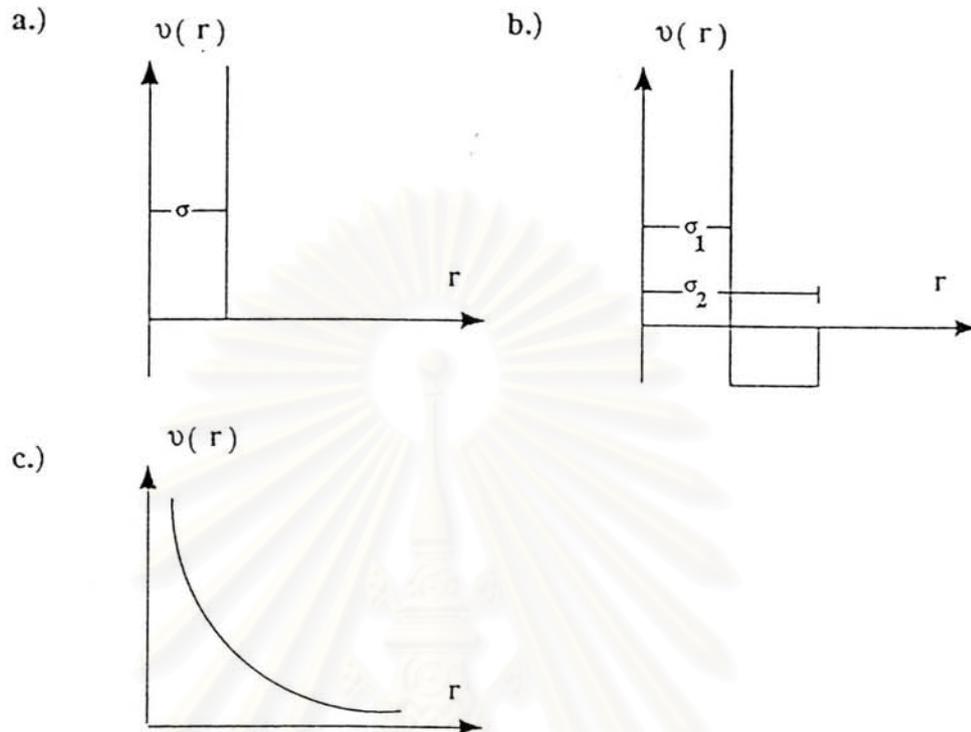


**Figure 2.1** a) The hard-sphere potential ; b) The square-well potential ; c) The soft-sphere potential with repulsion parameter  $K=1$

## 2.9 Specification of the system for this study

The Molecular Dynamics simulation have been performed for three systems, consisting of,

- 1) One  $K^+$  and 215 ammonia molecules at an average temperature of 240 K, without consideration of long-range interaction,
- 2) One  $I^-$  and 215 ammonia molecules at an average temperature of 240 K, without consideration of long-range interaction,
- 3) One  $K^+$ , one  $I^-$  and 214 ammonia molecules at an average temperature of 240 K, taken into account long-range interaction by applying Ewald summation methods for ions.

### 2.9.1 Intermolecular potential energy functions

The intermolecular potential energy functions have the concept of the potential energy surface for molecules, defined by the Born-Oppenheimer approximation for the separation of electronic and nuclear motion. Therefore, the potential energy surface can equal be thought of as the potential for the movement of atoms within a molecule or atoms in collision with one another.

In this study, the Molecular Dynamics simulations of dilute solution system containing one  $K^+$ , one  $I^-$ , and one KI in liquid ammonia will be performed. The intermolecular pair potential functions for  $K^+$ -ammonia,  $I^-$ -ammonia,  $K^+$ - $I^-$ , and ammonia-ammonia are required. The ammonia-ammonia intermolecular pair potential was obtained from literature [26] details given in Table 2.1, using a flexible model for ammonia by Spirko [38],

**Table 2.1** Ammonia-ammonia intermolecular potential, energies are given in units of kcal/mol and distances in Å .

---


$$V_{NN}(r) = 213.74/r + 802340.66/r^{12} - 195.88/r^6$$

$$V_{NH}(r) = -71.24/r + 0.15007\{\exp[-4.6(r-2.4)] - 0.003\exp[-2.3(r-2.4)]\}$$

$$V_{HH}(r) = 23.75/r + 700.32\exp(-3.7r)$$


---

The other intermolecular pair potentials had to be newly developed using *ab initio* calculations, in which the BSSE was corrected by applying the counterpoise method.

### 2.9.2 Construction of the intermolecular pair potential functions

To construct the  $K^+$ -ammonia,  $I^-$ -ammonia and  $K^+$ - $I^-$  intermolecular pair potentials by means of quantum mechanical calculations, the following steps are proposed ; (i) finding of the suitable basis set for the quantum chemical calculations, (ii) selection of dimer geometries, (iii) performance of the SCF calculations, corrected by applying the counterpoise method, (iv) fitting of

computed interaction energies to analytical functions, and (v) testing and improving of the quality of the functions.

#### (i) Finding of the suitable basis sets

We chose several kind of basis sets for the investigated systems. For the  $K^+$ -ammonia and  $I^-$ -ammonia systems, ammonia with bond lengths and bond angle from experiment [39] (N-H distance = 1.0124Å and H-N-H angle = 106.7°) was fixed at the origin of cartesian coordinate system, then, moved the ion ( $K^+$  or  $I^-$ ) at numerous positions (see details in the step (ii)). For  $K^+I^-$  system, we fixed one ion ( $K^+$  or  $I^-$ ) at the origin, then, put the another one at various distances.

Each basis sets used, we calculated total energies of each monomer, ammonia molecule and ion, and stabilization energies for pair of species and evaluated the BSSE by applying the counterpoise procedure. The best basis sets should give the lowest BSSE value at the corresponding distance, therefore, we compare and select the best one for the model systems.

#### (ii) Selection of geometries

For the  $K^+$ -ammonia and  $I^-$ -ammonia system, we fixed the ammonia molecule at the origin of cartesian coordinate system, then, ion ( $K^+$  or  $I^-$ ) was placed at numerous positions within the space around ammonia molecule, where  $0^\circ \leq \theta \leq 180^\circ$  and  $0^\circ \leq \phi \leq 60^\circ$  (according to its  $C_{3v}$  symmetry) as shown in Fig. 2.2.

สถาบันวิทยบริการ  
จุฬาลงกรณ์มหาวิทยาลัย

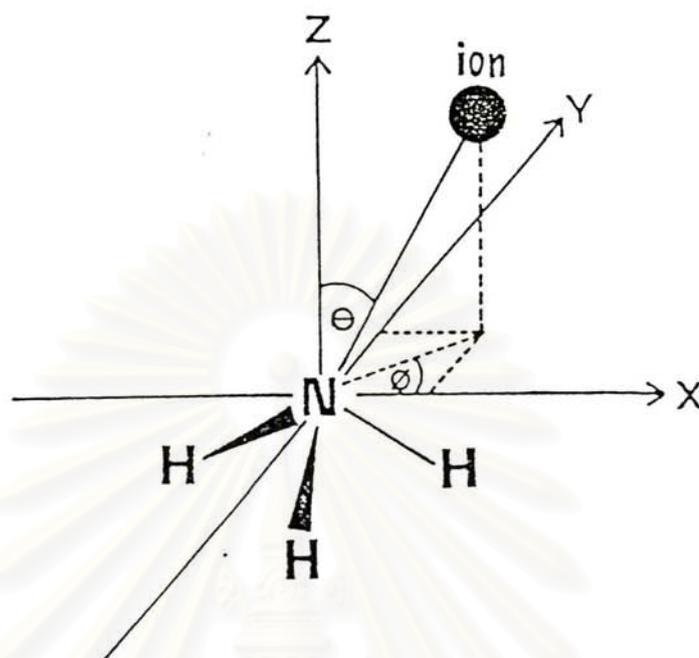


**Figure 2.2** Definition of geometric variables for the configurations of ion-ammonia system

Due to the  $C_{3V}$  symmetry of the ammonia molecule, only one-sixth of the whole space around molecule is required. Varying of the distance,  $r$  is based on the fact that it is necessary to extend the points to a distance where interaction energy approach zero. It should normally be at least equal to the cut-off limit employed in the simulation (see CHAPTER 3), except cases where the interaction energy approach zero before reaching this cut-off limit. The nearest distance also should relate to interparticle repulsion for low-temperature simulations for the reason that molecule would not reach at such configurations. By the way, it is very simply applied for  $K^+ - I^-$  system by fixing one ion ( $K^+$  or  $I^-$ ) at the origin, then, the another ion was moved.

### (iii) Performance of the SCF calculations

This calculations were performed by using Gaussian92 program. The suitable basis sets, selected from the step (i) are the extended basis sets with

double zeta quality, and taken from reference [40] for  $K^+$  and  $I^-$ , and the DZP basis sets from reference [41] for ammonia molecule. Number of energy points to construct the intermolecular potential functions are depended on the complexity of the system. The BSSE is corrected for all data points.

#### (iv) Fitting of computed interaction energies

All points of interaction energies of the pairs obtained from SCF procedure with BSSE correction, were fitted, using a multidimensional non-linear least-square procedure of the form,

$$\Delta E_{FIT} = \sum_{i=1}^n f(r_i) \quad \dots\dots\dots(2.32),$$

where  $f(r_i)$  denotes for potential energy function of  $r_i$ , the distance between the  $i$ -th atom of ammonia and ion ( $K^+$  or  $I^-$ ,  $n=4$ ) or between the  $K^+$  and  $I^-$  ( $n=1$ ). The result was formed in mathematical equation. The typical form and adjustable parameters for each function will be given in CHAPTER 4.

#### (v) Testing and improving of the functions

The procedure suggested by Beveridge [42] was used for testing the functions obtained from SCF calculations. The quality of the functions will be considered in two ways. First, the standard deviation of the interaction energies obtained from SCF method,  $\Delta E_{SCF}$  (equivalent to  $\Delta E$  and  $\Delta E_C$  from equation (2.24) and (2.25), respectively), and from the optimized function,  $\Delta E_{FIT}$ , should give the acceptable value, normally with a range of  $\pm 5\%$  [43]. In addition, the minimum energy point that shown the corresponding between the stabilization energy and distance obtained from  $\Delta E_{SCF}$  and  $\Delta E_{FIT}$  have to be take place at same distance.

#### 2.9.3 Investigation of non-additivity of pair potentials

To investigate how much the three-body effect influences the intermolecular pair potential, SCF calculations only for  $K^+-(NH_3)_n$  complexes with  $n = 2,3,4,6$  and  $8$  were performed. Due to a weak interaction between  $I^-$  and

ammonia, the non-additivity effect will not be considered. The  $K^+$  was fixed at the origin of cartesian coordinate system and ammonia molecules were positioned as  $C_{\infty}$ ,  $D_{3h}$ ,  $T_d$ ,  $O_h$ , and cubic symmetries with respect to nitrogen atoms for  $n = 2, 3, 4, 6$  and  $8$ , respectively. The geometries of their complexes are shown in Fig. 2.3.

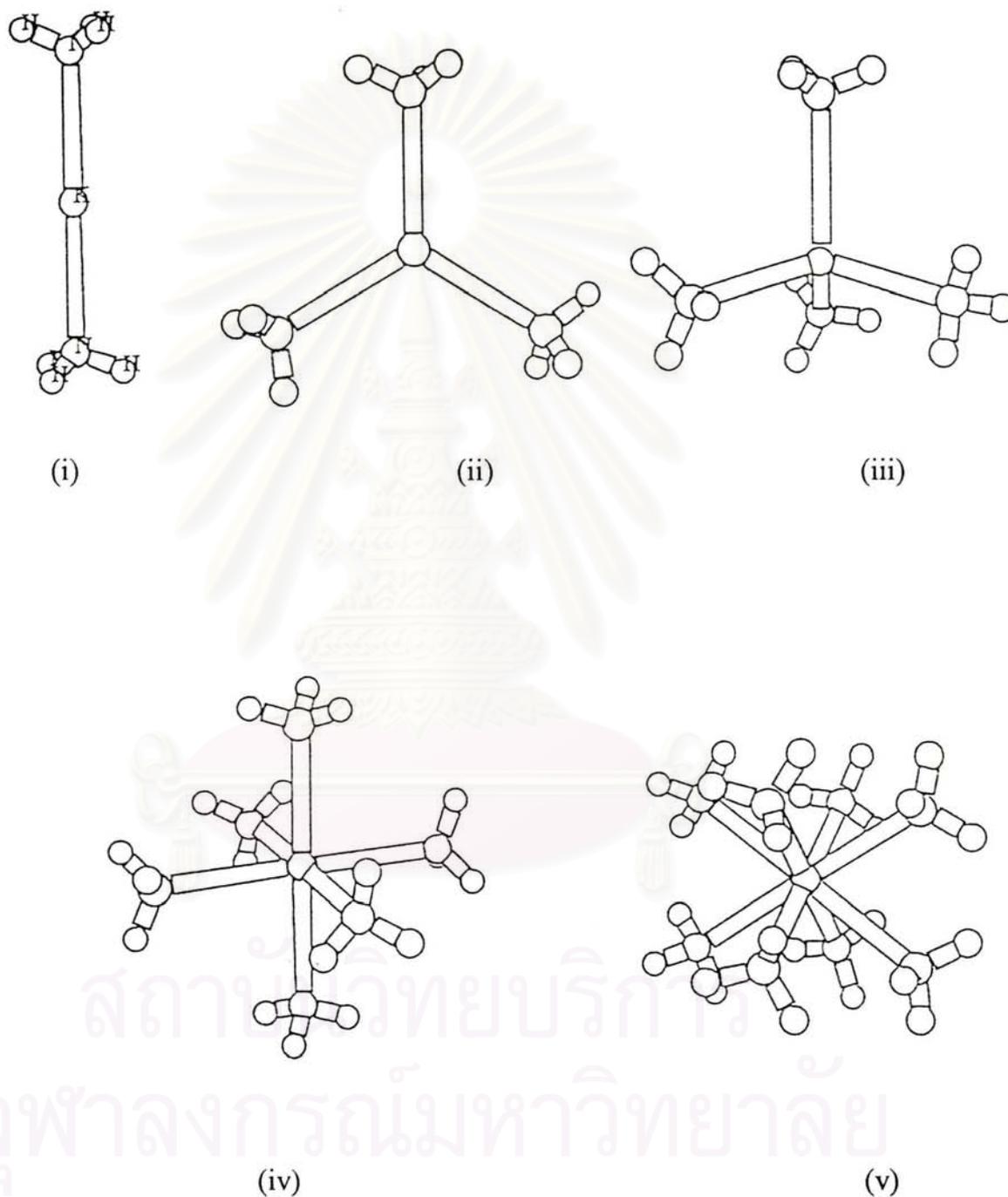


**Figure 2.3** Geometries of their  $K^+-(NH_3)_n$  complexes, (i)  $n=1$ , (ii)  $n=2$ , (iii)  $n=3$ , (iv)  $n=4$ , (v)  $n=6$  and (vi)  $n=8$

The  $n$   $K^+$ -nitrogen distances were optimized simultaneously. The average binding energy per ammonia molecule,  $\Delta E_{av1}$ , is computed as,

$$\Delta E_{av1} = \{E[ML_n] - E[M] - E[L_n]\} / n \quad \dots\dots\dots(2.33),$$

where  $E[ML_n]$ ,  $E[M]$  and  $E[L_n]$  denote the total energies calculated from the SCF method for the complexes in the  $K^+-(NH_3)_n$  configurations, for  $K^+$  and for  $n$  ammonia molecules in the corresponding  $K^+-(NH_3)_n$  configurations, respectively.

The *ab initio* calculations have been performed on a high performance workstation (IBM RISC/6000) at the Austrian-Thai Center for Computer Assisted Chemical Education and Research, Department of Chemistry, Faculty of Science, Chulalongkorn University.

In order to evaluate possible errors of the assumption of pairwise additivity of interaction due to many-body effects, average pair interaction energies between  $K^+$  and ammonia molecules in  $K^+-(NH_3)_n$  configurations were calculated and defined as,

$$\Delta E_{2FCN} = \sum_{i=1}^n \{E[ML_i] - E[M] - E[L_i]\} / n \quad \dots\dots\dots(2.34),$$

where  $E[ML_i]$  and  $E[L_i]$  are the total energies of any of the  $K^+-(NH_3)$  pairs in the  $K^+-(NH_3)_n$  complexes and of the ammonia monomer.

The corresponding percentage of non-additivity,  $\%E_1$  and  $\%E_2$ , together with the ligand-ligand repulsion energies,  $\Delta E_{rpl}$ , have been defined,

$$\%E_1 = 100(1 - \Delta E_{av1}^{n=1} / \Delta E_{av1}^{n \neq 1}) \quad \dots\dots\dots(2.35),$$

$$\%E_2 = 100(1 - \Delta E_{av1} / \Delta E_{2FCN}) \quad \dots\dots\dots(2.36),$$

$$\Delta E_{rpl} = E(L_n) - nE(L) \quad \dots\dots\dots(2.37).$$

## CHAPTER 3

### MOLECULAR DYNAMICS METHOD

Computer simulations provide a direct route from the microscopic details of a system (the masses of the atoms, the interaction between them, molecular geometry etc.) to macroscopic properties of experimental interest (the equation of state, transport coefficients, structural order parameters, and so on).

For a system of  $N$  atoms, let us use the abbreviation  $\Gamma$  for a particular point in phase space which has  $6N$  dimensions, and suppose that we can write the instantaneous value of some properties  $A$  (it might be the potential energy, density, heat capacity etc.) as a function  $A(\Gamma)$ . This function will change because of the involving in time of the system. It is reasonable to assume that the experimentally observable 'microscopic' property  $A_{\text{obs}}$  is really the time average of  $A(\Gamma)$  taken over a long time interval:

$$\begin{aligned} A_{\text{obs}} &= \langle A \rangle_{\text{time}} = \langle A(\Gamma(t)) \rangle_{\text{time}} \\ &= \lim_{\tau_{\text{obs}} \rightarrow \infty} \frac{1}{\tau_{\text{obs}}} \int_0^{\tau_{\text{obs}}} A(\Gamma(t)) dt \end{aligned} \quad \dots\dots\dots(3.1).$$

In fact, we clearly cannot hope to extend the integration for a long infinite time, but might be satisfied to average over a long finite time  $t_{\text{obs}}$ , as the equations of motion are usually solved on a step-by-step basis, i.e. a large finite number  $\tau_{\text{obs}}$  of time steps, of length  $\delta t = t_{\text{obs}}/\tau_{\text{obs}}$  are taken. In this case, we may write the equation (3.1) in the form,

$$A_{\text{obs}} = \langle A \rangle_{\text{time}} = \frac{1}{\tau_{\text{obs}}} \sum_{\tau=1}^{\tau_{\text{obs}}} A(\Gamma(t)) \quad \dots\dots\dots(3.2).$$

In the summation,  $\tau$  simply stands for an index running over the succession of time steps.

The calculation of time average by Molecular Dynamics method is not the approach to thermodynamic properties implicit in conventional mechanics. Because of the complexity of the time evolution of  $\Gamma(t)$  for large number of molecules. Gibbs suggested replacing the time average by the ensemble average. We regard an ensemble as a collection of points  $\Gamma$  in phase space that are distributed according to a probability density  $\rho(\Gamma)$ . This function is determined by the chosen fixed macroscopic parameters (NPT, NVT etc.), so we use the notation  $\rho_{NPT}$ ,  $\rho_{NVT}$ , or, in general,  $\rho_{ens}$ . Each point represents a typical system at any particular instant of time and evolved in time. According to the usual mechanic equations of motion, each system quite independently of the other systems. Consequently, in general, the phase space density  $\rho_{ens}(\Gamma)$  will change with time. To be useful, the prescription should satisfy some sensible conditions ;

a) the probability density  $\rho_{ens}(\Gamma)$  for the ensemble of interest should not change as the system evolves;

b) any 'reasonable' starting distribution  $\rho(\Gamma)$  should tend to this stationary solution as the simulation proceeds;

c) we should be able to argue that ergodicity holds, even though we cannot hope to prove this for realistic systems.

If these conditions are satisfied, then we should be able to generate, from an initial state, a succession of state points which, in the long term, are sampled in accordance with the desired probability density  $\rho_{ens}(\Gamma)$ . In this circumstances, the ensemble average will be equal to a kind of 'time average',

$$A_{obs} = \langle A \rangle_{ens} = \frac{1}{\tau_{obs}} \sum_{\tau=1}^{\tau_{obs}} A(\Gamma(t)) \quad \dots\dots\dots(3.3).$$

Molecular Dynamis is concerned with molecular motion and time evolution. The aim of a Molecular Dynamics simulation is to compute macroscopic properties of a chemical system assuming essentially that the

microscopic interaction potentials between the atoms and molecules constituting the system are known. The following assumptions for classical Molecular Dynamics simulations are required;

- The atoms and molecules constituting the chemical system are represented (modelled) by point masses and rigid bodies subject to the law of classical mechanics.

- The interaction potential between the point masses and/or rigid bodies under the influence of their mutual (and possible additional external) forces and torques are representative of the motions of the atoms and molecules in the chemical system.

- Statistical averages taken over an ensemble of phase space point of the trajectories over a sufficient length of time reproduce the structural and dynamical properties of the system.

For the simulation of homogeneous (or bulk) liquids, a few more assumptions have to be made. These assumptions are stricted to the method where the number of particles and the density are kept constant during the simulation, as the method that is most often used in studies of model system of real liquids. There are two general assumptions;

- Number of particles used in the simulation are finited, usually a few hundred or less than ten thousand, and contained in a regular cell, normally a box with a constant density. This construction called, periodic boundary condition.

- The minimum distance convention is applied. This is a prescription for how the interaction potentials, and thus the interparticle forces, exerted by all particles  $j$  on a given particle  $i$  are to be computed, normally knows as cut-off limit.

### 3.1 Molecular Dynamics procedure

The steps in Molecular Dynamics simulation can be summarized as in Fig. 3.1

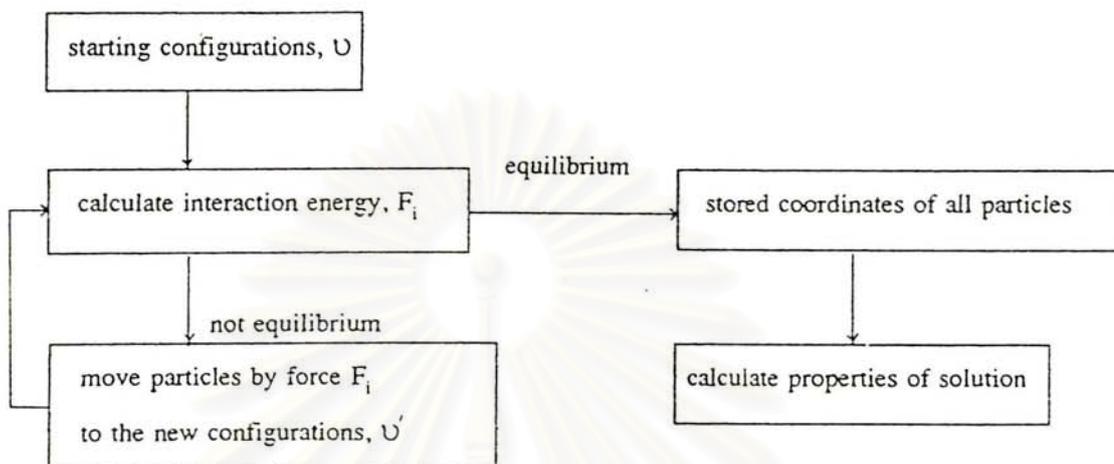


**Figure 3.1** The step in Molecular Dynamics simulation.

The actual simulation starts with reading in the starting configurations, velocities, forces and accelerations. The initial configuration has two simple forms, one uses the random configurations and another one starting from a lattice. In this study, we have made use the configurations of  $\text{Li}^+$ -ammonia system [26]. The predictor-corrector algorithm used in this step required the knowledge of positions, velocities and forces of two successive time steps.

The force  $F_i(j)$  on an atom  $i$  caused by other particles  $j$  can be calculated from the change in energy between its current position and its positions in a small distance away according to Newton's equation of motion. For an isolated system composed of  $N$  particles, the translational motions are given by

$$m_i \frac{d^2 r_i}{dt^2} = F_i(r_1, r_2, \dots, r_N) \dots\dots\dots(3.4),$$

where

$$F_i = -\nabla V_i(r_1, r_2, \dots, r_N) \quad \dots\dots\dots(3.5),$$

$V$  is potential at the instant time  $t$ , assuming, for simplicity, a pairwise additive potential, and the absence of external forces, then

$$V(r_1, r_2, \dots, r_N) = \sum_{ij} V_{ij}(r_{ij}) \quad ; \quad r_{ij} = r_i - r_j \quad \dots\dots\dots(3.6).$$

The force acting on particle  $i$  is given by

$$F_i = \sum_j F_{ij} \quad \dots\dots\dots(3.7),$$

where

$$F_{ij} = -F_{ji} = -\frac{\partial V_{ij}(r_{ij})}{\partial r_{ij}} \quad \dots\dots\dots(3.8).$$

### 3.2 The predictor-corrector algorithm

There are finite difference methods for solution of ordinary differential equation such as the equation of motions. One of the principle finite difference methods namely the predictor-corrector routine will be selected. The general idea is as follows. Given the molecular positions, velocities, and other dynamic information at time  $t$ , we attempt to obtain the positions, velocities etc. at a later time  $t+\delta t$ . The equations are solved on a step-by-step basis, which  $\delta t$  will be significantly smaller than the typical time taken for a molecule to travel its own length. If the classical trajectory is continuous, then an estimate of the positions, velocities etc. at time  $t+\delta t$  may be obtained by Taylor expansion about time  $t$ ,

จุฬาลงกรณ์มหาวิทยาลัย

$$\begin{aligned}
r^P(t+\delta t) &= r(t) + \delta t v(t) + 1/2 \delta t^2 a(t) + 1/6 \delta t^3 b(t) + \dots \\
v^P(t+\delta t) &= v(t) + \delta t a(t) + 1/2 \delta t^2 b(t) + \dots \\
a^P(t+\delta t) &= a(t) + \delta t b(t) + \dots \\
b^P(t+\delta t) &= b(t) + \dots
\end{aligned}
\tag{3.9}$$

The superscript marks these as 'predicted' values, just as  $r$  and  $v$  stand for the complete set of positions and velocities, so  $a$  is short for all the accelerations, and  $b$  denotes all the third time derivatives of  $r$ . If we truncate the expansion, remaining just the terms given explicitly, then we seem to have achieved our aim of (approximately) advancing the values of the stored coordinates and derivatives from one time step to the next. However, an equation above will not generate correct trajectories as time advances, because we have not introduced the equation of motion. We shall be 'correcting' them by calculating the correct accelerations  $a^c(t+\delta t)$  from the new positions  $r^P$ , the forces at time  $t+\delta t$ . The size of the error in the prediction step can be estimated;

$$\Delta a(t+\delta t) = a^c(t+\delta t) - a^P(t+\delta t) \tag{3.10}.$$

Then, this error, and the results of the predictor step, are fed into the corrector step, which read typically,

$$\begin{aligned}
r^c(t+\delta t) &= r^P(t+\delta t) + c_0 \Delta a(t+\delta t) \\
v^c(t+\delta t) &= v^P(t+\delta t) + c_1 \Delta a(t+\delta t) \\
a^c(t+\delta t) &= a^P(t+\delta t) + c_2 \Delta a(t+\delta t) \\
b^c(t+\delta t) &= b^P(t+\delta t) + c_3 \Delta a(t+\delta t)
\end{aligned}
\tag{3.11}$$

The idea is that  $r^c(t+\delta t)$  etc. are now better approximations to the true positions, velocities etc. Gear [44-45] has discussed the 'best' choice for the coefficients  $c_0, c_1, c_2, c_3, \dots$  (i.e. the choice leading to optimum stability and accuracy of the trajectory). The general scheme of a stepwise Molecular Dynamics simulation, based on a predictor-corrector algorithm, may be summarized as follows,

- a) predict the positions, velocities, accelerations etc. at a time  $t+\delta$  using the current values of these quantities;
- b) evaluate the forces, and hence accelerations  $a_i = f_i/m_i$ , from the new positions;
- c) correct the predicted positions, velocities, accelerations etc., using the new accelerations;
- d) calculate any variables of interest, such as the energy, virial, order parameters, ready for the accumulation of time averages, before returning to a) for the next step.

### 3.3 Periodic boundary conditions

The problem of surface effects can be overcome by implementing periodic boundary conditions [46]. The cubic box is replicated throughout space to form an infinite lattice. There are no walls at the central box, and thus no surface particles. The walls of the cubic box are transparent and particles can move freely between the cubic box and its periodic replica. As a replica particle moves into the cubic box whenever a particle moves from the cubic box into a replica cubic box (and thus become a replica particle). Particles in the replica cubic box are often also called 'mirror particles'. A two dimensional version of such a periodic system is shown in Fig. 3.2. The duplicate boxes are labelled A, B, C, etc, in an arbitrary fashion. As particle 1 moves through a boundary, its images, 1A, 1B, etc. (where the subscript specified in which box the image lies) move across their corresponding boundaries.

สถาบันวิทยบริการ  
จุฬาลงกรณ์มหาวิทยาลัย

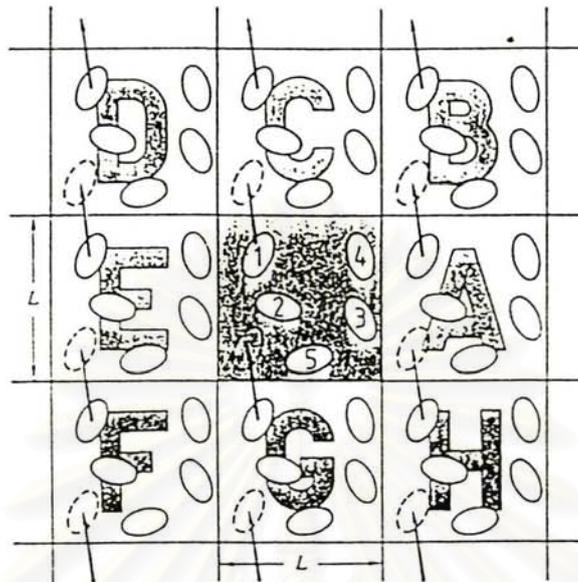


**Figure 3.2** The periodic boundary condition.

The use of periodic boundary conditions inhibits the occurrence of long-wavelength fluctuations. For a cube of side  $L$ , the periodicity will suppress any density waves with a wavelength greater than  $L$ . Thus, it would not be possible to simulate a liquid close to the gas liquid critical point, where the range of critical fluctuations is macroscopic. Furthermore, transitions which are known to be first order often exhibit the characteristics of higher order transitions when model in a small box because of the suppression of fluctuations.

### 3.4 Cut-off limit

To calculate properties of systems subject to periodic boundary conditions, in the case of Molecular Dynamics, the forces acting on all molecules. Consider how we would calculate the force on molecule 1, or those contributions to the potential energy involving molecule 1, assuming pairwise additivity. We have to include interactions between molecule 1 and every other molecule  $i$ ,

therefore, there are  $N-1$  terms in this sum and of course is impossible to calculate in practice. For a short-range potential energy function, we normally a cut-off distance of less than at half of the box length, called cut-off limit. The cut-off distance must be no greater than a half for consistency with the minimum image convention as shown in Fig. 3.3. However, this approximate breaks down for a very long-range Coulombic interaction. This forces are a serious problem for the computer simulator, since their range is greater than half the box length. The results caused by a given ion in which could be charged, since the number of cations and anions need not balance at any instant. There are two methods which can be used to tackle the problem of long-range forces. The lattice methods, such as the Ewald sum, include the interaction of an ion or molecule with all its periodic images. The another method called the reaction field methods, assume that the interaction from molecules beyond a cut-off distance can be handled in an average way, using macroscopic electrostatics. Both methods use well-known idea from the theory of electrostatics. In particular, a charge distribution within a spherical cavity polarizes the surrounding medium. This polarization, which depends upon the relative permittivity of the medium, has an effect on the charge distribution in the cavity.

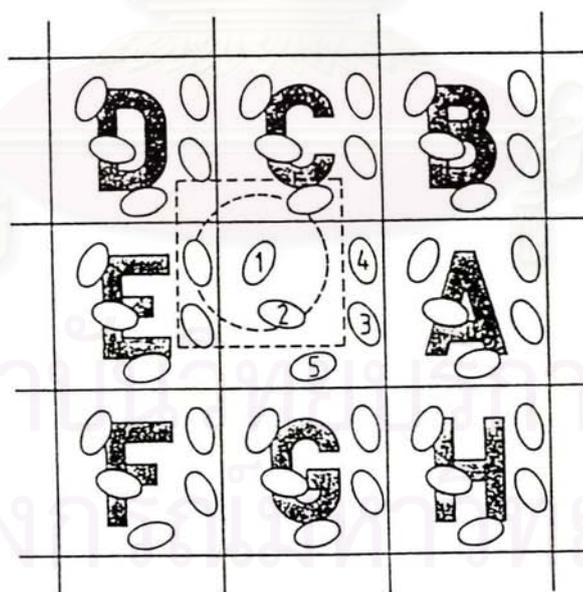


**Figure 3.3** The minimum image convention in a two-dimensional system

### 3.5 Long-range interaction

A long-range interaction is often defined as one in which the spatial interaction falls off no faster than  $r^{-d}$  where  $d$  is the dimensionality of the system. The charge-charge, charge-dipole, dipole-dipole and charge-quadrupole interactions are the examples of such interaction. The two methods to handle long-range interaction will be shown as following,

#### 3.5.1 The Ewald sum

This procedure is a technique for efficiently summing the interaction between an ion and all its periodic images [47]. In Fig. 3.2, ion 1 interacts with ion 2, 2A, 2B, and all the other images of 2. The potential energy can be written as

$$V^{ZZ} = \frac{1}{2} \sum_n \left( \sum_{i=1}^N \sum_{j=1}^N Z_i Z_j \left| \mathbf{r}_{ij} + \mathbf{n} \right|^{-1} \right) \quad \dots\dots\dots(3.12),$$

where  $Z_i, Z_j$  are the charges. The sum over  $n$  is the sum over all simple cubic lattice points. The prime indicates that we omit  $i = j$  for  $n = 0$ . For long-range potentials, this sum is conditionally convergent, i.e. the result depends on the order in which we add up the terms. As we add further terms to the sum, we are building up our infinite system in roughly spherical layer. When we adopt this approach, we must specify the nature of the medium surrounding the sphere, in particular its relative permittivity (dielectric constant).

In the Ewald method, each point charge is surrounded by a charge distribution of equal magnitude and opposite sign, which spreads out radially from the charge. The Fourier transforms of the cancelling distributions (one for each original charge) are added, and the total transformed back into real space. This is an important correction.

### 3.5.2 The reaction field method

The reaction field method is a field on a dipole introduced without the assumption of periodicity. The basic in the simulation consists of two parts; the first is a short-range contribution from molecules situated within a cut-off sphere or 'cavity'  $R$ , and the second arises from molecules outside  $R$  which are considered to form a dielectric continuum ( $\epsilon_s$ ) producing a reaction field within the cavity. Whenever a molecule enters or leaves the cavity surrounding another, a discontinuous jump occurs in the energy due to direct interactions within the cavity and in the reaction field contribution. These change do not exactly cancel, and the result is poor energy conservation. In addition, spurious features appear in the radial distribution function at  $r = r_c$ . These problems may be avoided by tapering the interactions at the cavity surface.

### 3.6 Shifted and shifted-force potentials

In Molecular Dynamics simulation, the truncation of the intermolecular potential at a cut-off introduced some difficulties in defining a consistent potential and force. The function  $V(r_{ij})$  use in a simulation contains a discontinuity at  $r_{ij} = r_c$ ; whenever a pair of molecules crosses this boundary, the total energy will not be conserved. We can avoid this by shifting the potential function by an amount  $V_c = V(r_c)$ , i.e. using instead the function,

$$V^S(r_{ij}) = \begin{cases} V(r_{ij}) - V_c & r_{ij} \leq r_c \\ 0 & r_{ij} > r_c \end{cases} \quad \dots\dots\dots(3.13),$$

where  $V^S(r_{ij})$  and  $V_c$  are shifted potential and potential at cut-off limit, respectively. However, its contribution to the total energy varies from time step to time step, since the total number of pairs within cut-off range varies. The force between a pair of molecules is still discontinuous at  $r_{ij} = r_c$ . Whereas the total

energy must be conserved, the shifted-force potential method is introduced : the potentials have been changed to the form,

$$V^{\text{SF}}(r_{ij}) = \begin{cases} V(r_{ij}) - V_c - \left(\frac{dV(r_{ij})}{dr_{ij}}\right)_{r_{ij}=r_c} (r_{ij} - r_c) & r_{ij} \leq r_c \\ 0 & r_{ij} > r_c \end{cases} \dots\dots\dots(3.14),$$

where  $V^{\text{SF}}$  is shifted-force potential and  $\frac{dV(r_{ij})}{dr_{ij}}$  is a small linear term added to the potential, and its derivative is zero at the cut-off distance.

### 3.7 Neighbouring algorithm

The potential and the force are set zero for distances longer than a specified cut-off limit. In the inner loop of the programs, we consider a molecule  $i$  and loop over all molecules  $j$  to calculate the minimum image separations. If molecules are separated by distances greater than the potential cut-off, the program skips to the end of the inner loop, avoiding expensive calculations, and considers the next neighbour. In this method, the time to examine all pair separations is proportional to  $N^2$ . Verlet [48-49] suggested a technique for improving the speed of a program by maintaining a list of the neighbours of a particular molecule, which is updated at intervals. Between updates of the neighbour list, the program does not check through all the  $j$  molecules, but just those appearing on the list. The number of pair separations explicitly considered is reduced and saved time in looping through  $j$ .

สถาบันวิทยบริการ  
จุฬาลงกรณ์มหาวิทยาลัย

### 3.8 Calculation of macroscopic properties

#### 3.8.1 Structural properties

The structural quantities is characterized by a set of distribution functions for the atomic positions. One of the most simplest important of which is the pair radial distribution function (RDF), or simply  $g_{\alpha\beta}(r)$ . This function gives the probability of finding particle  $\beta$  at the distance  $r$  away from particle  $\alpha$ . The function is usually normalized to 1 at large  $r$  and can be calculated from,

$$g_{\alpha\beta}(r) = \frac{V}{N} \left\langle \frac{N(\Delta r)}{4\pi r^2 \delta r} \right\rangle \quad \text{.....(3.15),}$$

where  $V$ ,  $N$  represent the volume and the total number of the atoms.  $N(\Delta r)$  is the number of pairs which are  $r_1$  to  $r_1 + \delta r$  apart.

The another one quantity that usually displays relatively with the pair radial distribution is the average coordination number, or simply  $n_{\alpha\beta}(r)$ . The results are shown the number of particle  $\beta$  distributed surrounding the particle  $\alpha$  at distance  $r$ . It is normally calculated from  $g_{\alpha\beta}(r)$  in the form,

$$n_{\alpha\beta}(r) = \frac{N}{V} \int g_{\alpha\beta}(r) 4\pi r^2 dr \quad \text{.....(3.16),}$$

where  $\frac{N}{V}$  is number density of the number of pairs in the simulation volume.

#### 3.8.2 Dynamical properties

The resulting quantity is a function of the time difference  $t$ : it is a 'time correlation function'. For identical phase functions,  $C_{AA}(t)$  is called an autocorrelation function and its time integral (from  $t = 0$  to  $t = \infty$ ) is a correlation time  $t_A$ . This functions are of great interest in Molecular Dynamics simulation because,

- a) they give a clear picture of the dynamics in a fluid;
- b) their time integrals  $t_A$  may often be related directly to macroscopic transport coefficients;
- c) their Fourier transforms  $C_{AA}(\omega)$  may often be related to experimental spectra.

We use  $\tau$  to label successive steps, i.e.  $t = \tau\delta t$ . The definition of time-average, in a discretized form, allows us to write the non-normalized autocorrelation function of  $A(t)$  as,

$$\begin{aligned} C_{AA}(\tau) &= \langle A(\tau) A(0) \rangle \\ &= \frac{1}{\tau_{\max}} \sum_{\tau_0=1}^{\tau_{\max}} A(\tau_0) A(\tau_0 + \tau) \end{aligned} \quad \dots\dots\dots(3.17),$$

where  $A(\tau)$  and  $A(0)$  are dynamical variables of the system, such as position, velocity, density etc. Here, we average over  $\tau_{\max}$  time origins the product of  $A$  at time  $\tau_0\delta t$  and at a time  $\tau\delta t$  later. The velocity autocorrelation function,

$$C_{VV}(t) = \langle V_i(0)V_i(t) \rangle \quad \dots\dots\dots(3.18),$$

where  $V_i(t)$  is the center-of-mass velocity of a single molecule, is often of great interest because its time integral relates to the self-diffusion coefficient, whereas its temporal Fourier transform is a measure of the 'density of states'. The self-diffusion coefficient,  $D$  obtained from the velocity autocorrelation function can be written in the form,

$$D = \frac{1}{3} \int C_{VV}(t) dt \quad \dots\dots\dots(3.19).$$

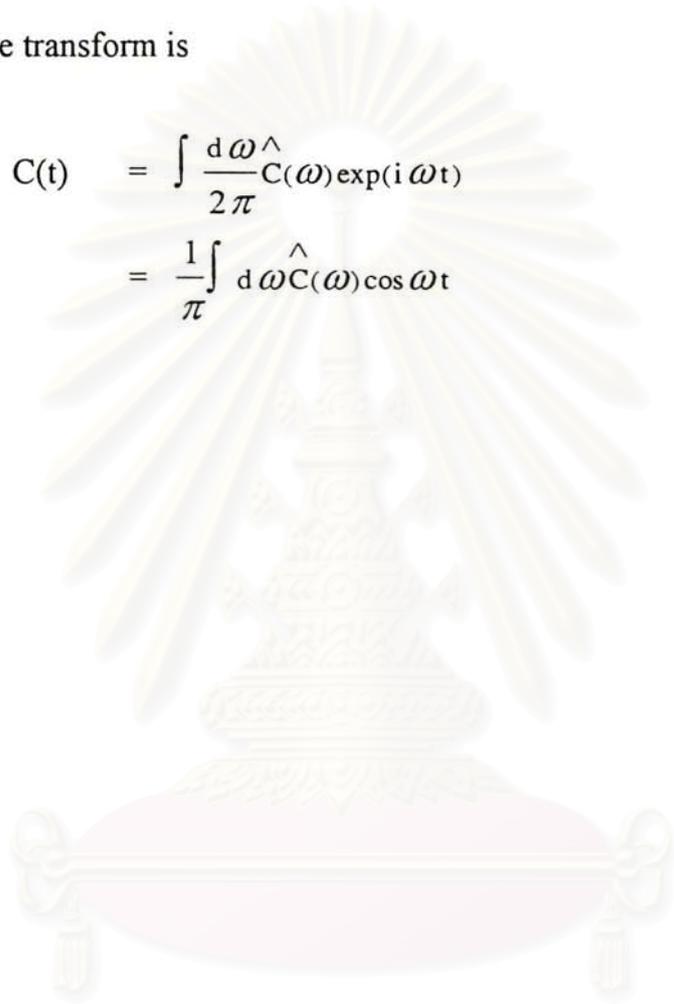
The results of computer simulations must often be transformed between time and frequency domains or between normal space and reciprocal space. To be

compared with experiment, a time correlation function  $C(t)$  is usually transformed to produce a spectrum  $\hat{C}(\omega)$ ,

$$\hat{C}(\omega) = \int dt C(t) \exp(-i \omega t) \quad \dots\dots\dots(3.20),$$

and the converse transform is

$$\begin{aligned} C(t) &= \int \frac{d\omega}{2\pi} \hat{C}(\omega) \exp(i \omega t) \\ &= \frac{1}{\pi} \int d\omega \hat{C}(\omega) \cos \omega t \quad \dots\dots\dots(3.21). \end{aligned}$$



สถาบันวิทยบริการ  
จุฬาลงกรณ์มหาวิทยาลัย

## CHAPTER 4

### RESULTS

#### Part A : Intermolecular potentials

##### 4.1 Suitable basis sets for the atoms of the systems

Since the DZP (Double Zeta including Polarization function) have been successfully used for developing of the potential functions for the study of liquid ammonia [26],  $\text{Li}^+$ -ammonia [26] and  $\text{Na}^+$ -ammonia [58] systems, it will be, again, applied for the  $\text{K}^+$ -ammonia and the  $\text{I}^-$ -ammonia systems without testing. For  $\text{K}^+$  and  $\text{I}^-$ , extended basis sets, taken from reference [40], have been examined. The calculated stabilization energies with ( $\Delta E_{\text{BSSE}}$ ) and without BSSE ( $\Delta E_{\text{SCF}}$ ) at the correspondingly optimal distances,  $r_{\text{BSSE}}$  and  $r_{\text{SCF}}$ , are summarized in Table 4.1 - Table 4.3.

สถาบันวิทยบริการ  
จุฬาลงกรณ์มหาวิทยาลัย

**Table 4.1** Testing of basis sets for the  $K^+$ -ammonia. (Interaction energies and r in kcal/mol and Å, respectively.)

Basis sets	Basis functions	$\Delta E_{SCF}$	$\Delta E_{BSSE}$	BSSE ( $\Delta E_{BSSE} - \Delta E_{SCF}$ )	$r_{SCF}$	$r_{BSSE}$	$r_{shift}$ ( $r_{BSSE} - r_{SCF}$ )	CPU time (sec)
STO-3G	21/63	-41.48	-22.34	19.14	2.50	2.70	0.2	6
DZV	26/67	-40.25	-20.49	19.76	2.60	3.00	0.4	12
DZP *	60/121	-27.12	-18.51	8.61	2.60	2.90	0.3	190
14s/9p/5d *	96/116	-20.94	-19.26	1.68	2.80	2.90	0.1	380

**Table 4.2** Testing of basis sets for the  $I^-$ -ammonia. (detail see Table 4.1.)

Basis sets	Basis functions	$\Delta E_{SCF}$	$\Delta E_{BSSE}$	BSSE	$r_{SCF}$	$r_{BSSE}$	$r_{shift}$	CPU time (sec)
16s/12p/8d *	122/150	-4.69	-4.37	0.32	4.20	4.20	0.0	490

**Table 4.3** Testing of basis sets for the  $K^+ - I^-$  system. (detail see table 4.1.)

Basis sets	Basis functions	$\Delta E_{SCF}$	$\Delta E_{BSSE}$	BSSE	$r_{SCF}$	$r_{BSSE}$	$r_{shift}$	CPU time (sec)
14s/9p/5d ( $K^+$ )	158/166	-98.99	-97.21	1.78	3.20	3.20	0.0	1200
16s/12p/8d ( $I^-$ )	122/150							

\* DZP basis sets for ammonia molecule taken from gaussian92 program

## 4.2 Intermolecular pair potentials

### 4.2.1 $K^+$ -ammonia pair potential

The 673 SCF energies points for the  $K^+$ -ammonia dimers, obtained from the extended 14s/9p/5d basis sets for  $K^+$  and DZP basis set for ammonia molecule (see Table 4.1 to Table 4.3) including BSSE, were fitted to the analytical form,

$$\Delta E_{FIT} = \sum_{i=1}^4 \frac{A_i}{r_i^4} + B_i \exp(-C_i r_i) + 332.15 \frac{q_i q_{K^+}}{r_i} \dots\dots\dots(4.1).$$

where  $r_i$  is the distance between the  $i$ -th atom of ammonia and  $K^+$ ,  $q_i$  and  $q_{K^+}$  are the net charges of the  $i$ -th atom of ammonia and of  $K^+$ , respectively. The final optimized parameters,  $A_i$ ,  $B_i$  and  $C_i$  are given in Table 4.4. The  $\Delta E_{BSSE}$  and the  $\Delta E_{FIT}$  are compared in Fig. 4.1 and Fig. 4.2.

**Table 4.4** Final optimized parameters for the interaction of N and H atoms of ammonia with  $K^+$ . (interaction energies and  $r$  in kcal/mol and Å, respectively).

Atom	q	A	B	C
N	-0.8022	-1.83758E+03	3.55782E+04	2.72920E+00
H	0.2674	1.41815E+02	-1.45075E+01	0.64894E+00

Characteristics of the fit :

Minimum energy included in the fit	= -19.26 kcal/mol
Weighting level	= -20.00 kcal/mol
Maximum energy included in the fit	= 30.00 kcal/mol
Standard deviation	= 0.72
% error	= 3.71

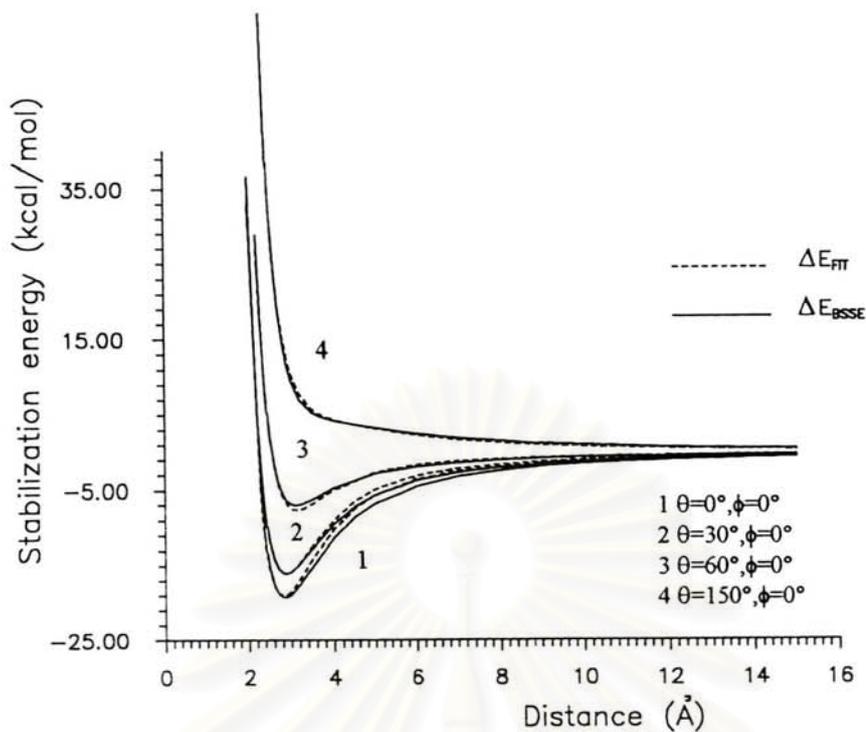


**Figure 4.1** Comparison of the stabilization energies obtained from the SCF calculations with BSSE,  $\Delta E_{\text{BSSE}}$  and from the potential function,  $\Delta E_{\text{FIT}}$  using the final values of the fitting parameters as given in Table 4.4 (see Fig. 2.1 for  $\theta$  and  $\phi$ ).

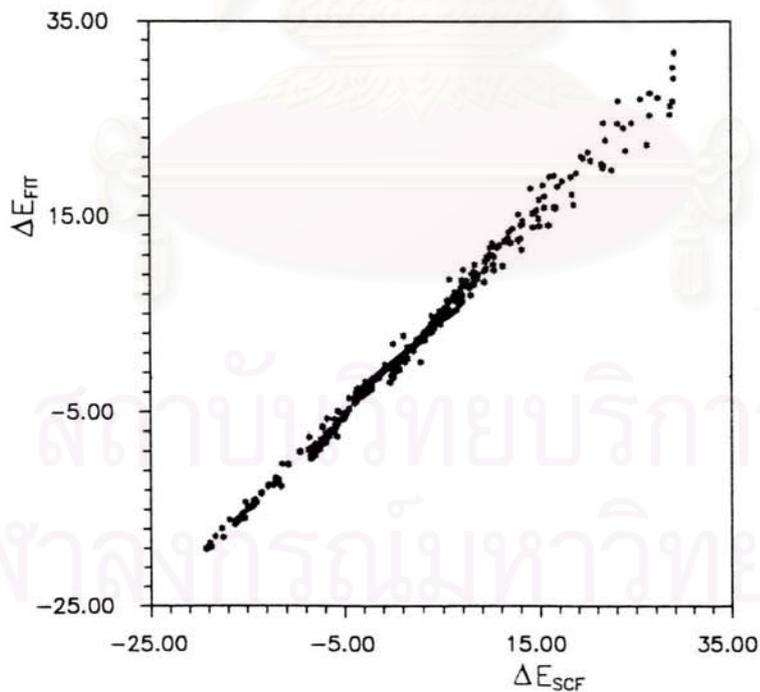


**Figure 4.2** Comparison of the  $\Delta E_{\text{BSSE}}$  and  $\Delta E_{\text{FIT}}$ .

#### 4.2.2 $\Gamma$ -ammonia pair potential

The same procedure, as for the  $K^+$ -ammonia system, is applied to develop the  $\Gamma$ -ammonia pair potential. The analytical function of the form,

$$\Delta E_{FIT} = \sum_{i=1}^4 \frac{A_i}{r_i^5} + B_i \exp(-C_i r_i) + 332.15 \frac{q_i q_{\Gamma^-}}{r_i} \dots\dots\dots(4.2),$$

is considered as the best one to represent the 601 points of  $\Gamma$ -ammonia interaction energies. The parameters are defined as equation (4.1). The final optimized parameters and characteristics of the fit are given in Table 4.5. The  $\Delta E_{BSSSE}$  versus the  $\Delta E_{FIT}$  are plotted in Fig. 4.3 and Fig. 4.4.

**Table 4.5** Final optimized parameters for the interaction of N and H atoms of ammonia with  $\Gamma^-$ . (interaction energies and r in kcal/mol and Å, respectively).

Atom	q	A	B	C
N	-0.8022	-1.50393E+04	5.40927E+04	2.28178E+00
H	0.2674	6.03316E+02	7.62496E+01	0.85205E+00

Characteristics of the fit :

Minimum energy included in the fit	= -4.51 kcal/mol
Weighting level	= -5.00 kcal/mol
Maximum energy included in the fit	= 30.00 kcal/mol
Standard deviation	= 0.83
% error	= 18.30

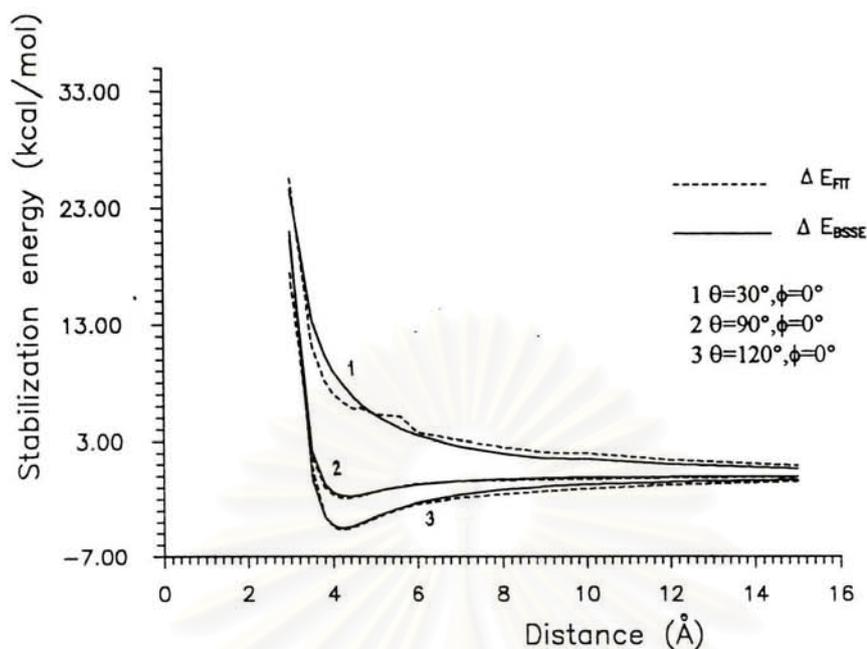


**Figure 4.3** Comparison of the stabilization energies obtained from the SCF calculations with BSSE,  $\Delta E_{\text{BSSE}}$  and from the potential function,  $\Delta E_{\text{FIT}}$  using the final values of the fitting parameters as given in Table 4.54 (see Fig. 2.1 for  $\theta$  and  $\phi$ ).

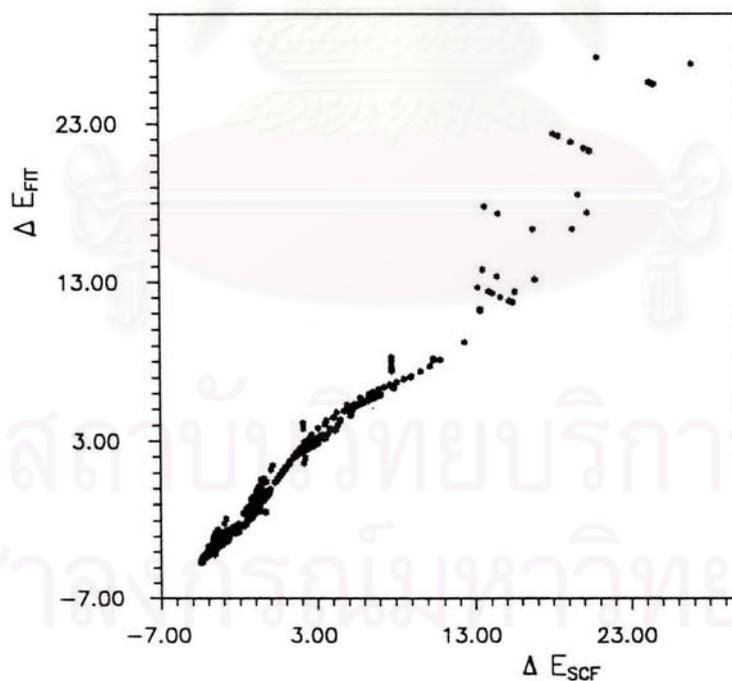


**Figure 4.4** Comparison of the  $\Delta E_{\text{BSSE}}$  and  $\Delta E_{\text{FIT}}$ .

### 4.2.3 $K^+ - I^-$ pair potential

The optimal form of the function for the 54 points of  $K^+ - I^-$  interaction energies are

$$\Delta E_{FIT} = \frac{A}{r^4} + \frac{B}{r^6} + C \exp(-Dr) + 322.15 \frac{q_{K^+} q_{I^-}}{r} \dots \dots \dots (4.3).$$

The final fitted parameters are given in Table 4.6. The plots are shown in Fig. 4.5 and Fig. 4.6.

**Table 4.6** Final optimized parameters for the interaction of  $I^-$  with  $K^+$ . (interaction energies and  $r$  in kcal/mol and Å, respectively).

Atom	q	A	B	C	D
$I^-$	-1.00	-1.50098E+03	3.30362E+03	4.41245E+04	2.44564E+00

Characteristics of the fit :

Minimum energy included in the fit	= -97.36 kcal/mol
Weighting level	= -100.00 kcal/mol
Maximum energy included in the fit	= 20.00 kcal/mol
Standard deviation	= 0.10
% error	= 0.11

สถาบันวิทยบริการ  
จุฬาลงกรณ์มหาวิทยาลัย

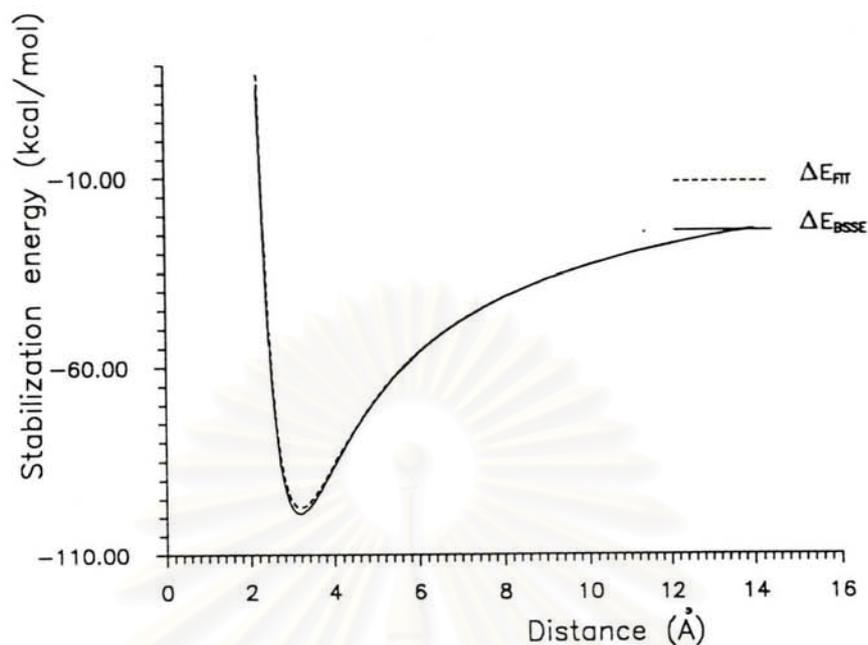


**Figure 4.5** Comparison of the stabilization energies obtained from the SCF calculations with BSSE,  $\Delta E_{\text{BSSE}}$  and from the potential function,  $\Delta E_{\text{FIT}}$  using the final values of the fitting parameters as given in Table 4.54 (see Fig. 2.1 for  $\theta$  and  $\phi$ ).

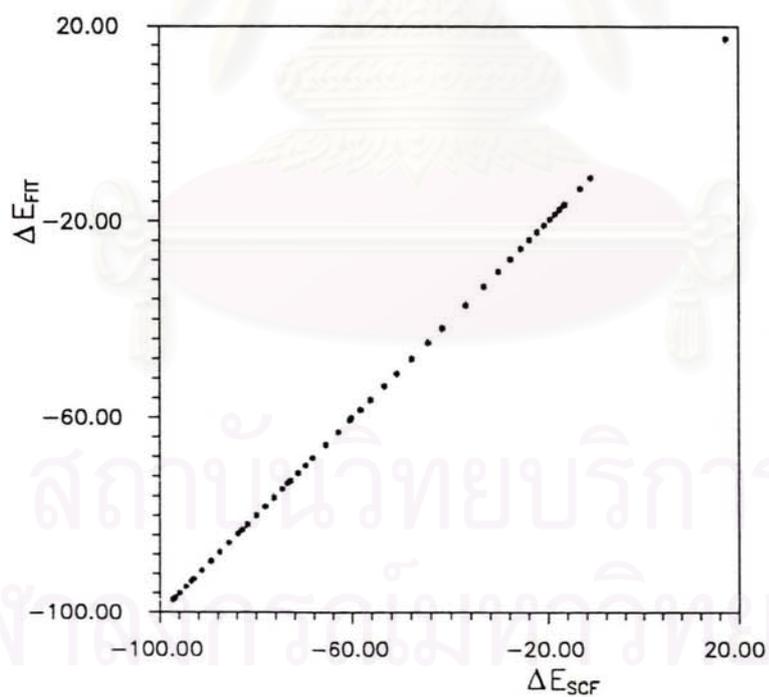


**Figure 4.6** Comparison of the  $\Delta E_{\text{BSSE}}$  and  $\Delta E_{\text{FIT}}$ .

### 4.3 SCF calculations on the non-additivity

The  $\Delta E_{av1}$ ,  $\Delta E_{2FCN}$ ,  $\%E_1$ ,  $\%E_2$  and  $\Delta E_{rpl}$ , as defined in equation (2.33) to equation (2.37), are summarized in Table 4.7.

**Table 4.7** The  $K^+$ -ammonia interactions complexes, as defined in equation (2.33) - (2.37), and optimized nitrogen distances ( $r_{M-N}$ ) for the different  $K^+-(NH_3)_n$  (interaction energies and  $r$  in kcal/mol and Å, respectively).

n	$r_{M-N}$	$\Delta E_{av1}$	$\%E_1$	$\Delta E_{2FCN}$	$\%E_2$	$\Delta E_{rpl}$
1	2.85	-19.31	0	-19.31	0	0.0
2	2.89	-18.44	5	-19.22	4	0.91
3	2.90	-18.17	6	-19.32	6	3.69
4	2.92	-17.57	10	-19.27	9	9.35
6	2.94	-16.80	15	-19.31	13	23.81
8	2.98	-15.20	27	-19.09	20	76.25

สถาบันวิทยบริการ  
จุฬาลงกรณ์มหาวิทยาลัย

## Part B : Molecular Dynamics simulation

### 4.4 Structural properties

#### 4.4.1 $K^+$ -ammonia system

With the time step of  $1.25 \times 10^{-16}$  s, the  $K^+$ -ammonia system reaches equilibrium after 200,000 moved (250 ps). The atom-atom RDFs and the running integration numbers, as defined in equation (3.15) and equation (3.16), respectively, have been calculated from 60,000 configurations of the system after equilibration and plotted in Fig. 4.7 and Fig. 4.8. Their characteristics are summarized in Table 4.8.

**Table 4.8** Characteristic values of the radial distribution functions,  $g_{\alpha\beta}(r)$  for the  $K^+$ -ammonia solution ;  $r_{M1}$ ,  $r_{M2}$  and  $r_{m1}$  are the distance in Å, where  $g_{\alpha\beta}(r)$  has first and second maximum and first minimum, respectively.  $n_{\alpha\beta}(r_{m1})$  is running integration numbers, integrated up to  $r_{m1}$ .

$\alpha\beta$	$r_{M1}$	$g_{\alpha\beta}(r_{M1})$	$r_{m1}$	$g_{\alpha\beta}(r_{m1})$	$n_{\alpha\beta}(r_{m1})$	$r_{M2}$
N-N	3.41	2.01	5.01	0.77	12.2	6.46
N-H	3.74	1.34	5.23	0.84	40.4	6.58
H-H	3.85	1.26	5.41	0.93	45.3	6.44
$K^+$ -N	2.88	8.22	4.04	0.0	8.7	5.85
$K^+$ -H	3.38	3.31	4.35	0.46	27.5	5.86

สถาบันวิทยบริการ  
จุฬาลงกรณ์มหาวิทยาลัย

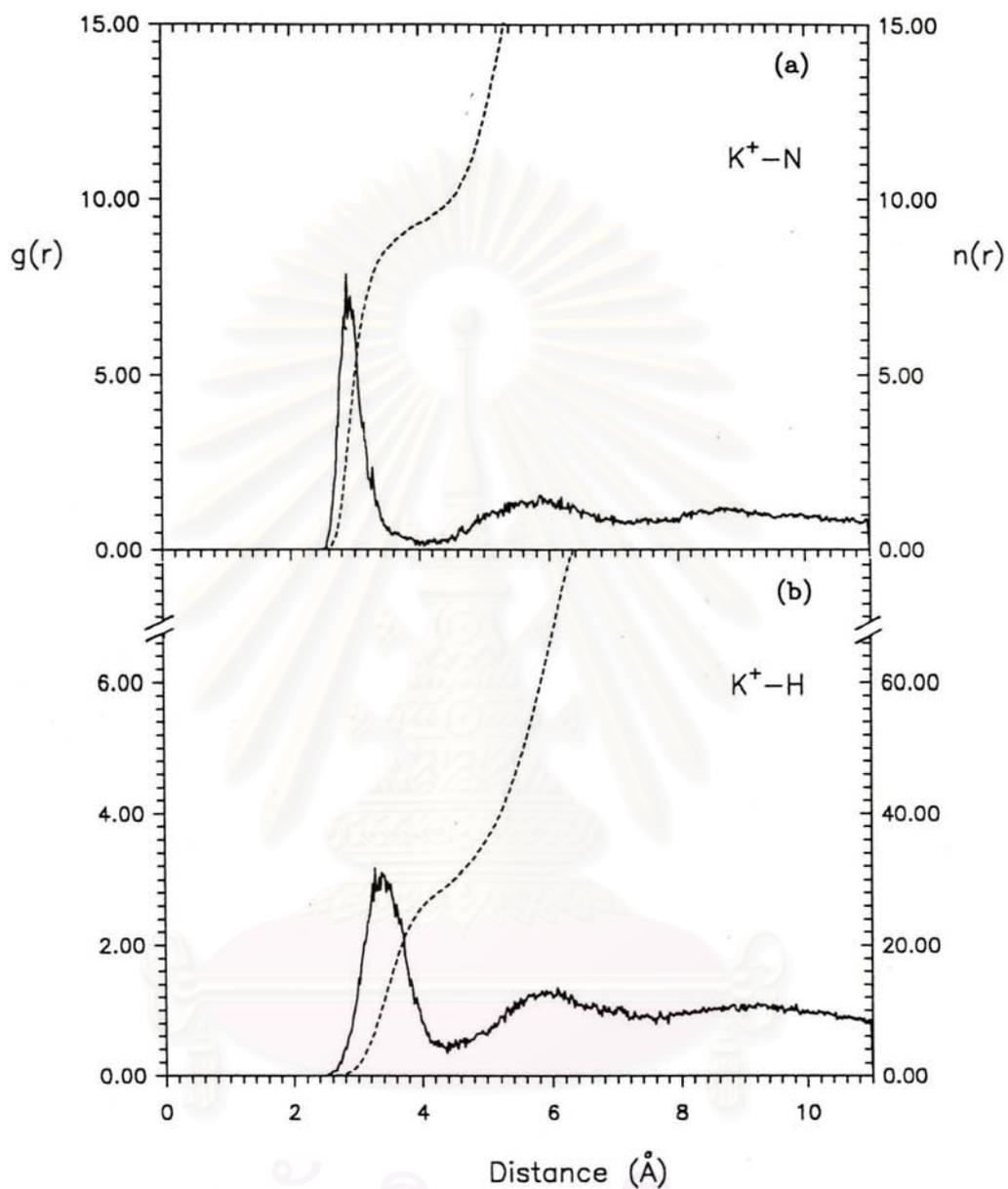


**Figure 4.7** Atom-atom radial distribution functions and running integration numbers from the Molecular Dynamics simulation of one  $K^+$  in liquid ammonia at 240 K. (a)  $K^+$ -N ; (b)  $K^+$ -H.

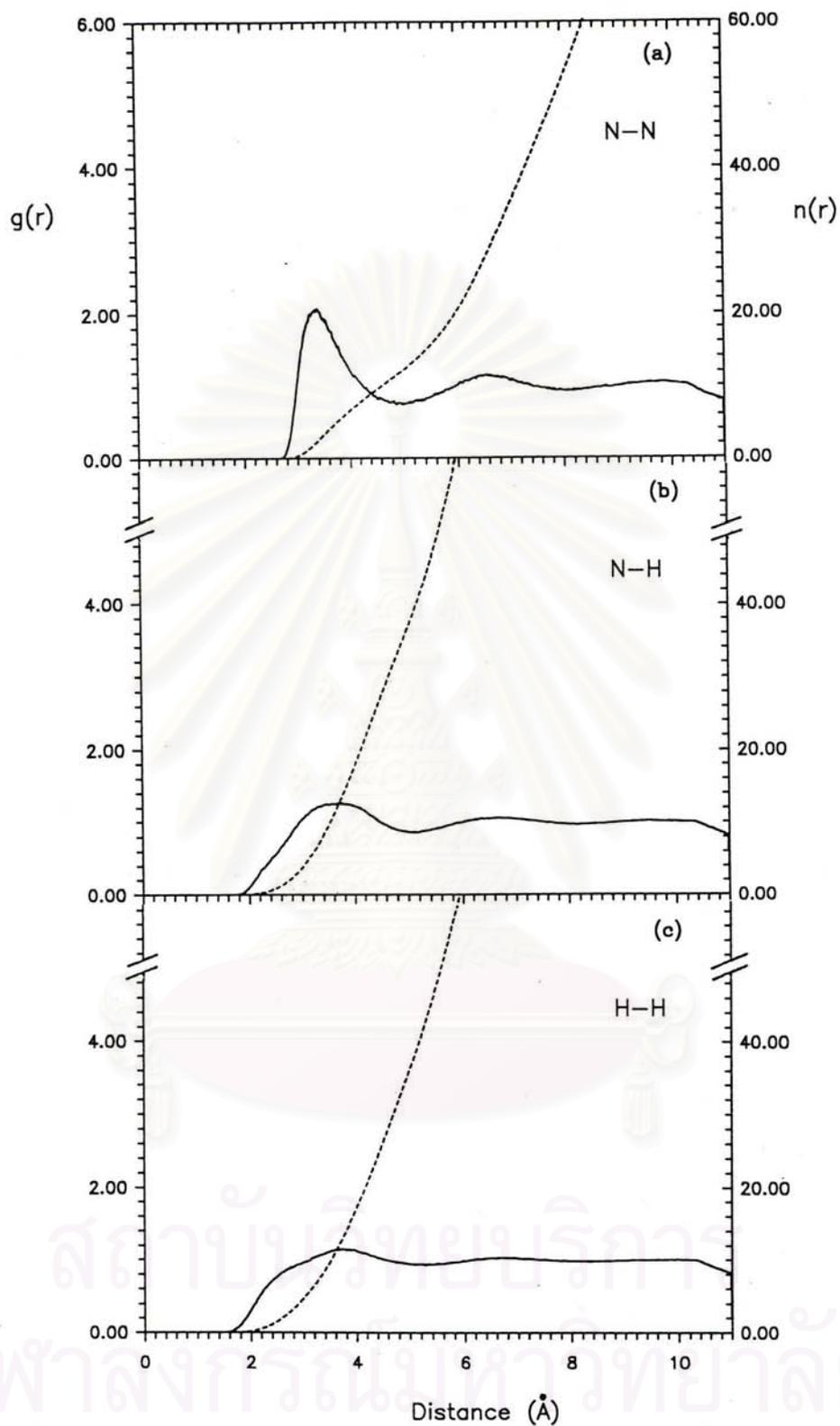


**Figure 4.8** Atom-atom radial distribution functions and running integration numbers from the Molecular Dynamics simulation of one  $\text{K}^+$  in liquid ammonia at 240 K. (a) N-N ; (b) N-H ; (c) H-H

#### 4.4.2 $\Gamma$ -ammonia system

Characteristics of the RDFs for the  $\Gamma$ -ammonia system, investigated from 60,000 configurations after equilibration, are collected in Table 4.9. The plots are shown in Fig. 4.9 and Fig. 4.10.

**Table 4.9** Characteristic values of the radial distribution functions,  $g_{\alpha\beta}(r)$  for the  $\Gamma$ -ammonia solution ;  $r_{M1}$ ,  $r_{M2}$  and  $r_{m1}$  are the distance in Å, where  $g_{\alpha\beta}(r)$  has first and second maximum and first minimum, respectively.  $n_{\alpha\beta}(r_{m1})$  is running integration numbers, integrated up to  $r_{m1}$ .

$\alpha\beta$	$r_{M1}$	$g_{\alpha\beta}(r_{M1})$	$r_{m1}$	$g_{\alpha\beta}(r_{m1})$	$n_{\alpha\beta}(r_{m1})$	$r_{M2}$
N-N	3.34	2.11	4.95	0.76	11.9	6.49
N-H	3.69	1.27	5.15	0.86	39.5	6.62
H-H	3.76	1.15	5.19	0.94	42.1	6.71
$\Gamma$ -N	4.14	2.82	5.45	0.55	15.9	7.06
$\Gamma$ -H	3.94	1.41	5.34	0.84	46.0	7.01

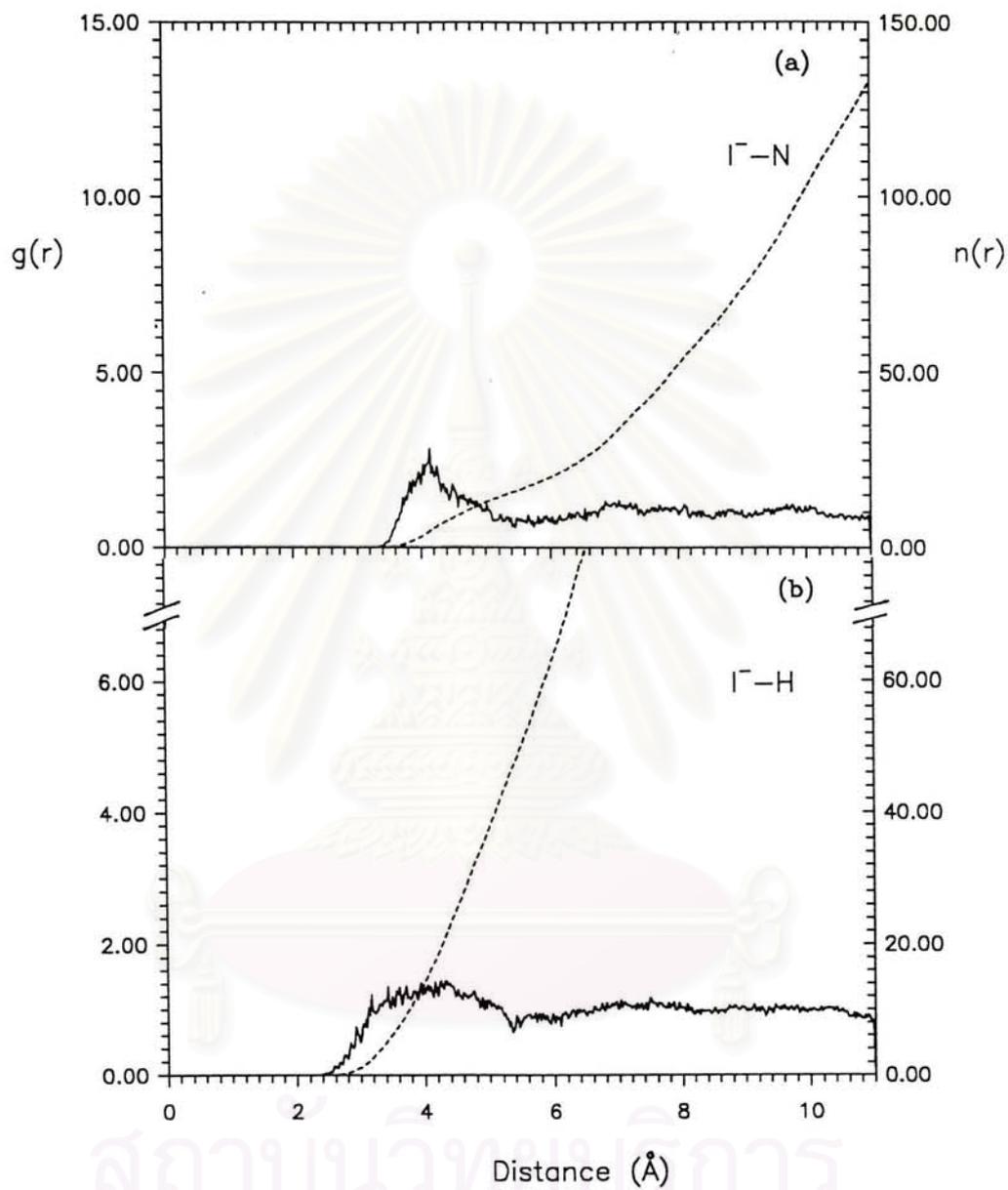


**Figure 4.9** Atom-atom radial distribution functions and running integration numbers from the Molecular Dynamics simulation of one  $\text{I}^-$  in liquid ammonia at 240 K. (a)  $\text{I}^-$ -N ; (b)  $\text{I}^-$ -H

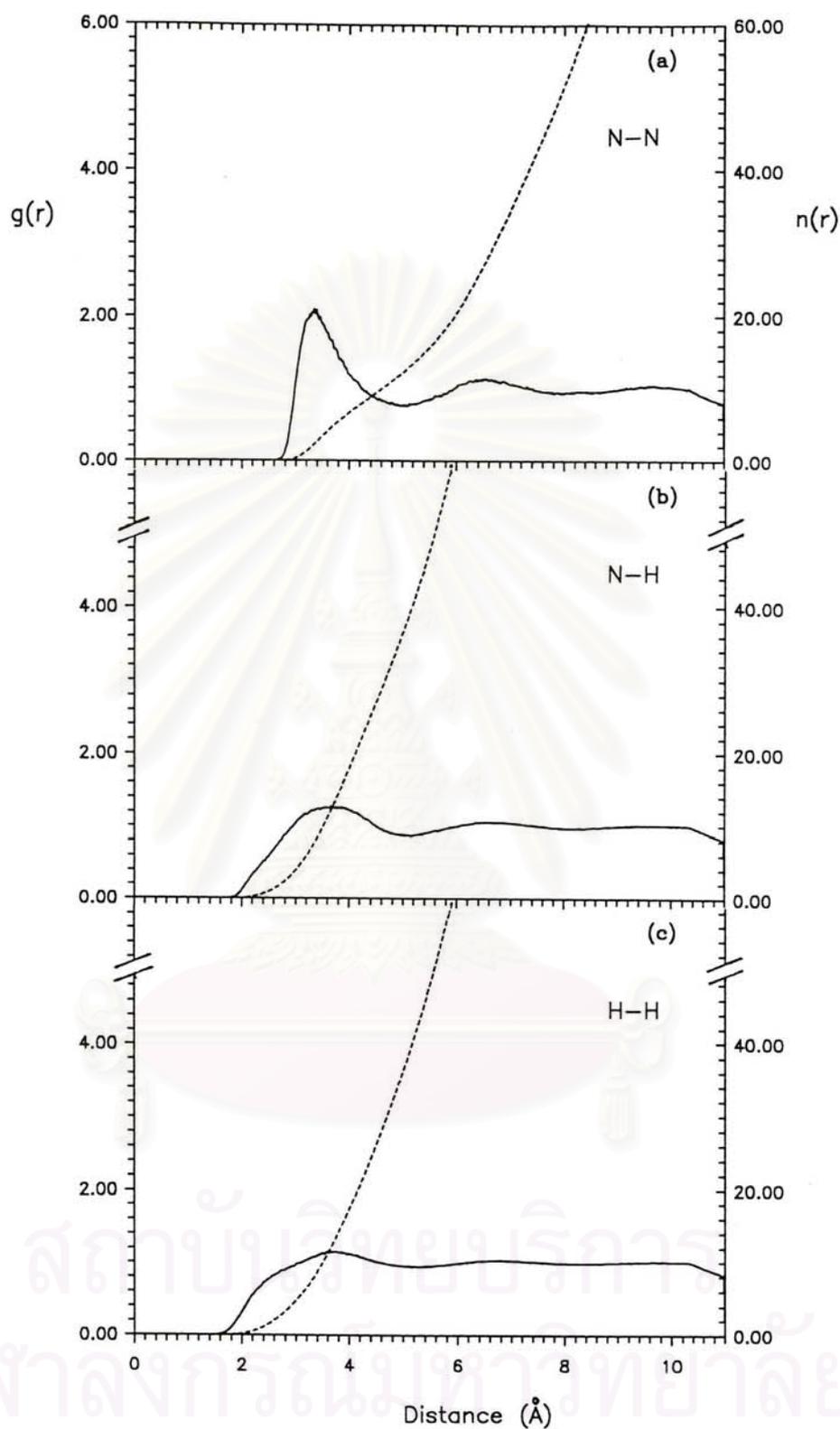


**Figure 4.10** Atom-atom radial distribution functions and running integration numbers from the Molecular Dynamics simulation of one  $\Gamma^-$  in liquid ammonia at 240 K. (a) N-N ; (b) N-H ; (c) H-H

#### 4.4.3 $K^+I^-$ -ammonia system

As for the cases of the  $K^+$ -ammonia and  $I^-$ -ammonia simulations, the atom-atom RDFs and the corresponding coordination numbers for the  $K^+I^-$  solution are plotted in Fig. 4.11 to Fig. 4.13 and summarized in Table 4.10.

**Table 4.10** Characteristic values of the radial distribution functions,  $g_{\alpha\beta}(r)$  for the  $K^+I^-$ -ammonia solution.  $r_{M1}$ ,  $r_{M2}$  and  $r_{m1}$  are the distance in Å, where  $g_{\alpha\beta}(r)$  has first and second maximum and first minimum, respectively.  $n_{\alpha\beta}(r_{m1})$  is running integration numbers, integrated up to  $r_{m1}$ .

$\alpha\beta$	$r_{M1}$	$g_{\alpha\beta}(r_{M1})$	$r_{m1}$	$g_{\alpha\beta}(r_{m1})$	$n_{\alpha\beta}(r_{m1})$	$r_{M2}$
N-N	3.23	2.08	4.86	0.87	11.5	6.14
N-H	3.67	1.27	4.97	0.93	37.4	6.42
H-H	3.61	1.16	5.19	0.98	41.9	6.64
$K^+$ -N	2.69	13.4	3.97	0.0	8.9	5.78
$K^+$ -H	3.35	3.28	4.31	0.42	27.8	5.83
$I^-$ -N	4.07	2.73	5.52	0.56	15.1	7.04
$I^-$ -H	4.02	1.37	5.43	0.72	44.5	7.13

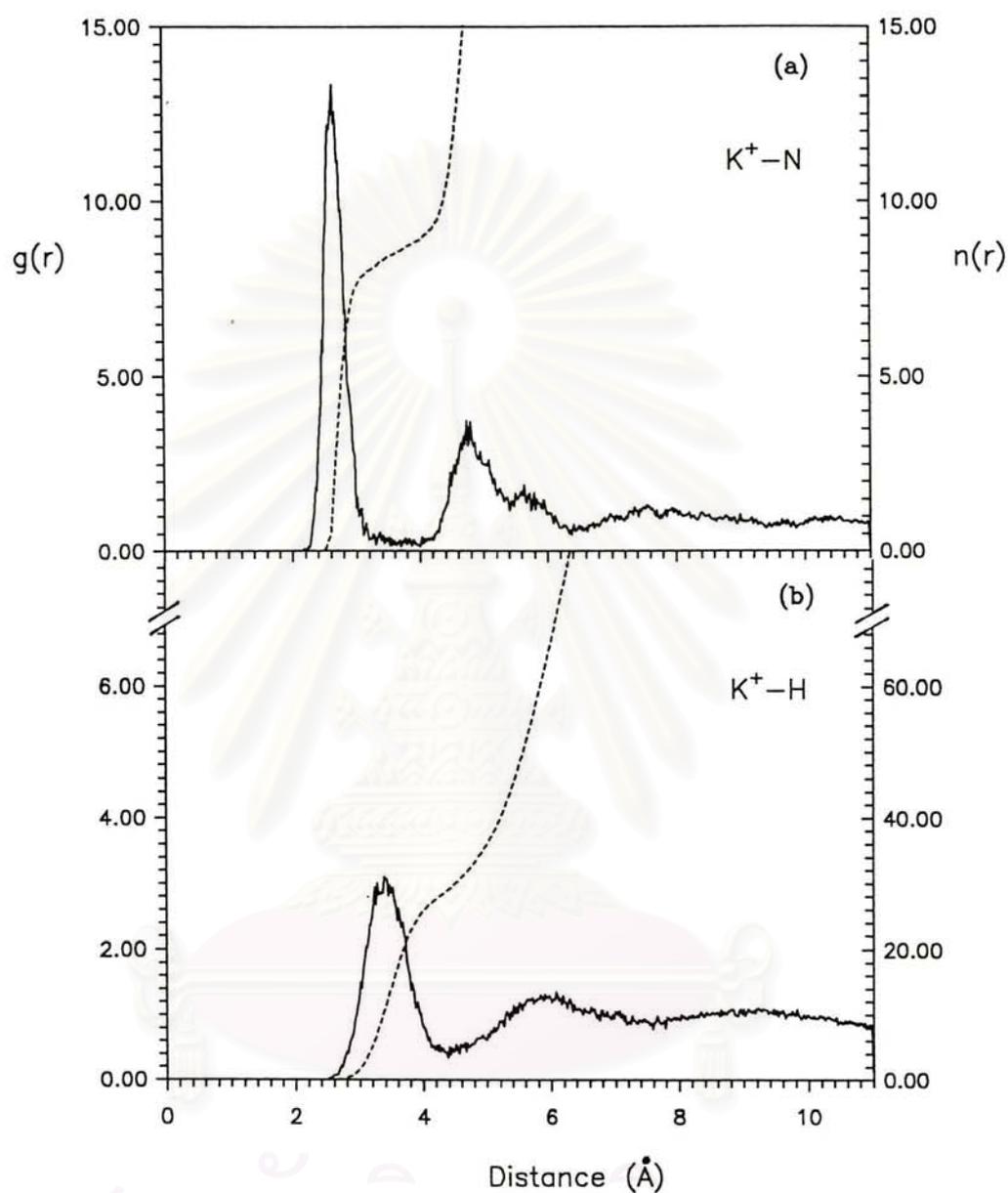


**Figure 4.11** Atom-atom radial distribution functions and running integration numbers from the Molecular Dynamics simulation of one  $K^+$  and one  $I^-$  in liquid ammonia at 240 K. (a)  $K^+$ -N ; (b)  $K^+$ -H

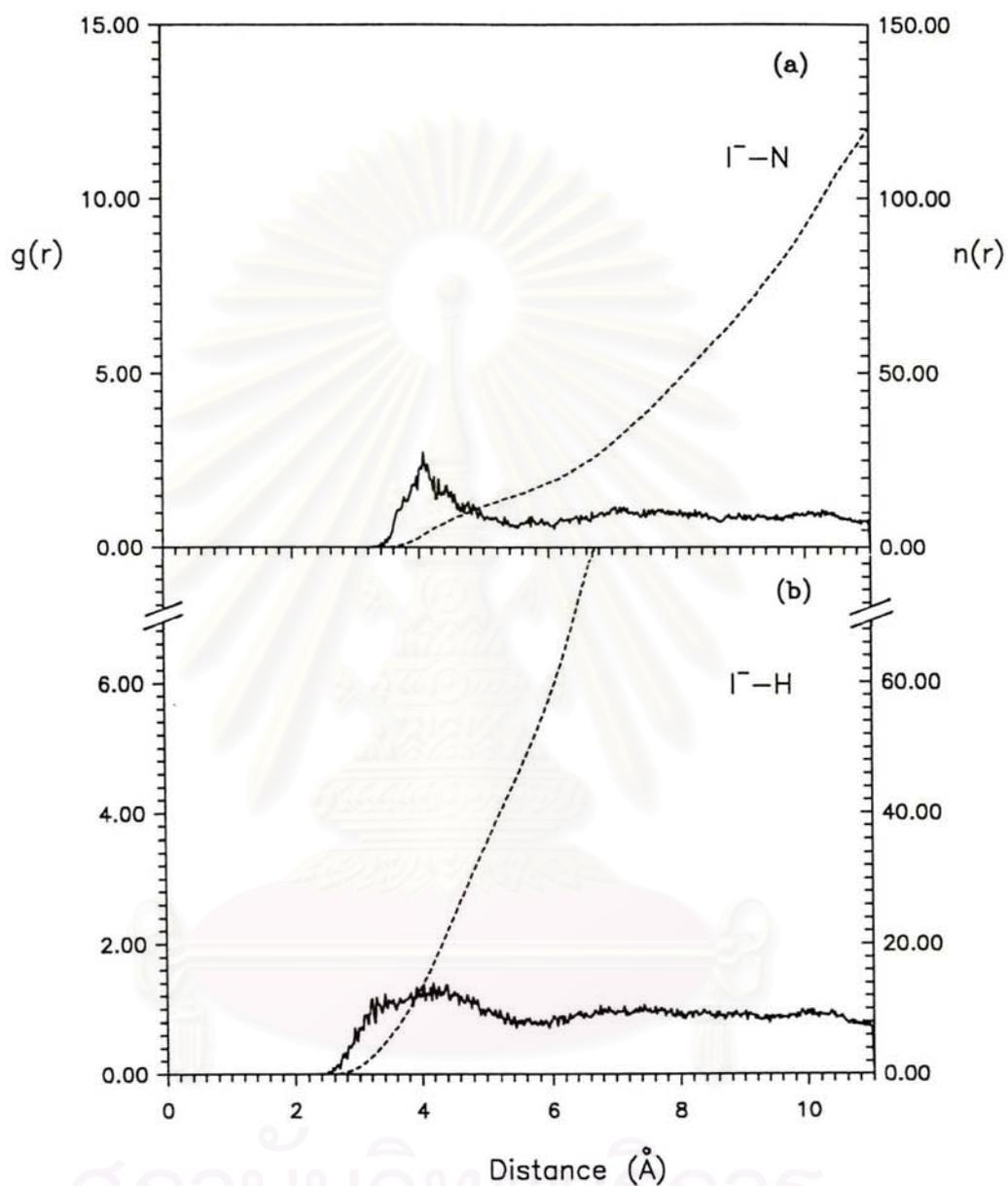


**Figure 4.12** Atom-atom radial distribution functions and running integration numbers from the Molecular Dynamics simulation of one  $K^+$  and one  $I^-$  in liquid ammonia at 240 K. (a)  $I^-$ -N ; (b)  $I^-$ -H

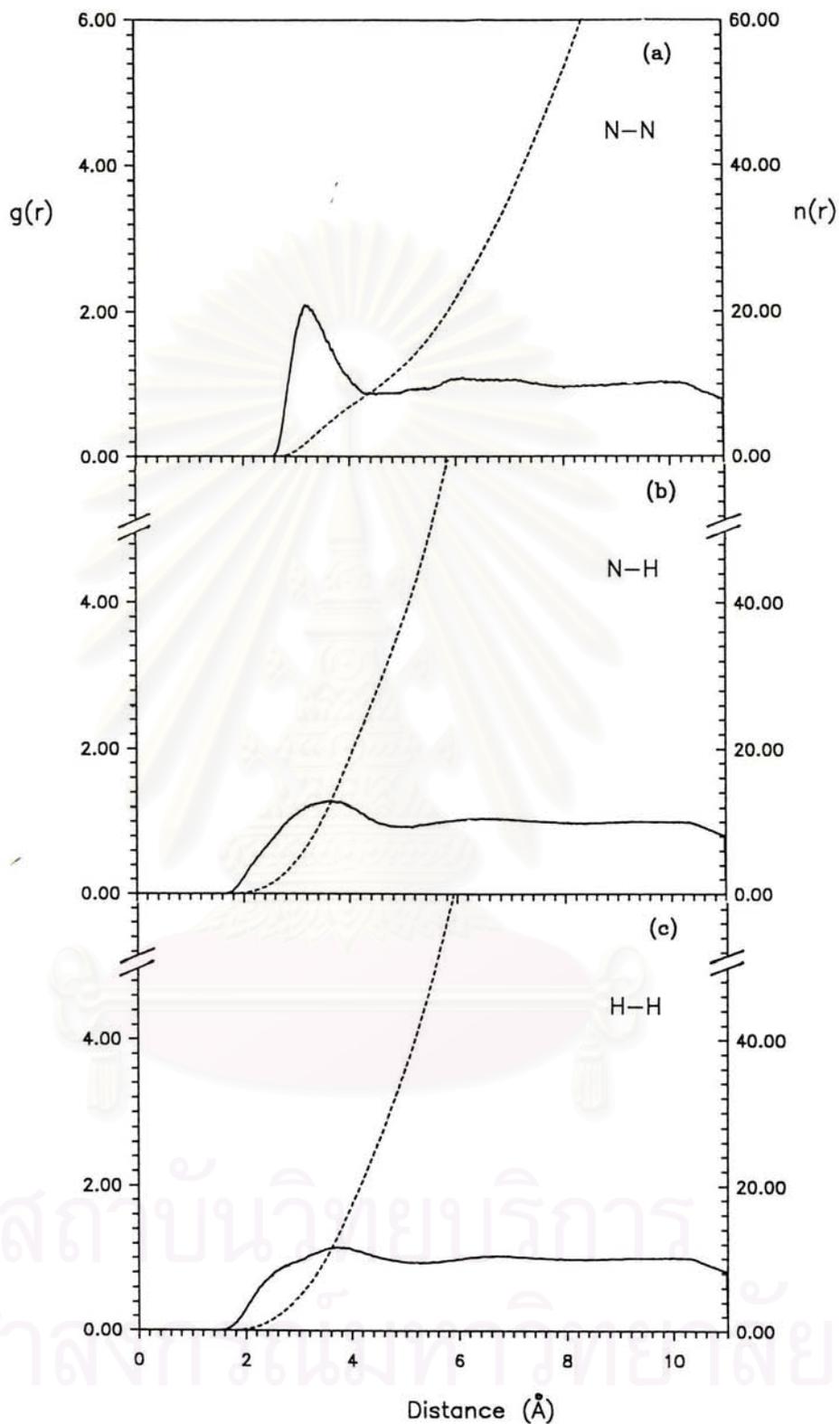
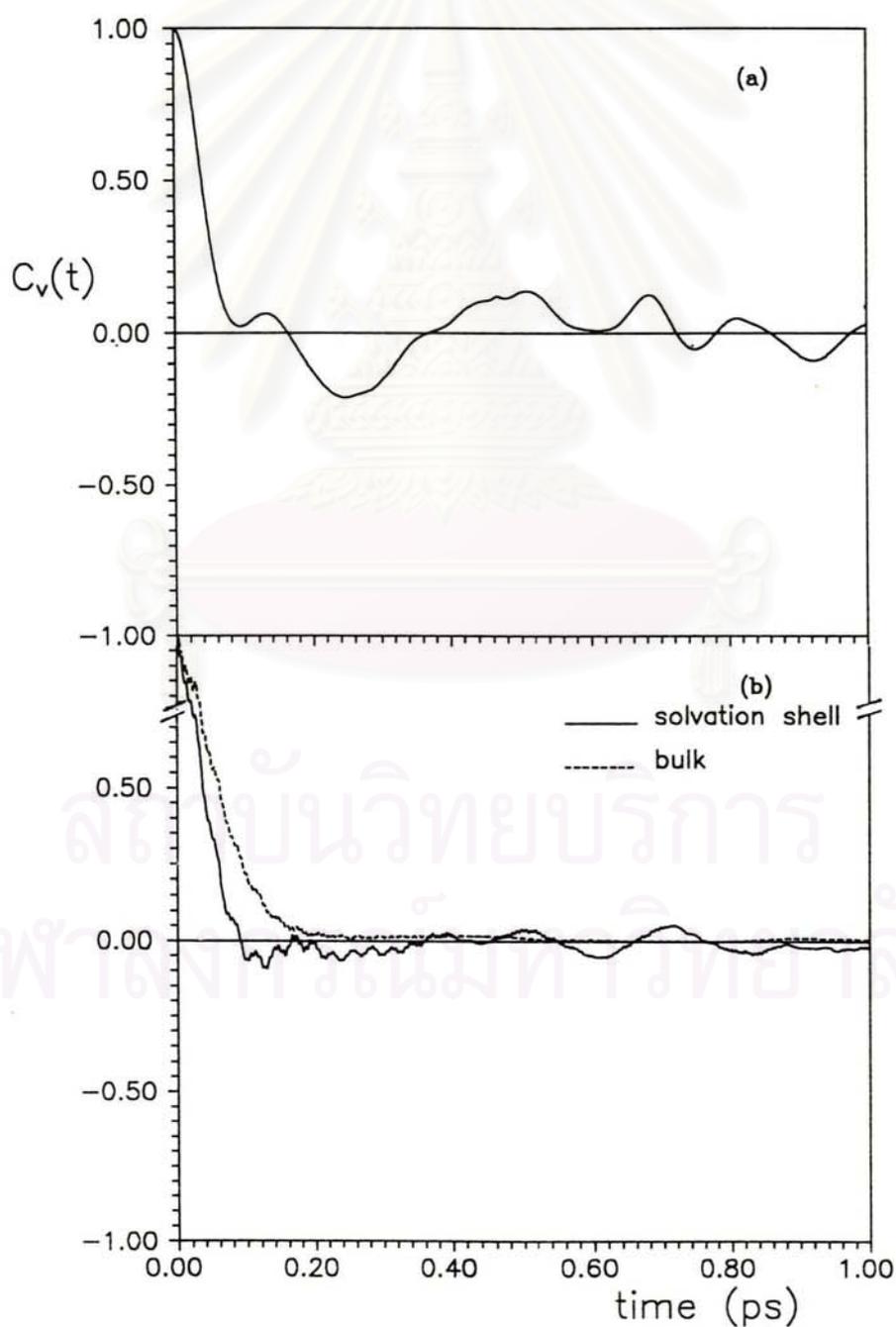


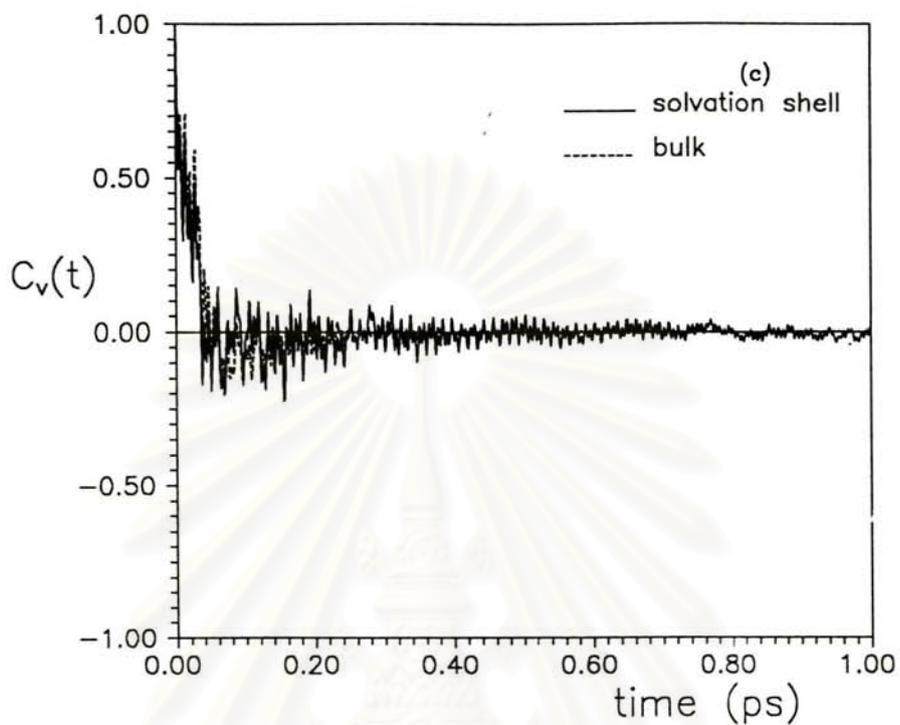
**Figure 4.13** Atom-atom radial distribution functions and running integration numbers from the Molecular Dynamics simulation of one  $\text{K}^+$  and one  $\text{I}^-$  in liquid ammonia at 240 K. (a) N-N ; (b) N-H ; (c) H-H

## 4.5 Dynamical properties

### 4.5.1 $K^+$ -ammonia system

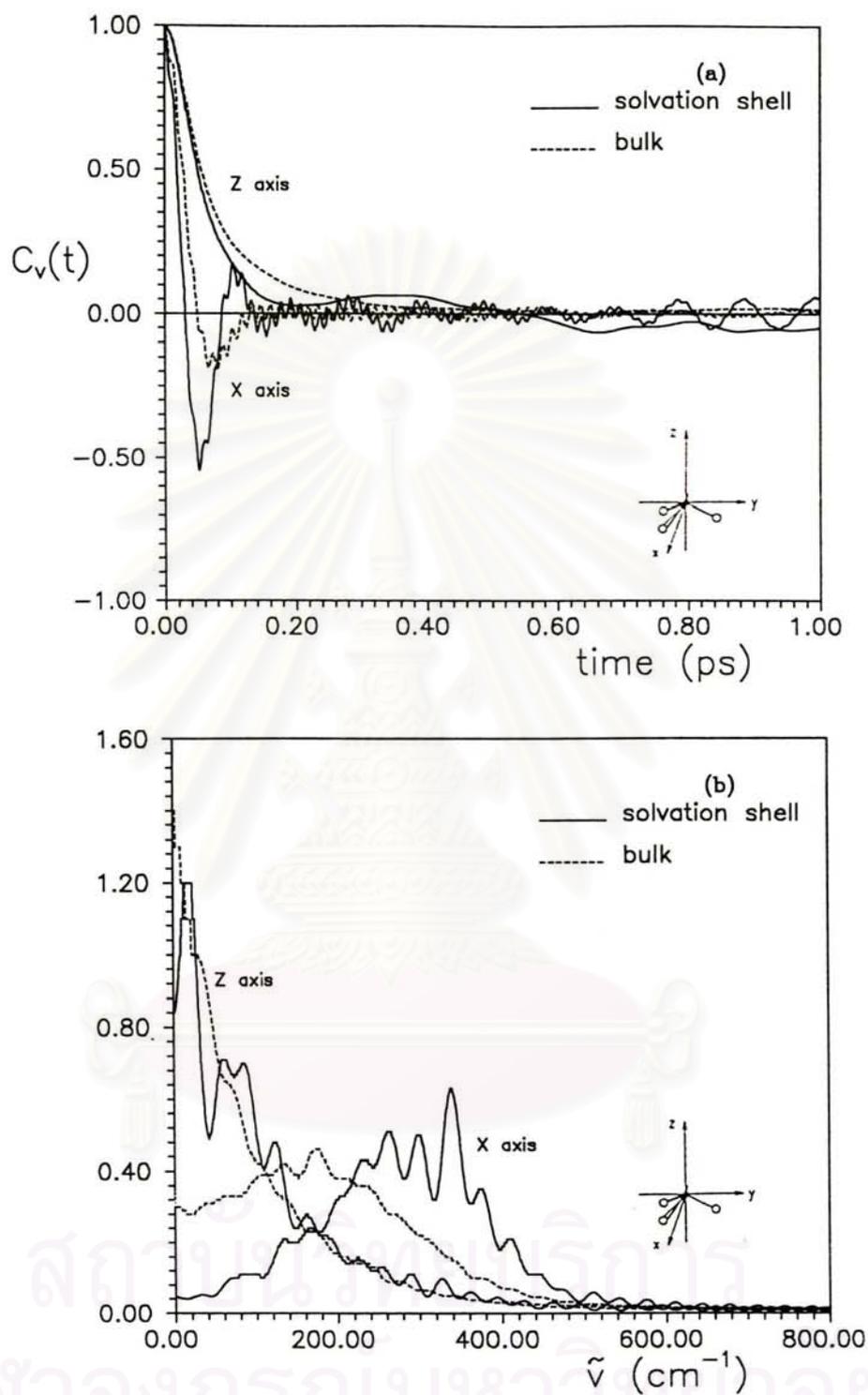
The normalized velocity autocorrelation functions (ACFs or  $C_v(t)$ , see equation (3.18)) and their Fourier transform ( $C(\omega)$ , see equation (3.20)), have been calculated separately for bulk ammonia and ammonia molecules in the first solvation shell of  $K^+$ , and plotted in Fig. 4.14 to Fig. 4.17. Fluctuation of the temperature of each particle and of the system have been also examined and drawn in Fig. 4.18.



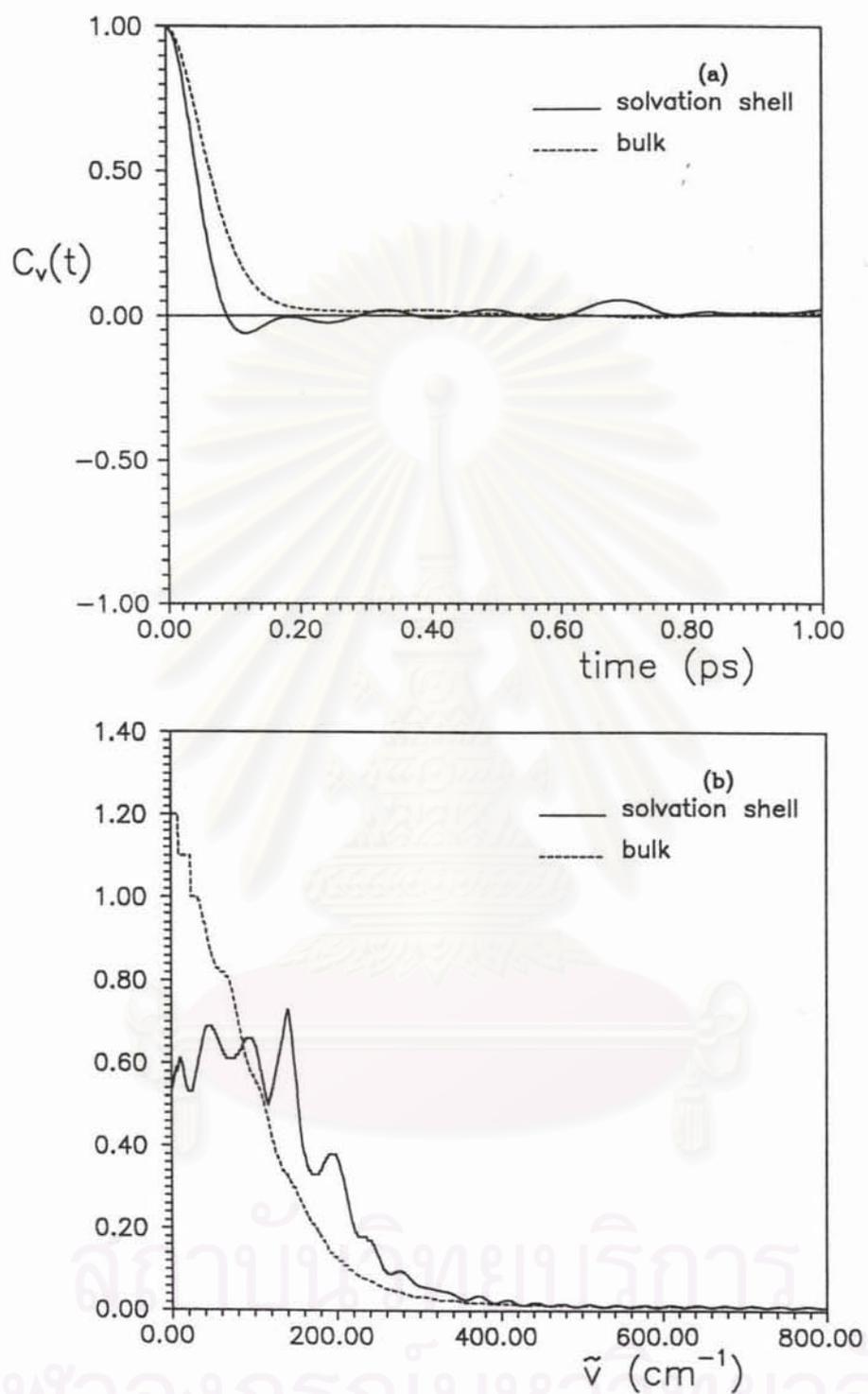


**Figure 4.14** Normalized velocity autocorrelation function functions of (a)  $K^+$  ; (b) N atom and (c) H atom, obtained from the Molecular Dynamics simulation of one  $K^+$  in liquid ammonia at 240 K.

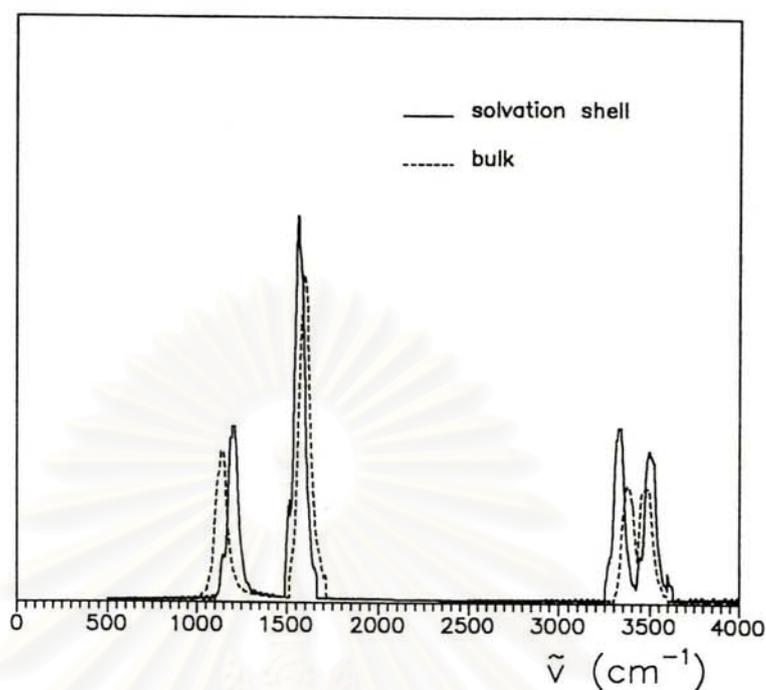
สถาบันวิทยบริการ  
จุฬาลงกรณ์มหาวิทยาลัย



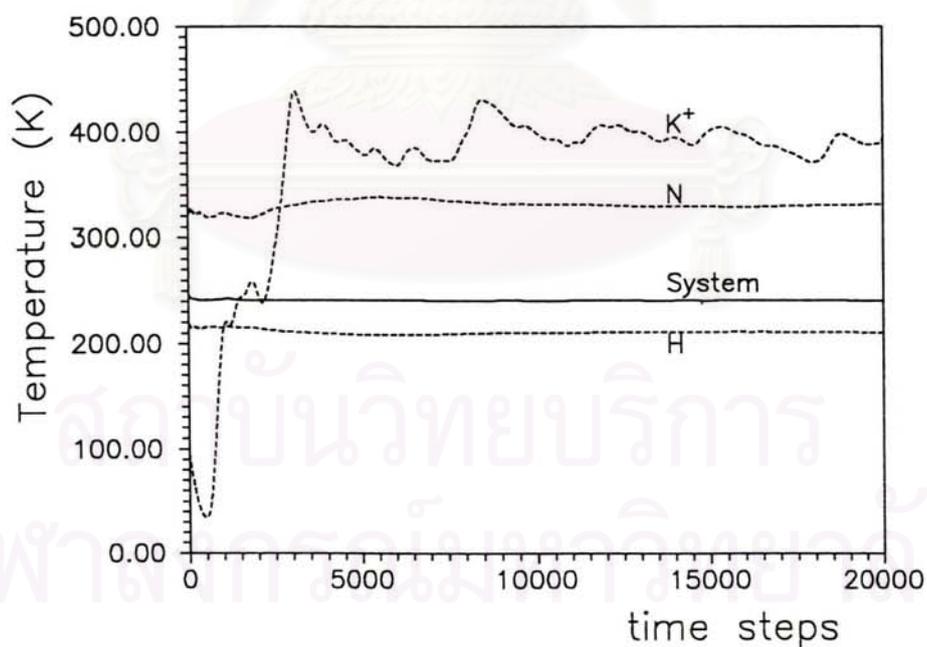
**Figure 4.15** (a) Normalized velocity autocorrelation functions of ammonia molecules about the x and z axis ; (b) their Fourier transforms, calculated from the Molecular Dynamics simulation of one  $\text{K}^+$  in liquid ammonia at 240 K.



**Figure 4.16** (a) Normalized center-of-mass velocity autocorrelation functions of ammonia molecules ; (b) their Fourier transforms, calculated from the Molecular Dynamics simulation of one  $\text{K}^+$  in liquid ammonia at 240 K.



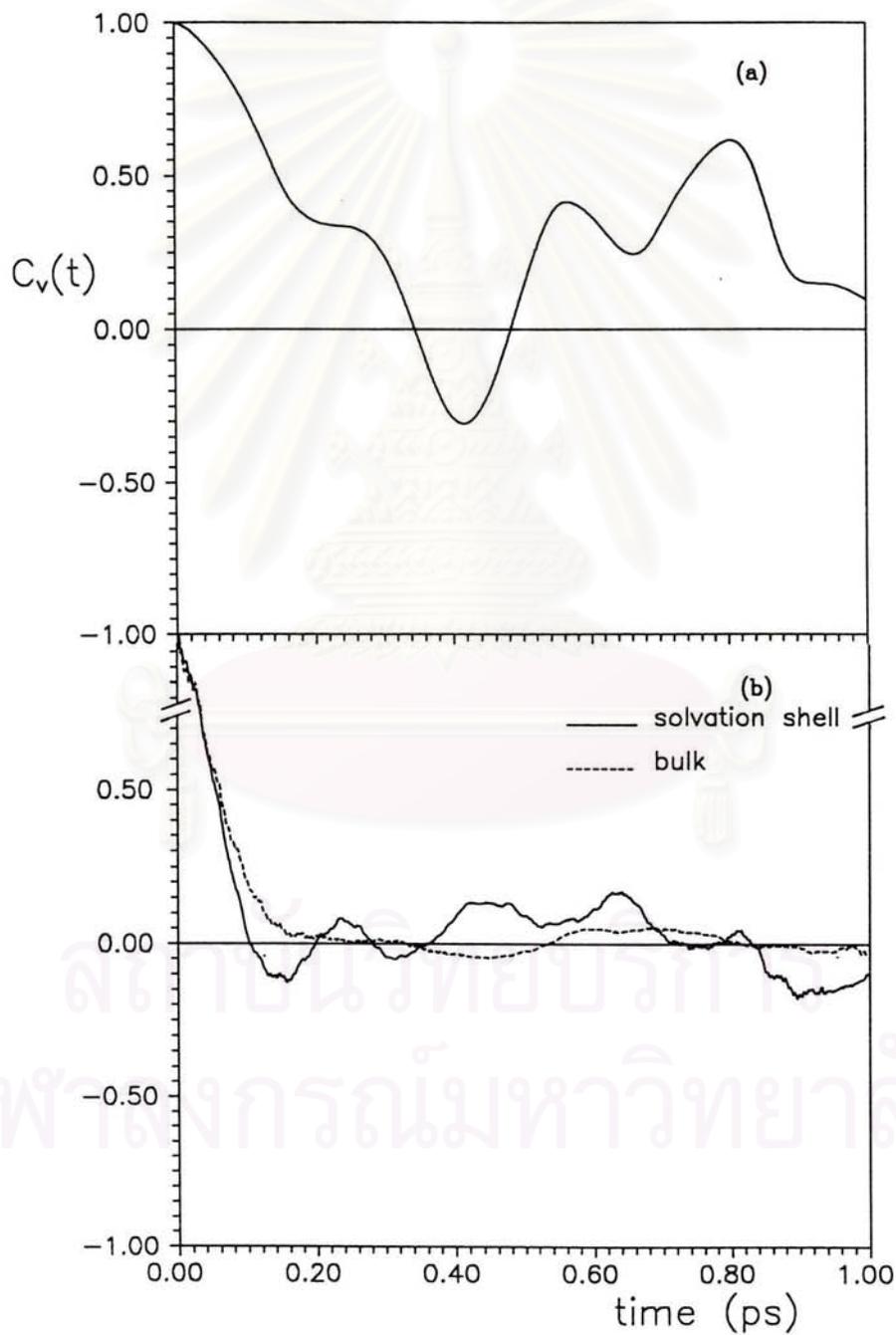
**Figure 4.17** Fourier transforms of the hydrogen velocity autocorrelation functions for bulk ammonia and ammonia in the solvation shell of  $K^+$ , calculated from the Molecular Dynamics simulation of one  $K^+$  in liquid ammonia at 240 K.

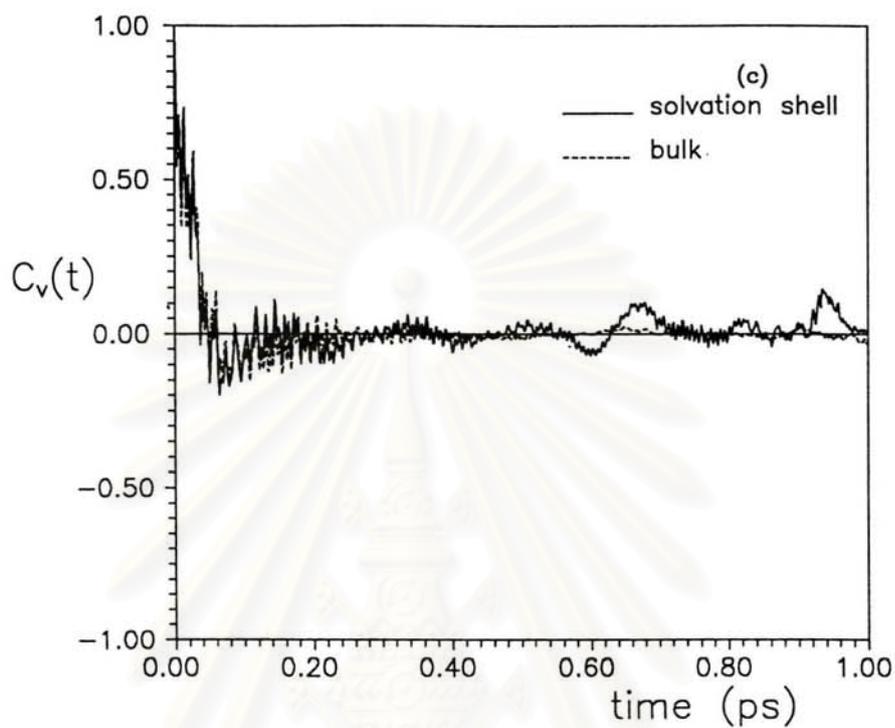


**Figure 4.18** Temperature changes of the Molecular Dynamics simulation of one  $K^+$  in liquid ammonia.

#### 4.5.2 $\Gamma$ -ammonia system

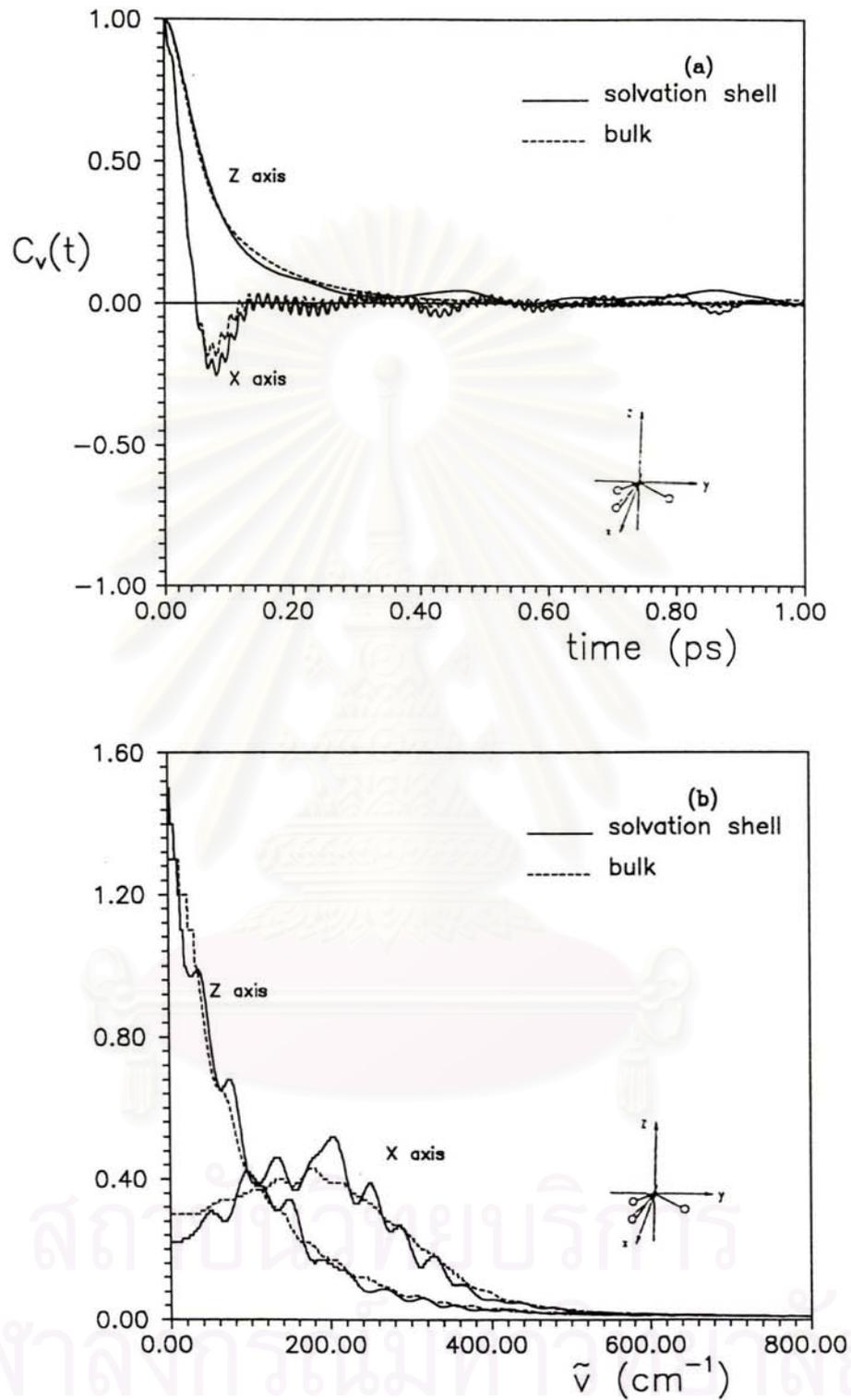
The same as the  $K^+$ -ammonia system, the normalized velocity autocorrelation functions, their Fourier transforms and the temperature changes have been plotted in Fig. 4.19 to Fig. 4.23.



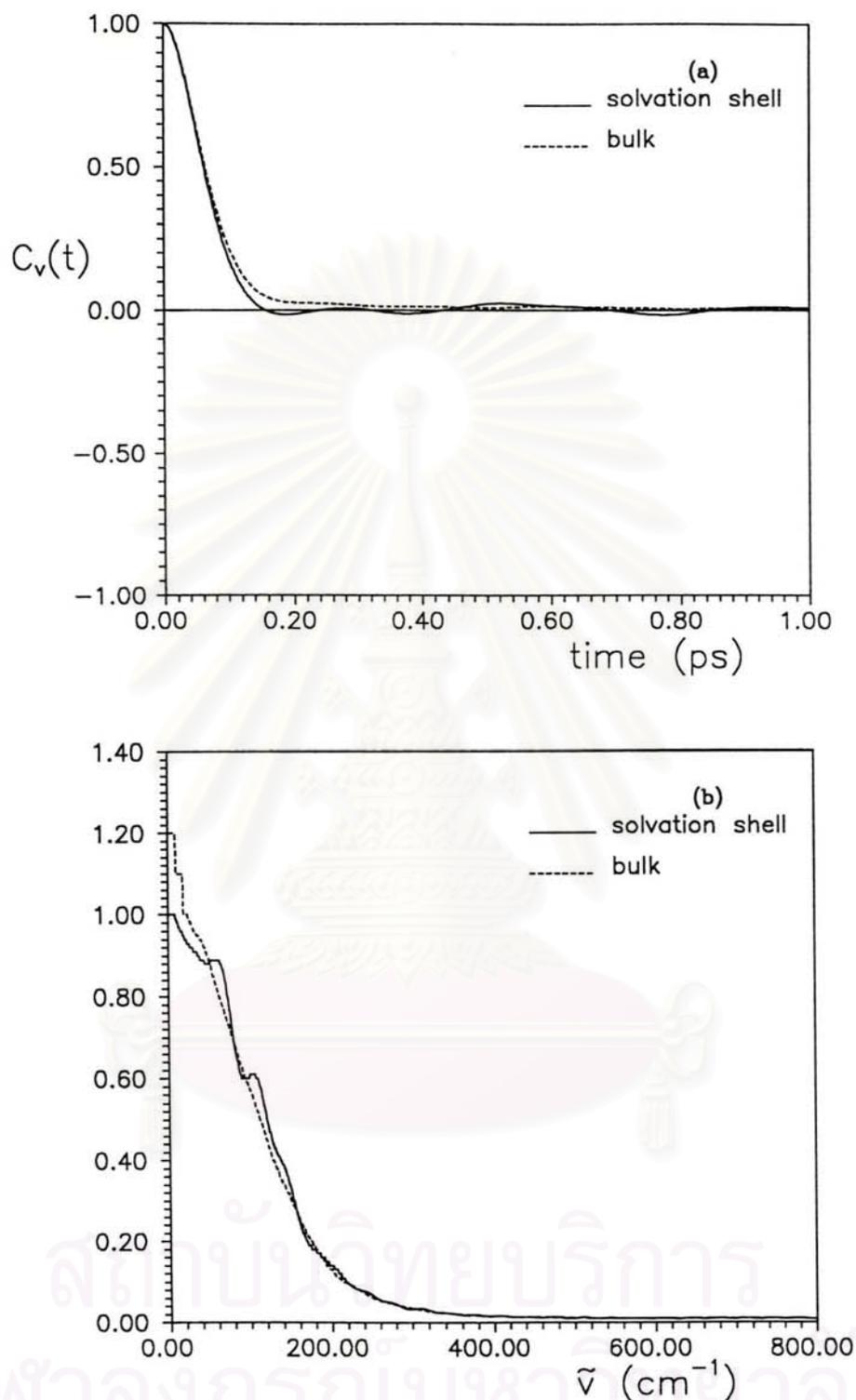


**Figure 4.19** Normalized velocity autocorrelation function functions of (a)  $\Gamma^-$  ; (b) N atom and (c) H atom, obtained from the Molecular Dynamics simulation of one  $\Gamma^-$  in liquid ammonia at 240 K.

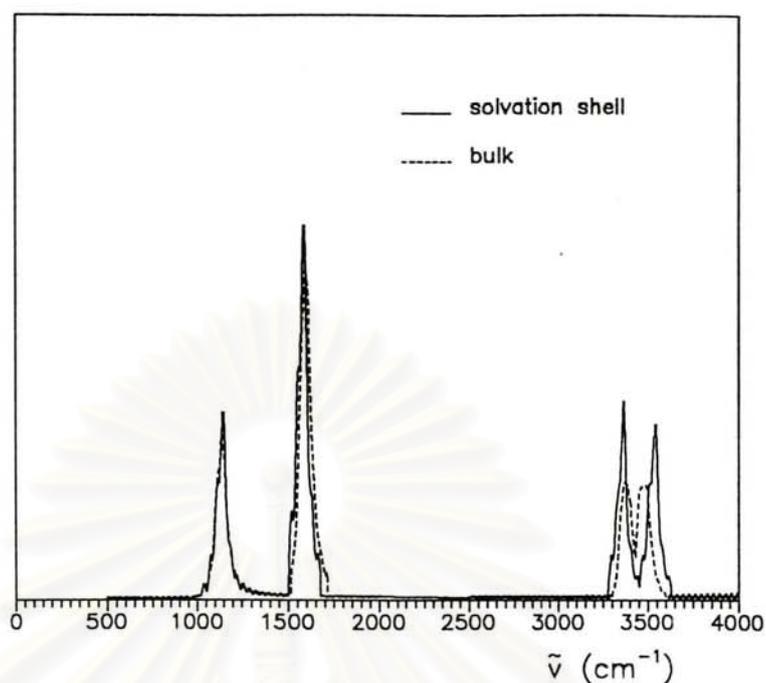
สถาบันวิทยบริการ  
จุฬาลงกรณ์มหาวิทยาลัย



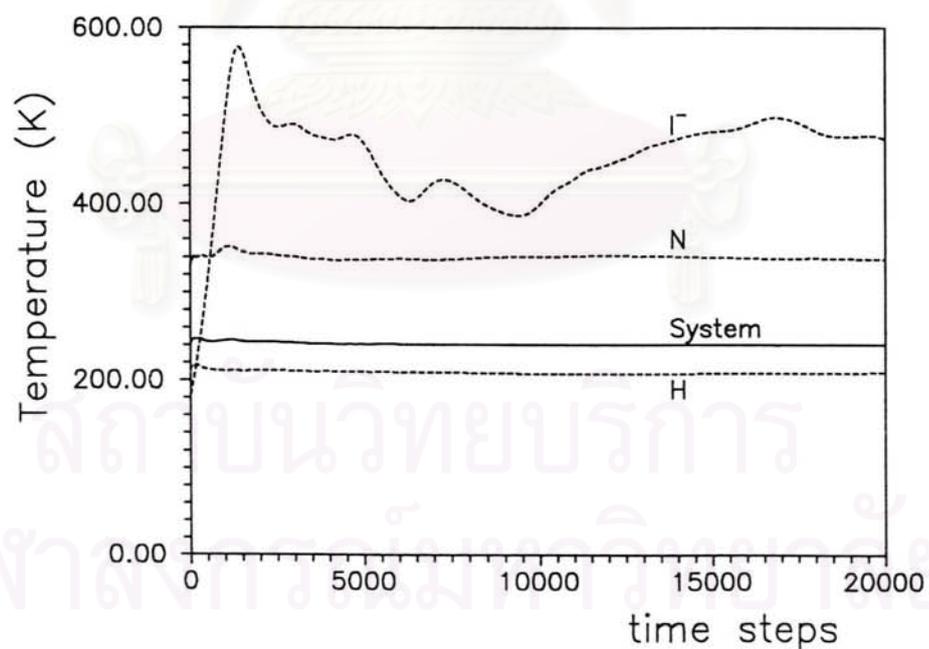
**Figure 4.20** (a) Normalized velocity autocorrelation functions of ammonia molecules about the x and z axis ; (b) their Fourier transforms, calculated from the Molecular Dynamics simulation of one  $\text{I}^-$  in liquid ammonia at 240 K.



**Figure 4.21** (a) Normalized center-of-mass velocity autocorrelation functions of ammonia molecules ; (b) their Fourier transforms, calculated from the Molecular Dynamics simulation of one  $\Gamma^-$  in liquid ammonia at 240 K.



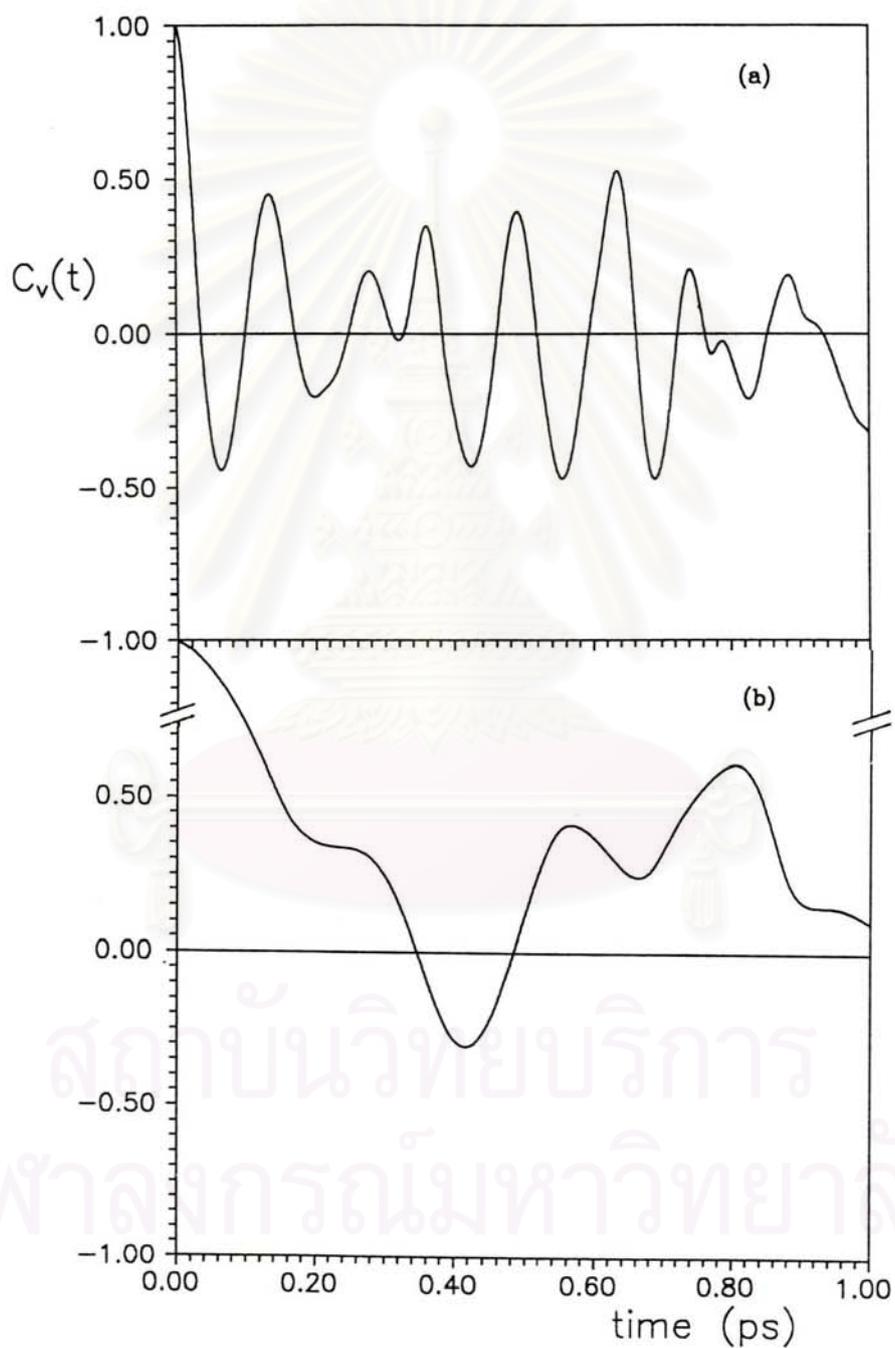
**Figure 4.22** Fourier transforms of the hydrogen velocity autocorrelation functions for bulk ammonia and ammonia in the solvation shell of  $\text{I}^-$ , calculated from the Molecular Dynamics simulation of one  $\text{I}^-$  in liquid ammonia at 240 K.

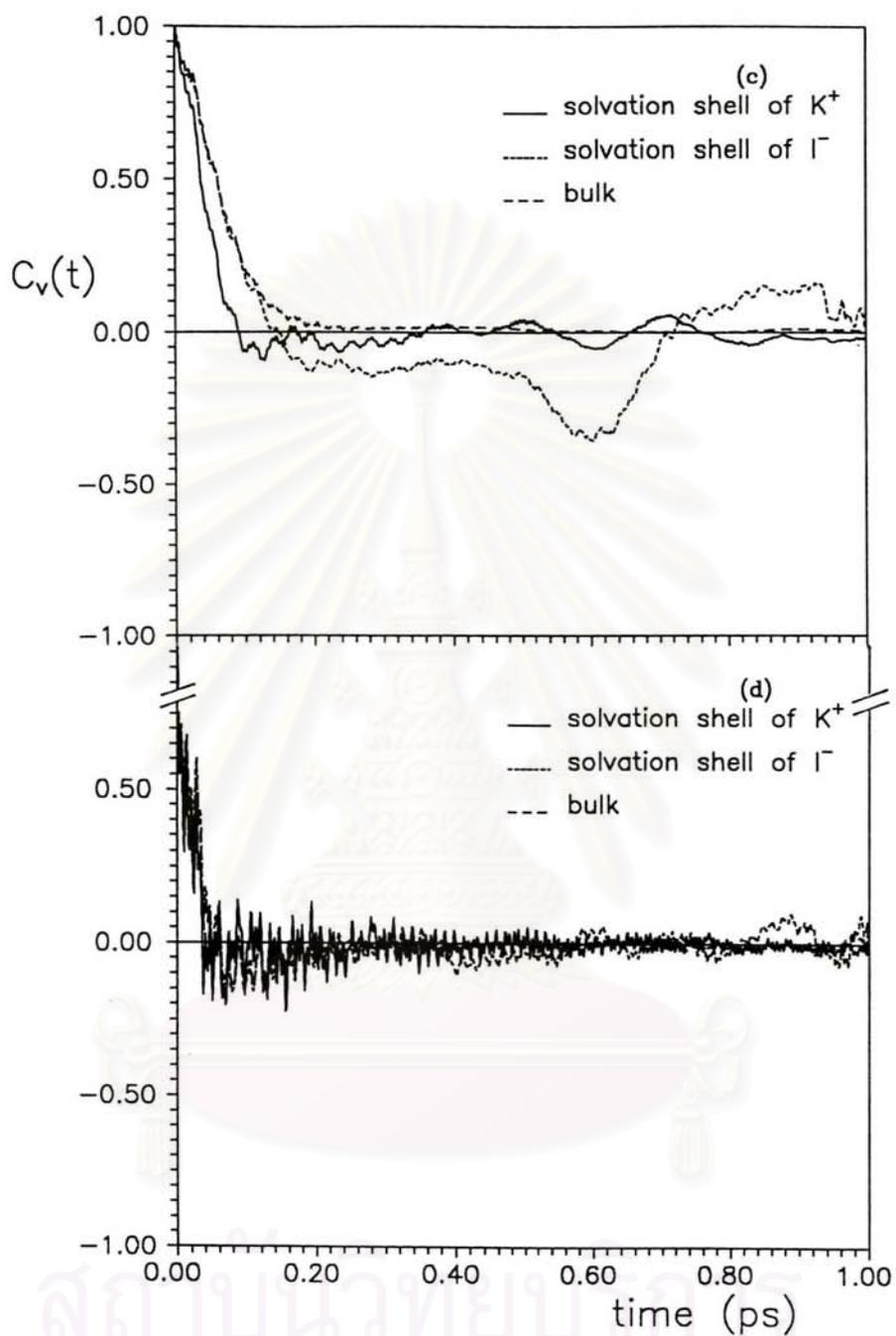


**Figure 4.23** Temperature changes of the Molecular Dynamics simulation of one  $\text{I}^-$  in liquid ammonia.

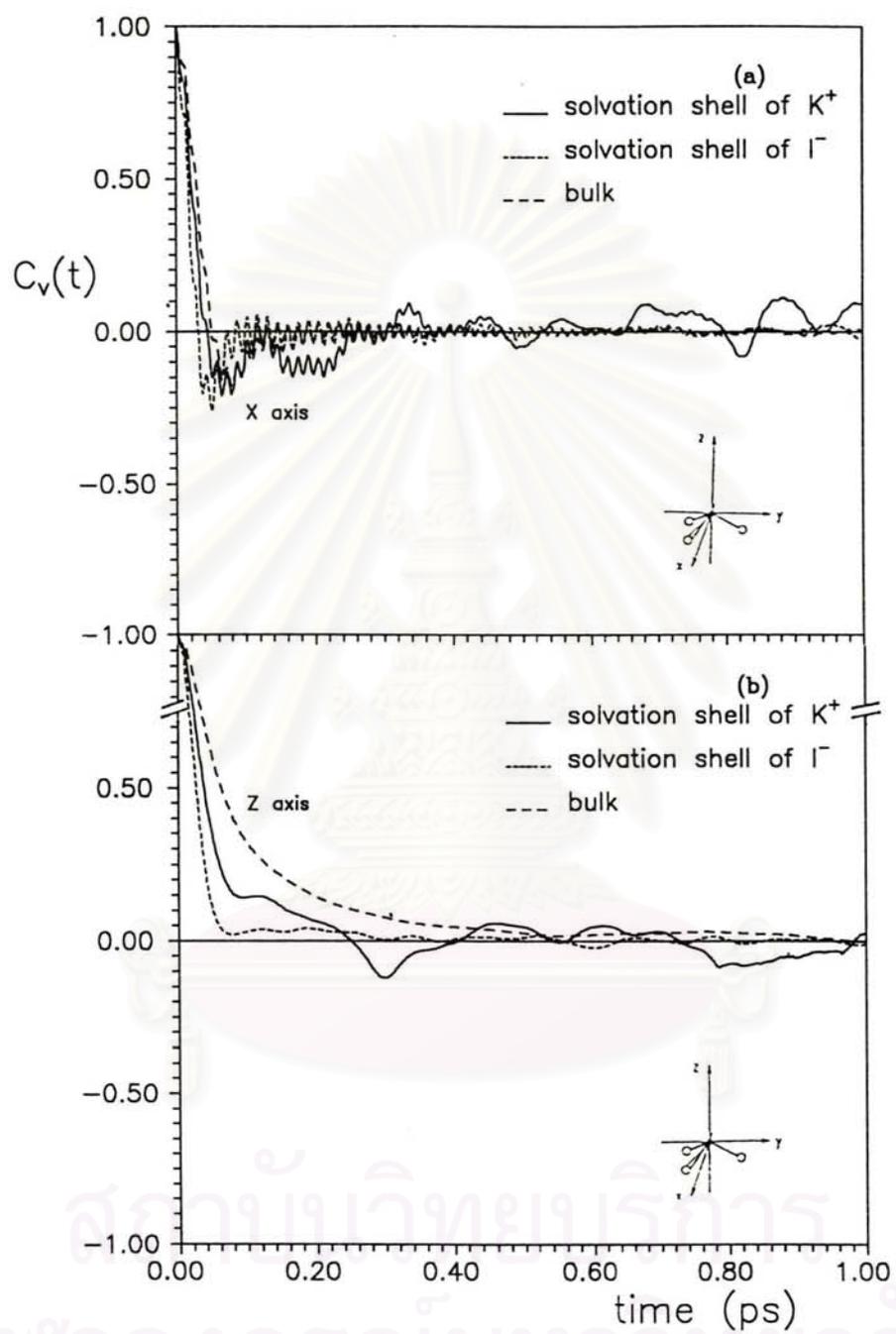
### 4.5.3 $K^+$ - $\Gamma$ -ammonia system

Their normalized velocity autocorrelation functions, Fourier transforms and temperature changes have been depicted in Fig. 4.24 to Fig. 4.28.





**Figure 4.24** Normalized velocity autocorrelation function functions of (a)  $K^+$  ; (b)  $I^-$  ; (c) N atom and (d) H atom, obtained from the Molecular Dynamics simulation of one  $K^+$  and one  $I^-$  in liquid ammonia at 240 K.



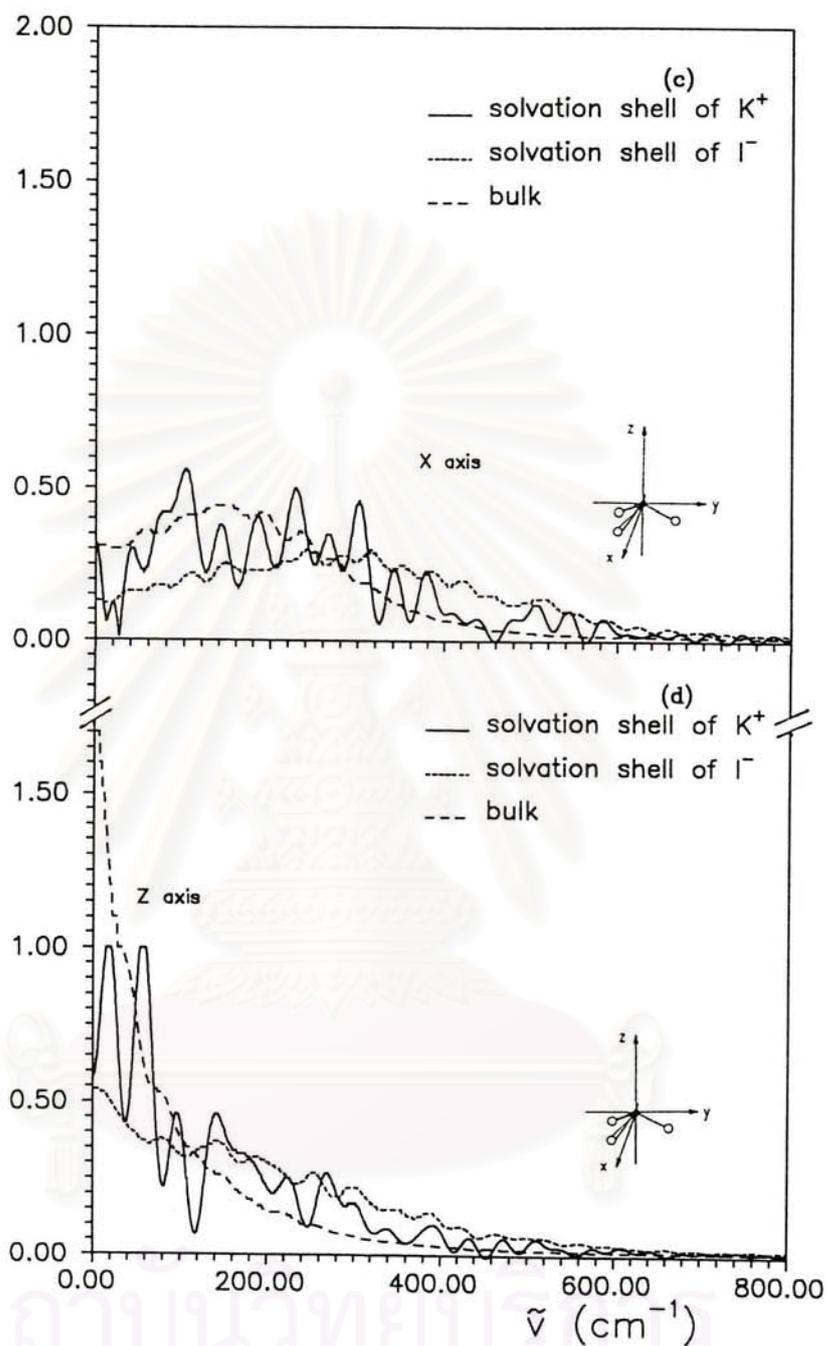


**Figure 4.25** (a) Normalized velocity autocorrelation functions of ammonia molecules about the x axis ; (b) Normalized velocity autocorrelation functions of ammonia molecules about the z axis ; (c) their Fourier transforms about the x axis; (d) their Fourier transforms about the z axis, calculated from the Molecular Dynamics simulation of one  $K^+$  and one  $I^-$  in liquid ammonia at 240 K.

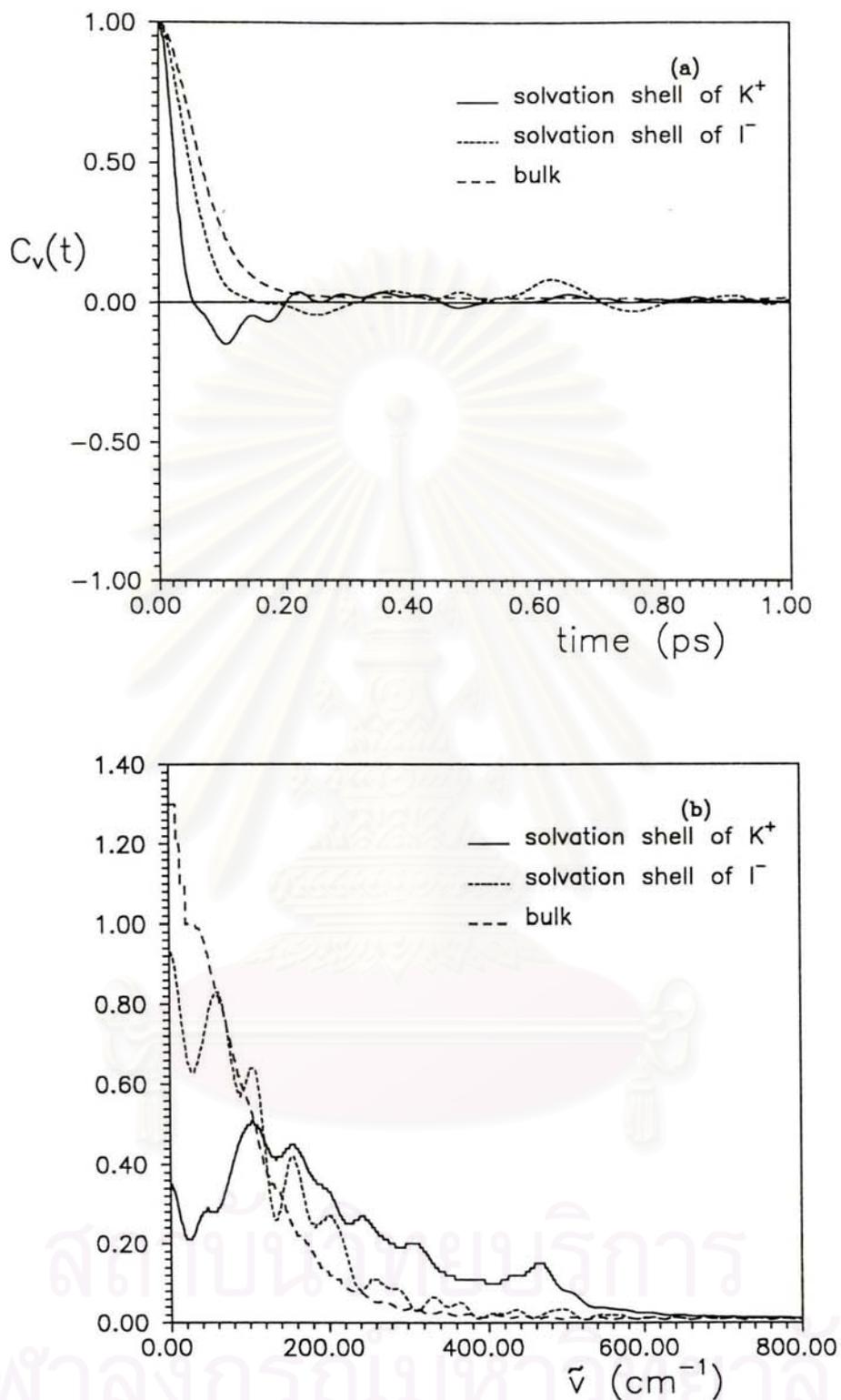


**Figure 4.26** (a) Normalized center-of-mass velocity autocorrelation functions of ammonia molecules ; (b) their Fourier transforms, calculated from the Molecular Dynamics simulation of one  $K^+$  and one  $I^-$  in liquid ammonia at 240 K.

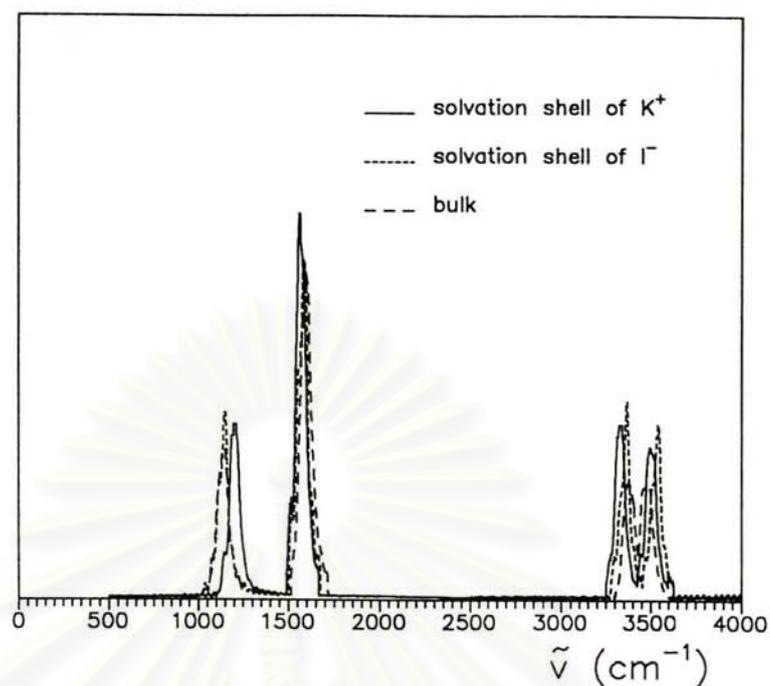


**Figure 4.27** Fourier transforms of the hydrogen velocity autocorrelation functions for bulk ammonia and ammonia in the solvation shell of  $K^+$  and  $I^-$ , calculated from the Molecular Dynamics simulation of one  $K^+$  and one  $I^-$  in liquid ammonia at 240 K.

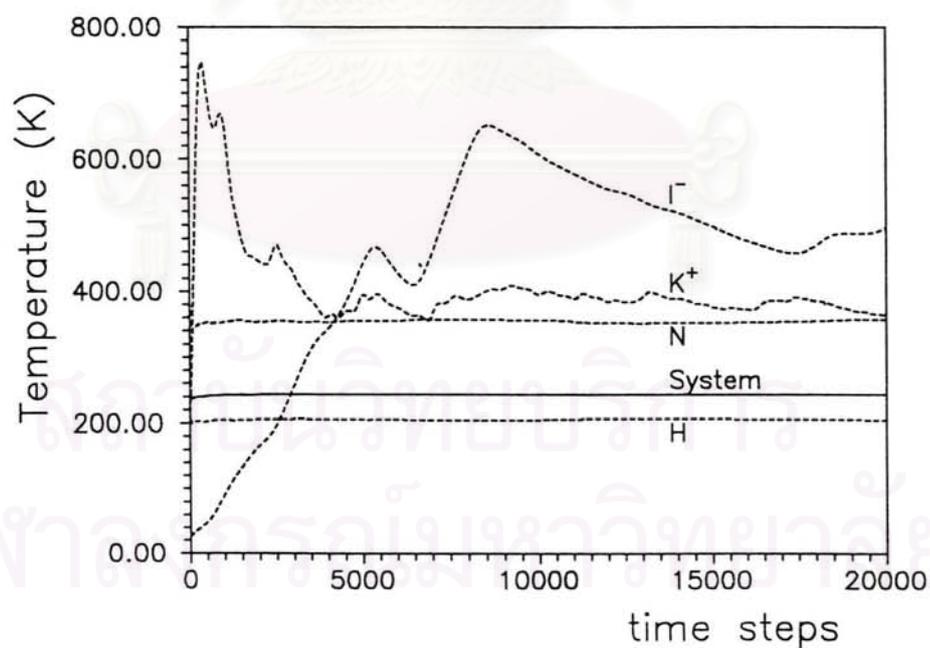


**Figure 4.28** Temperature changes of the Molecular Dynamics simulation of one  $K^+$  and one  $I^-$  in liquid ammonia.

## CHAPTER 5

### DISCUSSION

#### Part A : Intermolecular potential

The structural and dynamical properties of potassium iodide in liquid ammonia have been studied by Molecular Dynamics simulation, using the fitted functions obtained from SCF calculations to compute forces. The trust and the accuracy of the simulation results depend mainly on the quality of the basis sets and the fitted functions used. The best fitted functions should be good for representing both attractive and repulsive interaction energies.

#### 5.1 Suitable basis sets for the atoms of the systems

Because the basis set superposition error (BSSE) is one of the major factors limiting the accuracy of *ab initio* calculation [50]. The results taken from SCF calculations, in which the basis set superposition error was corrected by applying the counterpoise method,  $\Delta E_{\text{BSSE}}$ , and from the SCF calculations, without correction have been compared. In Table 4.1, the small basis sets, such as STO-3G or DZV, give a large basis set superposition error and large distance shift. There are two reasons that may be discussed. First, if BSSE is suspected, the correction must be performed in order to avoid a false result. The BSSE causes overestimation of the attraction contribution to the interaction energy and provides illegitimate increase of binding energy. It also influences the result of molecular geometry optimization and molecular charge distribution. Secondly, taking into account by applying the counterpoise method in the molecular calculations by using medium and small basis sets could give the values of interaction energy which are just close to those obtained by using more expensive and larger basis sets. However, for very poor atomic basis sets, by means of size and quality, it will

not provide effective improvement of the results even applying the counterpoise method.

In the part few years, the DZP basis set would have been the best choice for this purpose. According to the calculated results shown in Table 2.1, the DZP basis set causes the shift of the optimal  $K^+$ -ammonia distance by 0.3 Å. In addition, because of the available of the high performance computers, computational time is no more the main problem. Therefore, we design to use the large 14s/9p/5d and 16s/12p/8d basis sets for  $K^+$  and  $I^-$  (Table 4.1 to Table 4.3), respectively.

## 5.2 Intermolecular pair potential

For the  $K^+$ -ammonia intermolecular pair potential, the  $\Delta E_{BSSE}$  and the  $\Delta E_{FIT}$ , for various orientations shown in Fig. 4.1 and Fig. 4.2, are in good agreement. The function can represent very well, both for the attractive interaction region near the minimum and the repulsive interaction up to 30 kcal/mol.

The  $I^-$ -ammonia pair potential, (Fig. 4.3 and Fig. 4.4) does not represent well the  $\Delta E_{BSSE}$ , especially in the small repulsive region. The weak  $I^-$ -ammonia interaction (minimum interaction energy about -5 kcal/mol) make the function sensitive for the repulsive interaction, especially, for the repulsive regions up to 30 kcal/mol. Therefore, include of a high of a large repulsion would increase the standard deviation and, consequently, the percentual error in energy (18.3%, Table 4.5).

The orientation independent  $K^+ - I^-$  interactions in Fig. 4.5 and Fig. 4.6 show a high accuracy of the fit in all regions, both in terms of interaction energies and distance to the minimum.

## 5.3 SCF calculations on the non-additivity

As expected, increase of the cluster size causes the increase of the ion-nitrogen distances and the decrease of the stabilization energy per ammonia molecule,  $\Delta E_{av1}$ , (Table 4.7). In comparison with other ions in the most interesting case of octahedral complexes with water and ammonia molecules, their characteristics are summarized in Table 5.1.

**Table 5.1** Characteristics of the non-additivity (see Table 4.7) for the  $ML_n$  complexes, where M is metal ion, L is either water or ammonia molecule, and  $n=6$  (energies are in  $\text{Kcal.mol}^{-1}$ ,  $r_{\text{shift}}$ , from  $n=1$  to  $n=6$ , are in  $\text{\AA}$ .)

system	$r_{\text{shift}}$	% $E_1$	% $E_2$	$\Delta E_{\text{rpl}}$	ref.
$\text{Na}^+$ -water	0.22	>40	8	-	[51]
$\text{Mg}^{2+}$ -water	0.16	>40	15	-	[51]
$\text{Al}^{3+}$ -water	0.13	>40	21	-	[51]
$\text{Zn}^{2+}$ -ammonia	0.33	28	18	65.0	[52]
$\text{K}^+$ -ammonia	0.09	15	13	23.8	this work

The increase of  $\text{K}^+$ -nitrogen distance by 0.09  $\text{\AA}$  from  $n=1$  to 6 is not too large, as compared with the corresponding values for  $\text{Na}^+$ -water,  $\text{Mg}^{2+}$ -water,  $\text{Al}^{3+}$ -water and  $\text{Zn}^{2+}$ -ammonia by 0.22, 0.16, 0.13 and 0.33  $\text{\AA}$ , respectively. The accompanying drop in the interaction energy per solvent molecule, % $E_1$  is 15% for  $\text{K}^+$ -ammonia, compared to 28% of  $\text{Zn}^{2+}$ -ammonia and over 40% for all ion-water clusters. The assumption of pairwise additivity, % $E_2$  leads to an error of 13%, while the corresponding deviation for  $\text{Na}^+$ ,  $\text{Mg}^{2+}$ ,  $\text{Al}^{3+}$  in water and  $\text{Zn}^{2+}$  in ammonia are amount to 8%, 15%, 21% and 18%, respectively. The ligand-ligand repulsion energy per pair of interaction (total number of pair =  $n(n-1)/2$ ) of about 1-1.5 kcal/mol does not change much with the size of the cluster when compared with amount of 4-4.5 kcal/mol for  $\text{Zn}^{2+}$ -ammonia complexes. Thus, the  $\text{K}^+$ - $(\text{NH}_3)_n$  complexes are less stable than the  $\text{Zn}^{2+}$ - $(\text{NH}_3)_n$  complexes, the many-body effect is of less strength. Therefore, we may expect that neglect of many-body corrections in the Molecular Dynamics simulation will not give the large error for the structural properties, such as radial distribution functions, coordination number and the dynamical properties.

## Part B : Molecular Dynamics simulation

### 5.4 Structural properties

#### *a) Solvent structure*

The N-N radial distribution function for liquid ammonia from X-ray measurement [39] at 277 K exhibits a maximum at 3.37 Å and minimum at 5.3 Å, leading to the coordination number of 12. Since there is only one ion per 215 ammonia molecules or 2 ions in 214 ammonia molecules, the observed solvent properties are assumed to be identical with those of pure liquid ammonia. The MD results for the three systems, K<sup>+</sup>-ammonia, I<sup>-</sup>-ammonia and K<sup>+</sup>-I<sup>-</sup>-ammonia, agreed well with the X-ray data, especially for the coordination number and the height of the first peak of the radial distribution function. The characteristics of the N-N, N-H and H-H radial distribution functions, as depicted in Table 4.8 to Table 4.10 and Table 5.2, show only small deviation from a uniform distribution and they are not much different for the three systems. The relatively low contribution of hydrogen bonding to the structure of liquid ammonia is indicated by the disappearing of the shoulder at about 2.5 Å of the N-H RDFs for the three systems, in comparison with those of pure liquid [39]. This is in agreement with the value of 12 for the coordination number which also favours the picture of a close-packed structure rather than a hydrogen bond network.

#### *b) Solvation shell structure*

The K<sup>+</sup>-N RDF for both K<sup>+</sup>-ammonia and K<sup>+</sup>-I<sup>-</sup>-ammonia systems, show a well pronounced first peak at 2.88 Å and 2.69 Å (Fig. 4.7 and Fig. 4.11) with the corresponding integration numbers of 8.7 and 8.9 (Table 4.8 and Table 4.10), respectively. The obtained coordination numbers are in reasonable agreement with those observed for dilute solution of one K<sup>+</sup> and one KCl in water by means of MC, MD and X-ray methods (Table 5.2). Shift of the first maximum of the K<sup>+</sup>-N RDFs by ~ 0.2 Å to shorter distance in changing from the K<sup>+</sup>-ammonia to the K<sup>+</sup>-I<sup>-</sup>-ammonia systems and the split of the second peak, centered at 5.85 Å into 2 peaks at 4.70 Å and 5.78 Å can be described by the two-dimensional dipole orientation given in Fig. 5.1.

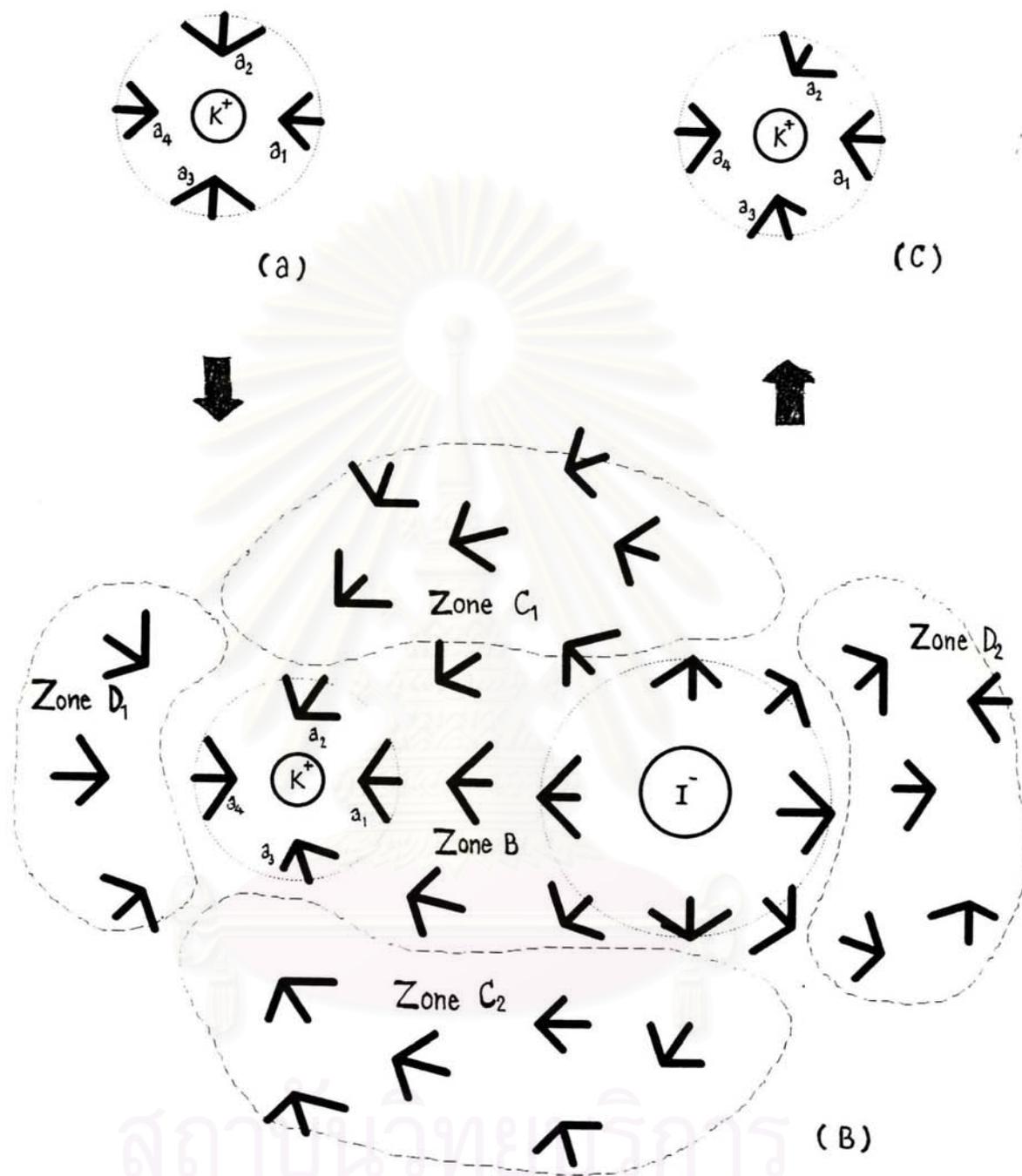


**Figure 5.1** Two-dimensional dipole orientation of ammonia molecules. (a) The ammonia molecule in the first solvation shell of  $K^+$  in the system consisting of one  $K^+$  in ammonia ; (b) The dipole orientation of ammonia molecules in the system consisting of one  $K^+$  and one  $I^-$  in ammonia ; (c) The orientation change of ammonia molecules in the solvation shell of  $K^+$  in the  $K^+-I^-$ -ammonia systems.

In the system consisting of one  $K^+$ , the second shell molecules, are weakly induced by the  $K^+$  (the  $K^+$ -ammonia interaction in the configuration where  $\theta = \phi = 0$ , Fig. 2.2, at 6 Å is about -5 kcal/mol, Fig. 4.1) and by the molecules in its first solvation shell. This causes the appear of second peak of the  $K^+$ -N RDFs at 5.85 Å. The  $K^+$ -N distances for the first shell molecules are interpreted, according to the first peak of the  $K^+$ -N RDFs, as 2.88 Å and assumed to be identical for all ammonias,  $a_1$  to  $a_4$  in Fig. 5.1a. The present of counter ion, the orientations of the solvent molecules is proposed as in Fig. 5.1b. Ammonia molecules in region B are induced, directly, by both ions, as well as their first shell molecules, therefore, parallel dipole orientations are promoted strongly by both ions. For the molecules in region C, both  $C_1$  and  $C_2$ , the induction, due to both ions and their first shell molecules, are partially out-of-phase, while those in region D orient themselves according, only, to each ion.

The above assumptions would lead to the following arrangements in the  $K^+$ - $I^-$ -ammonia system:

i) Molecules  $a_1$  to  $a_3$  (just some examples) is induced by the dipole oriented molecules in zone B and C. They are expected to bind tightly and closely to the  $K^+$ . This may lead to the shift of the first solvation position by 0.2 Å (Fig. 4.7a and Fig. 4.11a) to shorter distance in changing from the  $K^+$ -ammonia to the  $K^+$ - $I^-$ -ammonia systems, as well as the increase of the height of the  $K^+$ -N first peak. These effects have been significantly observed only for the  $K^+$  but not for  $I^-$  due to the stronger  $K^+$ -ammonia than the  $I^-$ -ammonia interactions by a factor of 4. In addition, shift of the  $K^+$ -N distance of 0.2 Å causes the increase of its interaction energy of only 0.69 kcal/mol (Fig. 4.1). This value is very close to the fluctuation due to the temperature effect.

ii) The high ordered solvent in zone B and C cause also the disappear of the second peak of the N-N RDF for the  $K^+$ - $I^-$ -ammonia system (Fig. 4.13a)

iii) Among the ammonia molecules in the first shell of the  $K^+$ , the  $K^+$ -N distance of the ammonia  $a_1$  is expected to be the shortest one, since it is induced by the most highly ordered molecules in zone B. The  $K^+$ -N distance for  $a_4$  is nearly not disturbed by the  $I^-$ , therefore, it should not be changed by the present of counter ion.

iv) Dipole vector of the molecules  $a_2$  and  $a_3$  in the first shell of  $K^+$  can not point toward the  $K^+$  because of the induction of the ammonia molecules in

zone B. This finding is supported by the difference between the first peak position of the  $K^+$ -N and  $K^+$ -H RDFs, 0.5 Å for the  $K^+$ -ammonia system (the difference between  $r_{MI}$  of  $K^+$ -N, 2.88 Å, and of  $K^+$ -H, 3.38 Å, Table 4.8) and 0.66 Å for the  $K^+$ - $I^-$ -ammonia system (Table 4.10). The corresponding vectors for the ammonia molecules pointing their dipole vectors toward the  $K^+$  is 0.38 Å.

v) The partial rotation of the molecules  $a_2$  and  $a_3$  as described in (iv) may also cause the moves of second shell molecules, located in zone C, to longer distances, while the molecule  $a_1$ , which points its dipole tightly toward the  $K^+$ , may cause the shortening of its  $K^+$ -N distance, as well as those of the molecules in zone B. This changes have been observed in terms of the split of the  $K^+$ -N second peak for the  $K^+$ - $I^-$ -ammonia system (Fig. 4.11a), as well as the increase of its height. In addition, sum of the integration numbers located under the first and the second splitted peaks of the  $K^+$ -N RDF for  $K^+$ - $I^-$ -ammonia system (for 18 and 31, respectively) are identical to those of 31 under the single-second peak for the  $K^+$ -ammonia system (Fig. 4.7a).

For the solvation shell of  $I^-$ , no significant difference on the characteristics of the  $I^-$ -N or  $I^-$ -H RDFs for the two systems,  $I^-$ -ammonia and  $K^+$ - $I^-$ -ammonia, have been found. The first shell coordination number between 15 to 16 (Table 4.9 and Table 4.10) is rather reasonable in comparison to those of between 6-8 for  $Cl^-$  (Table 5.2) (atomic radii of  $Cl^-$  and  $I^-$  are 2.20 Å and 1.81 Å, respectively). Slightly shift of the first maximum of the  $I^-$ -N RDFs by 0.07 Å to shorter distance, from 4.14 Å to 4.07 Å and of the in changing from the  $I^-$ -ammonia to the  $K^+$ - $I^-$ -ammonia system could be understood by the same reason as for  $K^+$ .

**Table 5.2** Characteristics of the first solvation shell of the solvation contained one ion or one molecule of salt in water and ammonia solvents. ( $\alpha\beta$ ,  $r_{M1}$  and  $n_{\alpha\beta}$  are pair of species, distance to the first maximum (in Å) and first shell coordination number, respectively.)

system	$\alpha\beta$	$r_{M1}$	$n_{\alpha\beta}$	method	ref.
KCl-water	K <sup>+</sup> -O	2.80	7.8	MD	[53]
		2.71	6.3	MC	[54]
		2.76	7.5	MD	[55]
		2.86	7.6	MD	[56]
		2.80	8.1	X-ray	[57]
	Cl <sup>-</sup> -O	3.16	7.6	MD	[53]
		3.25	8.4	MC	[54]
		3.29	7.2	MD	[55]
		3.23	5.9	MD	[56]
		3.14	6.0	X-ray	[57]
K <sup>+</sup> -ammonia	K <sup>+</sup> -N	2.88	8.7	MD	this work
	N-N	3.41	12.2	MD	this work
I <sup>-</sup> -ammonia	I <sup>-</sup> -N	4.14	15.9	MD	this work
	N-N	3.34	11.9	MD	this work
K <sup>+</sup> -I <sup>-</sup> -ammonia	K <sup>+</sup> -N	2.69	8.9	MD	this work
	I <sup>-</sup> -N	4.07	15.1	MD	this work
	N-N	3.23	11.5	MD	this work
Li <sup>+</sup> -ammonia	Li <sup>+</sup> -N	2.29	6.0	MD	[26]
Na <sup>+</sup> -ammonia	Na <sup>+</sup> -N	2.49	7.0	MD	[58]
Mg <sup>2+</sup> -ammonia	Mg <sup>2+</sup> -N	2.25	8.0	MC	[59]
Zn <sup>2+</sup> -ammonia	Zn <sup>2+</sup> -N	2.10	6.0	MC	[52]
		2.23	6.0	MD	[52]
pure ammonia	N-N	3.37	12.0	X-ray	[39]

## 5.5 Dynamical properties

A first overview over the particle motions can easily be gained by computing the velocity autocorrelation functions of the various particles in the system as obtained for  $K^+$ ,  $I^-$ , N atom, H atom and ammonia molecule. In the ammonia spectrum, the peak at the lowest frequencies should be associated with the hindered translations and vibrations of the molecule, while the intermediate peak reflects the bending vibration and the peak at the highest frequencies shows the stretching vibrations. The general shape of this spectrum is quite similar to the one obtained from a scan over the same frequency range in the infrared region. It must be stressed that the Fourier transforms of autocorrelation functions as reported here are not exactly equivalent to intensity functions in infrared or Raman spectroscopy, however, that there is some proportionality between the spectra reported here and the experimental results. We shall thus not base any conclusion here on intensity comparison between experimental and computed spectra and restrict our attention to the discussion of the positions of the peak maxima, at least as far as the comparison between experiments and simulations is concerned.

### *a) Hindered translational motions*

The normalized center-of-mass velocity autocorrelation functions of the ammonia molecules are presented separately for the bulk phase and for the solvation shell of the ions. The difference is more visible in liquid ammonia than in the case of aqueous electrolyte solution [60]. No significant differences have been found for the  $C_V(t)$  of bulk ammonia of the three systems,  $K^+$ -ammonia (Fig. 4.16a),  $I^-$ -ammonia (Fig. 4.21a) and  $K^+$ - $I^-$ -ammonia (Fig. 4.26a), except the faster decay of the first two systems, approached zero at a time range of about 0.5 ps, than the last one. The  $C_V(t)$  of ammonia molecules in the first shell of  $K^+$  approaches zero faster than those in the first shell of  $I^-$  for both systems with and without counter ion (salt-ammonia and ion-ammonia, respectively). These results relate to the strong interaction of  $K^+$ -ammonia than  $I^-$ -ammonia complexes. However, the  $C_V(t)$  of each ion in the two systems shows only small difference, the more fluctuation of the  $C_V(t)$  for the system containing the counter ion than the other one (Fig. 4.16a, Fig. 4.21a and Fig. 4.26a). These behaviour for the bulk indicates a relatively free translational motion, and is in agreement with the

conclusion drawn above that hydrogen bonding effects are not very important for the structure of the ammonia solution. The strong binding of the ammonia molecules to the solvation shell of ions leads to a more pronounced oscillation in their velocity autocorrelation functions than those of bulk ammonia.

The spectral densities of the velocity autocorrelation functions of the center-of-mass motion of the ammonia molecules reflect the hindered translation of these particles in the liquid. For bulk ammonia, Fig. 4.16b, Fig. 4.21b and Fig. 4.26b, the maximum at zero frequency are expected, for all simulations, due to the weak interaction between ammonia molecules. In the solvation shell of  $K^+$ , a maximum of the spectral density occur at about  $150\text{ cm}^{-1}$  for  $K^+$ -ammonia system and about  $110\text{ cm}^{-1}$  for the  $K^+$ - $I^-$ -ammonia system. These values lie within the range of the broad band found for similar systems, water in the hydration shell of  $Li^+$  (about  $50$  to  $250\text{ cm}^{-1}$ ) [60] and ammonia in the solvation shell of  $Li^+$  (about  $140\text{ cm}^{-1}$ ) [26]. In the solvation shell of  $I^-$ , a maximum at zero frequency were found in both  $I^-$ -ammonia and  $K^+$ - $I^-$ -ammonia systems. The reason is related to the weak  $I^-$ -ammonia interactions (Fig. 4.3).

The self-diffusion coefficients, calculated from the center-of-mass  $C_V(t)$  (see equation 3.19) for all simulations are summarized in Table 5.3. They are evaluated separately for ammonia molecules in the bulk and in the first shell of ions. Experimental value was also given [61] for comparison.

**Table 5.3** Calculated self-diffusion coefficient for ammonia molecules in the bulk and in the solvation shell of ions, obtained from the simulations at 240 K and from experimental result [61] at 240 K.

system	bulk ( $\text{cm}^2/\text{s}$ )	solvation shell of $K^+$ ( $\text{cm}^2/\text{s}$ )	solvation shell of $I^-$ ( $\text{cm}^2/\text{s}$ )
$K^+$ -ammonia	$1.3 \times 10^{-4}$	$6.1 \times 10^{-5}$	-
$I^-$ -ammonia	$1.0 \times 10^{-4}$	-	$7.4 \times 10^{-5}$
$K^+$ - $I^-$ -ammonia	$1.1 \times 10^{-4}$	$5.7 \times 10^{-5}$	$7.8 \times 10^{-5}$
ex.liq. ammonia	$5.3 \times 10^{-5}$	-	-

The less value of the self-diffusion coefficients of ammonia in the solvation shell of ions than bulk ammonia indicates, as expected, the binding of the molecules to the ions. The large discrepancy between the bulk phase values and the experimental one taken from literature for pure liquid ammonia is at present not fully understood. One reason might be that the ammonia-ammonia potential employed in this simulation is not sufficiently negative. However, it is a complicated problem to develop the ammonia-ammonia potential to represent all of its structural and dynamics properties. The high  $D$  value relates to the weak N-H interactions, and consequently, the disappear of the peak at  $\sim 2.5$  Å of the N-H RDFs (Fig. 4.8b, Fig. 4.10b and Fig. 4.13b). In contrast, the molecular dynamics values of Saporik *et al.* [62] and Klein *et al.* [63] are lower than the experimental ones, due to the strong N-H interactions (exhibited by the pronounce shoulder of the N-H RDFs at  $\sim 2.5$  Å).

#### *b) Librational motions*

The spectral densities of librational motions can be calculated from the Fourier transformation of one of the three components of the normalized velocity autocorrelation function of the hydrogen atoms [64-65]. Two of the  $C_v(t)$ s and the corresponding spectral densities of the librational motions of ammonia in the bulk and in the solvation shell of the ions, about  $x$  and the  $z$  axis, are presented in Fig. 4.15, Fig. 4.20 and Fig. 4.25 for the  $K^+$ -ammonia,  $I^-$ -ammonia and  $K^+$ - $I^-$ -ammonia systems, respectively. The rotation about the  $x$  axis shows a strong cation effect, i.e. the frequency increases from about  $170\text{ cm}^{-1}$  in the bulk to about  $340\text{ cm}^{-1}$  in the solvation shell of the  $K^+$  for the  $K^+$ -ammonia system and from  $150\text{ cm}^{-1}$  to  $330\text{ cm}^{-1}$  for the  $K^+$ - $I^-$ -ammonia system. The rotation about the dipole axis ( $z$ -axis) shows a rather free rotation as its maximum appears at zero frequency. The differences in the rotational motions of the bulk and solvated ammonia can be easily described on the basis of the structure of the solution. Strong solvation forces keep the N- $K^+$  vector parallel to the dipole vector of the solvated ammonia. Thus, the  $K^+$ -ammonia interactions hinder the motion around the  $x$ - or  $y$ -axis, but do not influence the rotation around the dipole axis.

Similar for those of  $K^+$ , the frequency about the  $x$ -axis increases from about  $180\text{ cm}^{-1}$  for the molecules in the bulk to about  $210\text{ cm}^{-1}$  (Fig. 4.20b) for the molecules in the first solvation shell of  $I^-$  for the  $I^-$ -ammonia system. The stronger  $K^+$ -ammonia interactions than the  $I^-$ -ammonia one causes the higher frequency of

motion about x-axis of the molecules in the first shell of  $K^+$  than those  $I^-$  (Fig. 4.26 b and Fig. 4.26c).

*c) Vibrational motion*

The spectral densities were calculated from the hydrogen atom autocorrelation functions of ammonia molecules in the bulk and in the solvation shell of the ions. From a symmetry coordinate analysis, which is similar to that developed by Bopp [64-65] for water, the symmetric and the asymmetric bending and stretching modes can be unambiguously identified (Fig. 4.17, Fig 4.22 and Fig. 4.27). The calculated results, as well as the experimental ones [66], are summarized in Table 5.4.

The effect of one or two ions on the intramolecular vibration of molecules in its solvation shell can not be measured experimentally, its investigation is one of the advantage of the Molecular Dynamics simulations. In the solvation shell of both  $K^+$  and  $I^-$  for all systems,  $K^+$ -ammonia,  $I^-$ -ammonia and  $K^+$ - $I^-$ -ammonia, the symmetric bending and the asymmetric stretching modes show a blueshift, while the two modes of vibrations, the asymmetric bending and the symmetric stretching, are redshift (Table 5.4). These shifts are consistent with those reported for  $Li^+$  in liquid ammonia [26]. Since the statistical uncertainties in the calculated frequencies are estimated to be about  $\pm 20 \text{ cm}^{-1}$ . Within this error margin, the following statements can be made: in both simulations and experiment. All symmetric modes, obtained from the simulations and experiment, are found at lower frequencies than the corresponding asymmetric ones, as depicted. From the qualitative agreement between simulated and measured frequencies it can be expected that the potential employed in the simulation leads to a qualitatively correct description of the effect of ions on the intramolecular properties of the ammonia molecules in the first solvation shell.

สถาบันวิทยบริการ  
จุฬาลงกรณ์มหาวิทยาลัย

**Table 5.4** Comparison of various vibrational frequencies taken from the simulations, calculated separately for bulk ammonia and ammonia in the solvation shell of ions, and from the experimental results.

mode	system							experimental liq. ammonia [66]
	MD (K <sup>+</sup> -ammonia)		MD (I <sup>-</sup> -ammonia)		MD (K <sup>+</sup> -I <sup>-</sup> -ammonia)			
	solvation shell of K <sup>+</sup>	bulk	solvation shell of I <sup>-</sup>	bulk	solvation shell of K <sup>+</sup>	solvation shell of I <sup>-</sup>	bulk	
sym.bend	1195	1138	1143	1135	1198	1142	1132	1066
asym.bend	1561	1595	1585	1593	1559	1587	1591	1638
sym.stretch	3321	3374	3363	3370	3317	3364	3376	3240
asym.stretch	3493	3476	3539	3472	3490	3538	3477	3379

สถาบันวิทยบริการ  
จุฬาลงกรณ์มหาวิทยาลัย

## REFERENCES

1. Hasen, J.P. and McDonald, I.R. 1986. Theory of simple liquids, (2nd ed.) Academic Press, New York.
2. Lennard-Jones, J.E. and Devonshire, A.F. (1939a). Critical and cooperative phenomena. III. A theory of melting and the structure of liquids. Proc. R.Soc.Lond. A169, 317-38.
3. Lennard-Jones, J.E. and Devonshire, A.F. (1939b). Critical and cooperative phenomena. IV. A theory of disorder in solids and liquids and the process of melting. Proc.R.Soc.Lond. a170, 464-84.
4. Metropolis, N., Rosenbluth, A.W., Rosenbluth, M.N., Teller, A.H., and Teller, E. 1953. Equation of state calculation by fast computing machines. J.Chem.Phys. 21, 1087-92.
5. Alder, B.J. and Wainwright, T.E. 1960. Studies in molecular dynamics. II. Behaviour of a small number of elastic spheres. J.Chem.Phys. 33, 1439-51.
6. Lie, G.C., Clementi, E. and Yoshimine, M. 1975. Study of the structural of molecular complexes XIII: Monte Carlo simulation of liquid water with a configuration interaction pair potential. J.Chem.Phys. 64(6), 2314-2323.
7. Swaminathan, S., Harrison, S.W. and Beveridge, D.L. 1977. Monte Carlo studies on the structure of a dilute aqueous solution of methane. J.Am.Chem.Soc. 100(8), 5705-5712.
8. Hagler, A.T. and Moulton, J. 1978. Computer simulation of the solvent structure around biological macromolecules. Nature 272(16), 248-256.
9. Jorgensen, W.L. and Ibrahim, M. 1980. Structure and properties of liquid ammonia. J.Am.Chem.Soc. 102(10), 3309-3315.
10. Jorgensen, W.L. 1981. Simulation of liquid ethanol including internal rotation. J.Am.Chem.Soc. 103(2), 345-350.
11. Bolis, G., Corongiu, G. and Clementi, E. 1981. Methanol in water solution at 300 K. Chem.Phys.Lett. 6(3), 299-306.
12. Jorgensen, W.L. and Madura, J.D. 1983. Solvation and conformation of methanol in water. J.Am.Chem.Soc. 105(6), 863-869.

13. Linse, P., Karlstrom, G. and Jonsson, B. 1984. Monte Carlo studies of a dilute aqueous solution of benzene. J.Am.Chem.Soc. 106(15), 4096-4102.
14. Byrnes, J.M. and Sandler, S.I. 1984. Monte Carlo simulation of liquid ethane. J.Chem.Phys. 80(2), 881-885.
15. Dietz, W. and Heinzinger, K. 1984. Structure of liquid chloroform: A comparison between computer simulation and neutron scattering results. Ber.Bunsenges.Phys.Chem. 88, 543-546.
16. Okazaki, S., Touhara, H. and Nakanishi, K. 1984. Computer experiments of aqueous solutions V: Monte Carlo calculation on the hydrophobic interaction in 5 mol % methanol solution. J.Chem.Phys. 81(2), 890-894.
17. Alagona, G., Ghio, C. and Kollman, P.A. 1985. Monte Carlo simulations of the solvation of the dimethyl phosphate anion. J.Am.Chem.Soc. 107(8), 2229-2238.
18. Bounds, D.G. 1985. A molecular dynamics study of the structure of water around the ions Li(I), Na(I), K(I), Ca(I), Ni(I) and Cl(I). Mol.Phys. 54(6), 1335-1355.
19. Rahman, A., Stillinger, F.H. and Lemberg, H.L. 1975. Study of a central force model for liquid water by molecular dynamics. J.Chem.Phys. 63(12), 5223-5230.
20. Narusawa, H. and Nakanishi, K. 1980. A simulation of preferential solvation in ternary Lennard-jones liquid mixtures by the molecular dynamics method. J.Chem.Phys. 73(8), 4066-4070.
21. Tanaka, H., Nakanishi, K. and Touhara, H. 1985. Computer experiments on aqueous solutions VII: Potential energy function for urea dimer and molecular dynamics calculation of 8 mol % aqueous solution of urea. J.Chem.Phys. 82, 5184-5190.
22. Sphor, E. and Heinzinger, K. 1986. Molecular dynamics simulation of a water/metal interface. Chem.Phys.Lett. 123(3), 218-220.
23. Probst, M.M., Radnai, T., Heinzinger, K., Bopp, P. and Rode, B.M. Molecular dynamics and x-ray investigation of an aqueous  $\text{CaCl}_2$  solution. J.Phys.Chem. 89(5), .
24. Palinkas, G. and Heinzinger, K. 1986. Hydration shell structure of the calcium ion. Chem.Phys.Lett. 126(3), 251-254.

25. Migliore, M. and Fornili, S.L., Spohr, E., Pakinkas, G. and Heinzinger, K. 1986. A molecular dynamics study of the structure of an aqueous KCl solution. Z.Naturforsch. 41a, 826-834.
26. Hannongbua, S., Ishida, T., Spohr, E. and Heinzinger, K. 1988. Molecular dynamics study of a lithium ion in ammonia. Z.Naturforsch. 43a, 572-582.
27. Lepoutre, G. and Seinko, M.J. 1964. Metal-ammonia solutions, Benjamin, Collogue Weyl I, New York.
28. Lagowski, J.J. and Seinko, M.J. 1970. Metal-ammonia solutions, Butterworths, Collogue Weyl II, London.
29. Jortner, J. and Kertner, N.R. 1973. Electrons in fluids, Springer, Collogue Weyl III, Berlin.
30. (a) Schrödinger, E. 1926. Ann.Physik, 79, 361. Representative general texts include; (b) Kemble, E.C. 1965. Fundamental Principles of Quantum Mechanics., McGraw-Hill, New York; (c) Levine, I.N. 1983. Quantum Chemistry, 3rd ed., Allyn and Bacon, Boston; (d) Pilar, F.L. 1968. Elementary Quantum Chemistry, McGraw-Hill, New York; (e) Hehre, W.J., Radom, L., Schleyer, P.v.R., and Pople, J.A. 1986. Ab initio Molecular Orbital Theory, John Wiley & Sons, Inc.
31. Born, M. and Oppenheimer, J.R. 1927. Ann.Physik, 84, 457.
32. Slater, J.C. 1930. Phys.Rev., 36, 57.
33. (a) Boys, S.F. 1950. Proc.Roy.Soc. (London), A200, 542. For a readable discussion of the properties and uses of gaussian functions in quantum mechanics, see: Shavitt, I. in Methods in Computational Physics vol.2, Wiley, New York, 1962.
34. For a discussion, see reference 30 (c), pp. 172-192.
35. Roothann, C.C.J. 1951. Rev.Mod.Phys., 23, 69.
36. Hall, G.G. 1951. Proc.Roy.Soc. (London), A205, 541.
37. Boys, S.F. and Bernardi, F. 1970. Mol.Phys., 19, 553.
38. Spirko, V. 1983. Vibrational anharmonicity and the inversion potential function of NH<sub>3</sub>. J.Mol.Spectrosc., 101, 30.
39. Narten, A.H. 1977. Liquid ammonia : Molecular correlation functions from x-ray diffraction. J.Chem.Phys., 66, 3117.
40. Husinaga, S. 1977. J.Chem.Phys., 66, 1382.

41. Dunning, T.H. and Hey, P.J. 1976. Modern Theoretical Chemistry. Plenum, New York.
42. Swaminathan, R.J., Whitehead, E. and Beveridge, D.L. 1977. J.Am.Chem.Soc. 99, 7817.
43. Hay, P.J. and Wadt, W.R. 1985. J.Chem.Phys., 82, 270.
44. Gear, C.W. 1966. The numerical integration of ordinary differential equations of various orders. Report ANL 7126, Argonne National Laboratory.
45. Gear, C.W. 1971. Numerical initial value problems in ordinary differential equations. Prentice-Hall, Englewood Cliffs, NJ.
46. Born, M. and Von Karman, Th. 1912. Über, Schwingungen in Raumgittern, Physik.Z., 13, 297-309.
47. Ewald, P. 1921. Die Berechnung optischer und elektrostatischer Gitterpotentiale. Ann.Phys., 64, 253-87.
48. Verlet, L. 1967. Computer 'experiments' on classical fluids. I. Thermodynamical properties of Lennard-Jones molecules. Phys.Rev., 159, 98-103.
49. Verlet, L. 1968. Computer 'experiments' on classical fluids. II. Equilibrium correlation functions. Phys. Rev., 165, 201-14.
50. Kolos, W. 1979. Theoret.Chim.Acta., 51, 219.
51. Probst, M.M. 1987. Chem.Phys.Lett., 137, 229.
52. Hannongbua, S., Kerdcharoen, T., and Rode, B.M. 1992. J.Chem.Phys., 96, 9.
53. Migliore, M., Fornili, S.L., Spohr, E., Pálinkás, G., and Heinzinger, K. 1986. Z.Naturforsch., 41a, 826-834.
54. Mezei, M. and Beveridge, D.L. 1981. J.Chem.Phys., 74, 6902.
55. Impey, R.W., Madden, P.A., and McDonald, I.R. 1983. J.Chem.Phys., 87, 5071.
56. Bounds, D.G. 1985. Mol.Phys., 54, 1335.
57. Pálinkás, G., Radnai, T., and Hajdu, F. 1980. Z.Naturforsch., 35a, 107.
58. Hannongbua, S. 1991. Aust.J.Chem., 44, 447-456.
59. Hannongbua, S. and Rode, B.M. 1992. J.Chem.Phys., 162, 257-263.
60. Szász, Gy.I. and Heinzinger, K. 1983. J.Chem.Phys., 79, 3467.
61. Garroway, A.N. and Cotts, R.M. 1973. Phys.Rev., A7, 635.
62. Kritsana, P. Sarik, Reinhart Ahlrichs and Stefan Brode, 1985. Mol.Phys. 6, 1247-1264.

63. Impey, R.W., and Klein, M.L. 1984. Chem.Phys.Lett., 104, 579.

64. Bopp, P. 1986. Chem.Phys., 196, 205.

65. Bopp, P., 1987. Habilitationsschrift, Technische Hochschule Darmstadt, Darmstadt.

66. Birchall, T. and Drummond, I.1859. J.Chem.Soc., A1970.



สถาบันวิทยบริการ  
จุฬาลงกรณ์มหาวิทยาลัย

## Appendix 1

---

Exponents and Coefficients for STO-3G basis set

atom	shell	exponent	coefficient	
N	S 3 1.00	.9910616896D+02	.1543289673D+00	
		.1805231239D+02	.5353281423D+00	
		.4885660238D+01	.4446345422D+00	
	SP 3 1.00	.3780455879D+01	-.9996722919D-01	.1559162750D+00
		.8784966449D+00	.3995128261D+00	.6076837186D+00
		.2857143744D+00	.7001154689D+00	.3919573931D+00
H	S 3 1.00	.3425250914D+01	.1543289673D+00	
		.6239137298D+00	.5353281423D+00	
		.1688554040D+00	.4446345422D+00	
K <sup>+</sup>	S 3 1.00	.7715103681D+03	.1543289673D+00	
		.1405315766D+03	.5353281423D+00	
		.3803332899D+02	.4446345422D+00	
	SP 3 1.00	.5240203979D+02	-.9996722919D-01	.1559162750D+00
		.1217710710D+02	.3995128261D+00	.6076837186D+00
		.3960373165D+01	.7001154689D+00	.3919573931D+00
	SP 3 1.00	.3651583985D+01	-.219620369D+00	.1058760429D-01
		.1018782663D+01	.2255954336D+00	.5951670053D+00
		.3987446295D+00	.9003984260D+00	.4620010120D+00
	SP 3 1.00	.5039822505D+00	-.308844121D+00	-.121546860D+00
		.1860011465D+00	.1960641166D-01	.5715227604D+00
		.8214006743D-01	.1131034442D+01	.5498949471D+00

จุฬาลงกรณ์มหาวิทยาลัย

## Exponents and coefficients for DZV basis set

atom	shell	exponent	coefficient
N	S 7 1.00	.5909000000D+04	.1190000000D-02
		.8875000000D+03	.9099000000D-02
		.2047000000D+03	.4414500000D-01
		.5984000000D+02	.1504640000D+00
		.2000000000D+02	.3567410000D+00
		.7193000000D+01	.4465330000D+00
		.2686000000D+01	.1456030000D+00
	S 2 1.00	.7193000000D+01	-.160405000D+00
		.7000000000D+00	.1058215000D+01
	S 1 1.00	.2133000000D+00	.1000000000D+01
	P 4 1.00	.2679000000D+02	.1825400000D-01
		.5956000000D+01	.1164610000D+00
		.1707000000D+01	.3901780000D+00
		.5314000000D+00	.6371020000D+00
P 1 1.00	.1654000000D+00	.1000000000D+01	
H	S 3 1.00	.1924060000D+02	.3282800000D-01
		.2899200000D+01	.2312080000D+00
		.6534000000D+00	.8172380000D+00
	S 1 1.00	.1776000000D+00	.1000000000D+01

สถาบันวิทยบริการ  
จุฬาลงกรณ์มหาวิทยาลัย

## Exponents and coefficients for DZP basis set

atom	shell	exponent	coefficient
N	S 6 1.00	.5909440000D+04	.2004000000D-02
		.8874510000D+03	.1531000000D-01
		.2047900000D+03	.7429300000D-01
		.5983760000D+02	.2533640000D+00
		.1999810000D+02	.6005760000D+00
		.2686000000D+01	.2451110000D+00
	S 1 1.00	.7192700000D+01	.1000000000D+01
	S 1 1.00	.7000000000D+00	.1000000000D+01
	S 1 1.00	.2133000000D+00	.1000000000D+01
	P 4 1.00	.2678600000D+02	.1825700000D-01
		.5956400000D+01	.1164070000D+00
		.1707400000D+01	.3901110000D+00
		.5314000000D+00	.6372210000D+00
P 1 1.00	.1654000000D+00	.1000000000D+01	
H	S 3 1.00	.1924060000D+02	.3282800000D-01
		.2899200000D+01	.2312080000D+00
		.6534000000D+00	.8172380000D+00
	S 1 1.00	.1776000000D+00	.1000000000D+01

สถาบันวิทยบริการ  
จุฬาลงกรณ์มหาวิทยาลัย

## Exponents and coefficients for extended basis set

ion	shell	exponent	coefficient
K <sup>+</sup>	S 1 1.00	0.19027034D+06	.1000000000D+01
	S 1 1.00	0.28613941D+05	.1000000000D+01
	S 1 1.00	0.65763284D+04	.1000000000D+01
	S 1 1.00	0.18822392D+04	.1000000000D+01
	S 1 1.00	0.61879246D+03	.1000000000D+01
	S 1 1.00	0.22519307D+03	.1000000000D+01
	S 1 1.00	0.88633194D+02	.1000000000D+01
	S 1 1.00	0.36582578D+02	.1000000000D+01
	S 1 1.00	0.11055775D+02	.1000000000D+01
	S 1 1.00	0.45094418D+01	.1000000000D+01
	S 1 1.00	0.11401467D+01	.1000000000D+01
	S 1 1.00	0.46956978D+00	.1000000000D+01
	S 1 1.00	0.76838944D-01	.1000000000D+01
	S 1 1.00	0.30578949D-01	.1000000000D+01
	P 1 1.00	0.11215660D+04	.1000000000D+01
	P 1 1.00	0.26708172D+03	.1000000000D+01
	P 1 1.00	0.86610217D+02	.1000000000D+01
	P 1 1.00	0.32629225D+02	.1000000000D+01
	P 1 1.00	0.13226649D+02	.1000000000D+01
	P 1 1.00	0.55847004D+01	.1000000000D+01
	P 1 1.00	0.21895464D+01	.1000000000D+01
	P 1 1.00	0.89115916D+00	.1000000000D+01
	P 1 1.00	0.33677344D+00	.1000000000D+01
	D 1 1.00	0.22380294D+02	.1000000000D+01
D 1 1.00	0.60329914D+01	.1000000000D+01	
D 1 1.00	0.19713966D+01	.1000000000D+01	
D 1 1.00	0.65363725D+00	.1000000000D+01	
D 1 1.00	0.19125306D+00	.1000000000D+01	
Γ	S 3 1.00	1.0249248D+06	2.2309664D-02
		1.5484313D+05	1.7069281D-1
		3.5646336D+04	8.6809665D-1
	S 1 1.00	1.0272630D+04	.1000000000D+01
	S 1 1.00	3.4344769D+03	.1000000000D+01
	S 1 1.00	1.2844313D+03	.1000000000D+01
	S 1 1.00	5.2564189D+02	.1000000000D+01
S 1 1.00	2.3074127D+02	.1000000000D+01	

S 1 1.00	8.7255217D+01	.1000000000D+01
S 1 1.00	3.9494464D+01	.1000000000D+01
S 1 1.00	0.14254520D+02	.1000000000D+01
S 1 1.00	0.76466089D+01	.1000000000D+01
S 1 1.00	0.30500598D+01	.1000000000D+01
S 1 1.00	0.17326181D+01	.1000000000D+01
S 1 1.00	0.87682364D+00	.1000000000D+01
S 1 1.00	0.63499302D+00	.1000000000D+01
S 1 1.00	0.25649761D+00	.1000000000D+01
S 1 1.00	0.10611694D+00	.1000000000D+01
P 3 1.00	7.2990410D+03	2.3438952D-02
	1.7678671D+03	1.8469444D-1
	5.9009433D+02	8.5540750D-1
P 1 1.00	2.3149387D+02	.1000000000D+01
P 1 1.00	1.0173176D+02	.1000000000D+01
P 1 1.00	4.7569119D+01	.1000000000D+01
P 1 1.00	2.2275404D+01	.1000000000D+01
P 1 1.00	1.0840897D+01	.1000000000D+01
P 1 1.00	5.2379498D+00	.1000000000D+01
P 1 1.00	2.5466334D+00	.1000000000D+01
P 1 1.00	0.12106848D+01	.1000000000D+01
P 1 1.00	0.57440921D+00	.1000000000D+01
P 1 1.00	0.24653310D+00	.1000000000D+01
P 1 1.00	0.91353229D-01	.1000000000D+01
D 11.00	0.37037639D+03	.1000000000D+01
D 11.00	0.10971047D+03	.1000000000D+01
D 11.00	0.41199216D+02	.1000000000D+01
D 11.00	0.17284607D+02	.1000000000D+01
D 11.00	0.78154415D+01	.1000000000D+01
D 11.00	0.37428153D+01	.1000000000D+01
D 11.00	0.16595878D+01	.1000000000D+01
D 11.00	0.65265908D+00	.1000000000D+01

สถาบันวิทยบริการ  
จุฬาลงกรณ์มหาวิทยาลัย

## Appendix 2

---

### Gaussian 92 input file

\$RunGauss

#HF Gen Geom=Coord Gfinput

Potassium(1+) in Ammonia

```
1 1
N 0.00000 0.00000 0.00000
H 0.93776 0.00000 -0.38147
H -0.46888 -0.81212 -0.38147
H -0.46888 0.81212 -0.38147
K 3.75000 6.49519 -12.99038

1 0
S 6 1.00
.5909440000D+04 .2004000000D-02
.8874510000D+03 .1531000000D-01
.2047900000D+03 .7429300000D-01
.5983760000D+02 .2533640000D+00
.1999810000D+02 .6005760000D+00
.2686000000D+01 .2451110000D+00
S 1 1.00
.7192700000D+01 .1000000000D+01
S 1 1.00
.7000000000D+00 .1000000000D+01
S 1 1.00
.2133000000D+00 .1000000000D+01
P 4 1.00
.2678600000D+02 .1825700000D-01
.5956400000D+01 .1164070000D+00
.1707400000D+01 .3901110000D+00
.5314000000D+00 .6372210000D+00
P 1 1.00
.1654000000D+00 .1000000000D+01
D 1 1.00
.8000000000D+00 .1000000000D+01
****

2 0
S 3 1.00
.1924060000D+02 .3282800000D-01
.2899200000D+01 .2312080000D+00
.6534000000D+00 .8172380000D+00
S 1 1.00
.1776000000D+00 .1000000000D+01
P 1 1.00
.1000000000D+01 .1000000000D+01
****
```

3 0

S 3 1.00

.1924060000D+02 .3282800000D-01

.2899200000D+01 .2312080000D+00

.6534000000D+00 .8172380000D+00

S 1 1.00

.1776000000D+00 .1000000000D+01

P 1 1.00

.1000000000D+01 .1000000000D+01

\*\*\*\*

4 0

S 3 1.00

.1924060000D+02 .3282800000D-01

.2899200000D+01 .2312080000D+00

.6534000000D+00 .8172380000D+00

S 1 1.00

.1776000000D+00 .1000000000D+01

P 1 1.00

.1000000000D+01 .1000000000D+01

\*\*\*\*

5 0

S 1 1.0

0.19027034E+06 1.0

S 1 1.0

0.28613941E+05 1.0

S 1 1.0

0.65763284E+04 1.0

S 1 1.0

0.18822392E+04 1.0

S 1 1.0

0.61879246E+03 1.0

S 1 1.0

0.22519307E+03 1.0

S 1 1.0

0.88633194E+02 1.0

S 1 1.0

0.36582578E+02 1.0

S 1 1.0

0.11055775E+02 1.0

S 1 1.0

0.45094418E+01 1.0

S 1 1.0

0.11401467E+01 1.0

S 1 1.0

0.46956978E+00 1.0

S 1 1.0

0.76838944E-01 1.0

S 1 1.0

0.30578949E-01 1.0

P 1 1.0

0.11215660E+04 1.0

P 1 1.0

0.26708172E+03 1.0

P 1 1.0

0.86610217E+02 1.0

P 1 1.0

0.32629225E+02 1.0

P 1 1.0

สถาบันวิทยบริการ  
 วิทยาลัย  
 ราชภัฏวชิรวิทยาดำรง

0.13226649E+02	1.0
P 1 1.0	
0.55847004E+01	1.0
P 1 1.0	
0.21895464E+01	1.0
P 1 1.0	
0.89115916E+00	1.0
P 1 1.0	
0.33677344E+00	1.0
D 1 1.0	
0.22380294E+02	1.0
D 1 1.0	
0.60329914E+01	1.0
D 1 1.0	
0.19713966E+01	1.0
D 1 1.0	
0.65363725E+00	1.0
D 1 1.0	
0.19125306E+00	1.0
****	



สถาบันวิทยบริการ  
จุฬาลงกรณ์มหาวิทยาลัย

**CURRICULUM VITAE**

Anan Tongraar

- 1969      Born December, 16th in Chonburi, Thailand  
            Father : Mr. Samart Tongraar  
            Mother : Mrs. Anong Tongraar
- 1976      Elementary School (Satit Piboonbumpen, Boorapa Univ.,Chonburi)
- 1983      High School (Satit Piboonbumpen, Boorapa Univ.,Chonburi)
- 1989      Bachelor of Science (Chemistry),  
            Chulalongkorn University, Bangkok
- 1993      Master degree student at Department of Chemistry,  
            Faculty of Science, Chulalongkorn University, Bangkok



สถาบันวิทยบริการ  
จุฬาลงกรณ์มหาวิทยาลัย